TÉCNICO LISBOA

The use of MSC derived hepatocyte-like cells (HLCs) in microfluidic culture systems: an approach for studying the metabolic syndrome

Joana Saraiva Rodrigues

Thesis to obtain the Master of Science Degree in

Biomedical Engineering

Supervisor(s): Professor Joana Paiva Gomes Miranda
and Professor Maria Margarida Fonseca Rodrigues Diogo

Examination Committee

Chairperson: Professor João Pedro Estrela Rodrigues Conde
Supervisor: Professor Joana Paiva Gomes Miranda
Member of the comittee: Professor Maria da Graça Tavares Soveral Rodrigues

November 2016

Acknowledgements

Firstly, I would like to express my gratitude to Professor Joana Miranda for accepting me as a master thesis student at the Chemical Biology and Toxicology (CBT) group, in iMed.ULisboa, Faculty of Farmacy, Universidade de Lisboa, and for giving me the opportunity to work in a field that I have always been very interested. I am also thankful for all the advices and for teaching me a precise methodology of work in the laboratory.

I am grateful to Professor Margarida Diogo who was always very helpful throughout my master's degree and for showing me the variety of investigation fields in Bioengineering.

I want to show my gratitude to all the members of the CBT team. I was very lucky to be in a pleasant work environment with the people I met in this group: Inês, Susana, Bernardo and Catarina. I am very grateful to Madalena Cipriano, for always being available to answer my questions, passing me her knowledge, for the suggestions to improve my work and for being patient with me. Thank you, Sérgio Camões, for our fun moments at the laboratory, for teaching me routine procedures and for helping me to solve my problems in the laboratory.

To the friends I made in the university, huge thanks for all the good times: Jorge, for your wonderful sense of humour moments, with you I am always laughing; Ana, for pushing me to the next level and for all our fun times; Catarina, for always being available either when I just want to go outside for a break or when I want to go to a party; João, for providing me so many funny moments just by being yourself. We also spent some bad times but we supported each other and that made all easier. Without you, Técnico would have been impossible to overcome. To my older friends, I am also thankful for showing interest in my studies and for cheering me up when needed. A special thanks to Texas for being my bestfriend.

Most importantly, I need to recognize the patience of my family, specially my mother and father. Thank you for always believing in my capacities, for giving me the opportunity to proceed my studies and for taking good care of me (specially my mother for bringing me sweets whenever I ask her).

Resumo

A síndrome metabólica, ou síndrome de resistência à insulina, afeta cerca de um quarto da população mundial. Três tipos celulares estão envolvidos no desenvolvimento desta doença, nomeadamente, adipócitos, miofibroblastos e hepatócitos. Assim, é crucial entender o papel da interação entre estes tipos celulares neste contexto. A utilização de dispositivos de microfluídica apresenta diversas vantagens, incluindo a possibilidade de estudar a comunicação entre vários tipos de células. Neste sentido, este trabalho focou-se na adaptação de células tipo-hepatócito (HLCs), derivadas de células estaminais mesenquimais da matriz do cordão umbilical (hnMSCs), a estes dispositivos e na avaliação do metabolismo energético destas células.

Neste trabalho, conseguimos adaptar o processo de diferenciação hepático ao dispositivo de microfluídica e manter HLCs funcionais até duas semanas. Verificou-se ainda a manutenção das suas atividades de biotransformação de fase I e de fase II, capacidade de armazenamento de glicogénio, presença de marcadores hepáticos (CK-18, ALB, HNF-4α, OATP-C e MRP-2) e produção de ureia e albumina, ao longo deste período. Além disto, as HLCs apresentaram níveis de expressão de genes envolvidos na glicólise/lipogénese (*PDK4*), gluconeogénese (*PEPCK* e *G6PASE*), metabolismo de ácidos gordos (*PPARA*) e de ácidos biliares (*FXR* e *CYP7A1*) e biogénese mitocondrial (*PGC-1A)* com tendência semelhante à observada a nível fisiológico, em resposta à insulina e ao glucagon.

Concluindo, foi possível adaptar e manter HLCs funcionais num dispositivo de microfluídica, mantendo as suas características ao longo do tempo em paralelo com a capacidade de resposta a estímulos hormonais. Deste modo, é possível futuramente utilizar estas células em estudos de interação celular nestes dispositivos de microfluídica.

Palavras-chave: Células tipo-hepatócito; Dispositivo de microfluídica; Insulina; Glucagon; Síndrome metabólico

Abstract

The metabolic syndrome, or insulin resistance syndrome, affects approximately one quarter of the world population. Three cell types are involved in its pathophysiology: adipocytes, myofibroblasts and hepatocytes. Therefore, it is crucial to understand the role of cell-to-cell interactions in the development of this disease. The use of microfluidic devices has several advantages including the possibility to study the communication between different cell types. Thus, this work focused on the adaptation of hepatocyte-like cells (HLCs), derived from human umbilical cord matrix-derived mesenchymal stem cells, to a microfluidic device, and to evaluate HLCs energy metabolism.

Herein, we were able to adapt the hepatic differentiation procedure to the microfluidic device and to maintain functional HLCs up to two weeks. Moreover, part of the hepatic differentiation process was successfully adapted to the microfluidic device. Maintenance of phase I and II biotransformation activities, glycogen storage, presence of hepatic markers (CK-18, ALB, HNF-4α, OATP-C and MRP2) and urea and albumin production were observed throughout this period. Most importantly, HLCs expressed genes regarding glycolysis and lipogenesis (*PDK4*), gluconeogenesis (*PEPCK* and *G6PASE*), fatty acid oxidation (*PPARA*), bile acid metabolism (*FXR* and *CYP7A1*) and mitochondrial function and biogenesis (*PGC-1A*) with similar trend to that observed in a physiologic context, in response to insulin and glucagon, and adapt their metabolism to fasting.

To conclude, it was possible to obtain functional HLCs of human origin in a microfluidic device that maintained its characteristics throughout culture time protocol. Moreover, the cells were capable of responding to insulin and to glucagon and to adapt their metabolism to fasting, setting up the roads for the possibility of using these cells to study cell-to-cell interactions in this microfluidic device.

Keywords: Hepatocyte-like cells; Insulin; Glucagon; Microfluidic devices; Metabolic syndrome

Index

List of Figures

Figure 11 - PAS staining of HLCs at D27 and D34, maintained in MM and DM revealed glycogen storage ability throughout culture time. The controls used were hnMSCs, rpHep and HLCs cultured in DM at D34 incubated with amylase. rpHep was used as a positive control. Scale bar = 100 µm.
Abbreviations: hnMSCs (undifferentiated human neonatal mesenchymal stem cells); rpHep (rat primary hepatocytes); MM (maintenance medium); DM (differentiation medium); D27, D34 (day 27, day 34 of the differentiation protocol)

Figure 12 - Immunocytochemical staining revealed the presence of specific hepatic markers: HNF-4α, ALB, OATP-C, MRP2 and CK-18 in HLCs maintained in both media, at D27 and D34. Cell nuclei were counterstained with DAPI. Scale bar = 50 µm.
Abbreviations: MM (maintenance medium); DM (differentiation medium); D27, D34 (day 27, day 34 of the differentiation protocol); HNF-4α (hepatocyte nuclear factor-4α); ALB (albumin); OATP-C (organic anion-transporting polypeptide-C); MRP2 (multidrug resistance protein 2); CK-18 (cytokeratin-18).

Figure 13 - Effect of culture time and medium composition on Phase I and II activities: a) EROD, b) ECOD and c) UGT activities. Data is represented as Average ± SEM (n=2-4). Undifferentiated hnMSCs and HepG2 cell line, rpHeps and cryopreserved hpHep are negative and positive controls, respectively (white bars). *, **, *** Significantly differs among the controls with $p < 0.05$, $p < 0.01$ and $p < 0.001$, respectively.
Abbreviations: rpHep (rat primary hepatocytes); hpHep (human primary hepatocytes); hnMSC (undifferentiated human neonatal mesenchymal stem cells); MM (maintenance medium); DM (differentiation medium); D27, D34 (day 27, day 34 of the differentiation protocol); EROD (7-ethoxyresorufin-O-deethylase); ECOD (7-ethoxycoumarin-O-deethylase); UGTs (uridine 5'-diphosphate glucuronosyltransferases).

Figure 14 - Genes used for energy metabolism study divided by metabolic pathways: glycolysis and lipogenesis, gluconeogenesis, fatty acid metabolism, bile acid metabolism and mitochondrial biogenesis and function.
Abbreviations: *PDK4* (pyruvate dehydrogenase kinase 4); *SREBP-1C* (Sterol regulatory element-binding protein 1-c); *CHREBP* (Carbohydrate response element binding protein); *GLUT1* (glucose transporter 1); *PEPCK* (phosphoenolpyruvate carboxylase); *G6PASE* (glucose-6-phosphatase); *PPARA* (peroxisome proliferator-activated receptor α); *CPT1A* (carnitine palmitoyltransferase 1 α); *ACOX1* (acyl-CoA oxidase 1); *FXR* (farnesoid X receptor); *CYP7A1* (cytochrome P450 enzyme cholesterol 7α-hydroxylase); *PGC-1A* (peroxisome proliferator γ-activated receptor coactivator 1-α); *PGC-1B* (Peroxisome proliferator γ-activated receptor coactivator 1-β); *ERRA* (Estrogen-related receptor α); *NRF1* (nuclear respiratory factor 1); *CYTC* (cytochrome C).

Figure 15 – Gene expression in HLCs throughout culture time in MM and DM regarding a) glycolysis and lipogenesis; b) gluconeogenesis; c) fatty acid metabolism; d) bile acid metabolism and **e) mitochondrial biogenesis and function.** The graphs represent HLCs' evolution in MM and DM relative to 8h-fasting at D34. Data is represented as Average ± SEM (n=2-6). *, **, *** Significantly differs from the different media composition and the days of differentiation with $p < 0.05$, $p < 0.01$ and $p < 0.001$, respectively.
Abbreviations: D27 (day 27 of the differentiation protocol); D34 (day 34 of the differentiation protocol), MM (maintenance medium), DM (differentiation medium); *PDK4* (pyruvate dehydrogenase kinase 4); *GLUT1/SLC2A1* (glucose transporter 1/solute carrier family 2 member 1); *PEPCK* (phosphoenolpyruvate carboxylase); *G6PASE* (glucose-6-phosphatase); *PPARA* (peroxisome proliferator-activated receptor α); *CPT1A* (carnitine palmitoyltransferase 1 α); *ACOX1* (acyl-CoA oxidase 1); *FXR* (farnesoid X receptor); *CYP7A1* (cytochrome P450 enzyme cholesterol 7α-hydroxylase); *PGC-1A* (peroxisome proliferator γ-activated receptor coactivator 1-α); *PGC-1B* (peroxisome proliferator γ-activated receptor coactivator 1-β); *ERRA* (estrogen-related receptor α); *NRF1* (nuclear respiratory factor 1); *CYTC* (cytochrome C).

Figure 16 – HLCs' adaptive response to fasting at D34. **Gene expression of specific genes of a) glycolysis and lipogenesis, b) gluconeogenesis, c) fatty acid metabolism, d) bile acid metabolism and e) mitochondrial biogenesis and function.** The graphs represent the fold induction of HLCs in response to 8h- and 10-fasting relative to MM. Grid lines represent fold induction equal to 0.8 and 1.2. Data is represented as Average ± SEM (n=2-6). *, **, *** Significantly differs from the different media composition and the days of differentiation with $p < 0.05$, $p < 0.01$ and $p < 0.001$, respectively. $^{\#}$, $^{\#\#}$, $^{\#\#\#}$ Significantly induced or repressed expression with $p < 0.05$, $p < 0.01$ and $p < 0.001$, respectively.
Abbreviations: *PDK4* (pyruvate dehydrogenase kinase 4); *SREBP-1C* (sterol regulatory element-binding protein 1-c); *CHREBP1* (carbohydrate response element binding protein); *GLUT1/SLC2A1* (glucose transporter 1/solute carrier family 2 member 1); *PEPCK* (phosphoenolpyruvate carboxylase); *G6PASE* (glucose-6-phosphatase); *PPARA* (peroxisome proliferator-activated receptor α); *CPT1A* (carnitine palmitoyltransferase 1 α); *ACOX1* (acyl-CoA oxidase 1); *FXR* (farnesoid X receptor); *CYP7A1* (cytochrome P450 enzyme cholesterol 7α-hydroxylase); *PGC-1A* (peroxisome proliferator γ-activated receptor coactivator 1-α); PGC-1B (Peroxisome proliferator γ-activated receptor coactivator 1-β); *ERRA* (estrogen-related receptor α); *NRF1* (nuclear respiratory factor 1); *CYTC* (cytochrome C).

Figure 17 – Gene expression in HLCs in response to insulin and glucagon regarding a) glycolysis and lipogenesis and b) gluconeogenesis. Grid lines represent fold induction equal to 0.8 and 1.2. Data is

represented as Average ± SEM (n=2-6). *, **, *** Significantly differs from the different media composition and the days of differentiation with $p < 0.05$, $p < 0.01$ and $p < 0.001$, respectively. #, ##, ### Significantly induced or repressed expression with $p < 0.05$, $p < 0.01$ and $p < 0.001$, respectively.
Abbreviations: HLCs (hepatocyte-like cells); hpHep (human cryopreserved hepatocytes); *PDK4* (pyruvate dehydrogenase kinase 4); *SREBP-1C* (sterol regulatory element-binding protein 1-c); *CHREBP1* (carbohydrate response element binding protein); *GLUT1/SLC2A1* (glucose transporter 1/solute carrier family 2 member 1); *GLUT2/SLC2A2* (glucose transporter 2/solute carrier family 2 member 2); *PEPCK* (phosphoenolpyruvate carboxylase); *G6PASE* (glucose-6-phosphatase).

Figure 18 – Gene expression in HLCs in response to insulin and glucagon regarding a) fatty acid metabolism, b) bile acid metabolism and c) mitochondrial biogenesis and function. Grid lines represent fold induction equal to 0.8 and 1.2. *, **, *** Significantly differs from the different media composition and the days of differentiation with $p < 0.05$, $p < 0.01$ and $p < 0.001$, respectively. #, ##, ### Significantly induced or repressed expression with $p < 0.05$, $p < 0.01$ and $p < 0.001$, respectively.
Abbreviations: HLCs (hepatocyte-like cells); hHeps (human cryopreserved hepatocytes), *PPARA* (peroxisome proliferator-activated receptor α); *CPT1A* (carnitine palmitoyltransferase 1 α); *ACOX1* (acyl-CoA oxidase 1); *FXR* (farnesoid X receptor); *CYP7A1* (cytochrome P450 enzyme cholesterol 7α-hydroxylase); *PGC-1A* (peroxisome proliferator γ-activated receptor coactivator 1-α); *PGC-1B* (peroxisome proliferator γ-activated receptor coactivator 1-β); *ERRA* (estrogen-related receptor α); *NRF1* (nuclear respiratory factor 1); *CYTC* (cytochrome C).

Figure 19 – HLCs morphology at D17 and the change from a fibroblast-like shape to a polygonal shape throughout the day of inoculation, in the microfluidic device: a) HLCs before trypsinization (scale bar = 500 µm); **b) HLCs 20 minutes after device inoculation** (scale bar = 500 µm); **c) HLCs 1 hour after device inoculation** (scale bar = 500 µm); **d) HLCs 2 hours after device inoculation** (scale bar = 100 µm).

Figure 20 - HLCs' morphology throughout culture time in the MD: **a) HLCs at D27 in MM** (scale bar = 500 µm); **b) HLCs at D27 in DM** (scale bar = 100 µm); **c) HLCs at D34 in MM** (scale bar = 100 µm); **d) HLCs at D34 in DM** (scale bar = 100 µm).

Figure 21 - Effect of culture time on a) urea and **b) albumin production HLCs cultured in MM and DM at D27 and D34.** Data is represented as Average ± SEM (n=4-5). Undifferentiated hnMSCs and HepG2 cell line, rpHeps and hpHeps are negative and positive controls, respectively (white bars). *, **, *** Significantly differs among the controls with $p < 0.05$, $p < 0.01$ and $p < 0.001$, respectively.
Abbreviations: rpHep (rat primary hepatocytes), hpHep (human primary hepatocytes) and hnMSC (undifferentiated human neonatal mesenchymal stem cells), MM (maintenance medium), DM (differentiation medium); D27 (day 27 of the differentiation protocol); D34 (day 34 of the differentiation protocol).

Figure 22 - Evolution in gene expression of HLCs in the microfluidic device and in plates throughout culture time, in a) MM and **b) DM.** The graphs represent the fold induction regarding gene expression of HLCs in MM and DM at D34 relative to D27. Grid lines represent fold induction equal to 0.8 and 1.2. Data is represented as Average ± SEM (n=2-4). *, **, *** Significantly differs from the different media composition and the days of differentiation with $p < 0.05$, $p < 0.01$ and $p < 0.001$, respectively. #, ##, ### Significantly induced or repressed expression with $p < 0.05$, $p < 0.01$ and $p < 0.001$, respectively.
Abbreviations: MD (microfluidic device); MM (maintenance medium); DM (differentiation medium); *PDK4* (pyruvate dehydrogenase kinase 4); *PEPCK* (phosphoenolpyruvate carboxylase); *G6PASE* (glucose-6-phosphatase); *PPARA* (peroxisome proliferator-activated receptor α); *CPT1A* (carnitine palmitoyltransferase 1 α); *ACOX1* (acyl-CoA oxidase 1); *FXR* (farnesoid X receptor); *CYP7A1* (cytochrome P450 enzyme cholesterol 7α-hydroxylase); *PGC-1A* (peroxisome proliferator γ-activated receptor coactivator 1-α).

Figure 23 - Comparison of microfluidic devices relative to plates in a) MM and **b) DM, in both days.** The graphs represent the fold induction of HLCs cultured in MD relative to plates. Grid lines represent fold induction equal to 0.8 and 1.2. Data is represented as Average ± SEM (n=2-4). *, **, *** Significantly differs from the different media composition and the days of differentiation with $p < 0.05$, $p < 0.01$ and $p < 0.001$, respectively. #, ##, ### Significantly induced or repressed expression with $p < 0.05$, $p < 0.01$ and $p < 0.001$, respectively.
Abbreviations: MD (microfluidic device); MM (maintenance medium); DM (differentiation medium); *PDK4* (pyruvate dehydrogenase kinase 4); *PEPCK* (phosphoenolpyruvate carboxylase); *G6PASE* (glucose-6-phosphatase); *PPARA* (peroxisome proliferator-activated receptor α); *CPT1A* (carnitine palmitoyltransferase 1 α); *ACOX1* (acyl-CoA oxidase 1); *FXR* (farnesoid X receptor); *CYP7A1* (cytochrome P450 enzyme cholesterol 7α-hydroxylase); *PGC-1A* (peroxisome proliferator γ-activated receptor coactivator 1-α).

Figure 24 - Gene expression levels in HLCs cultured in the microfluidic device or in 2D static cultures in a) D27 and b) D34. Fold induction of gene expression in HLCs cultured in MM relative to HLCs cultured in DM. Grid lines represent fold induction equal to 0.8 and 1.2. Data is represented as Average ± SEM (n=2-4). *, **, *** Significantly differs from the different media composition and the days of differentiation with $p < 0.05$, $p < 0.01$ and $p < 0.001$, respectively. #, ##, ### Significantly induced or repressed expression with $p < 0.05$, $p < 0.01$ and $p < 0.001$, respectively.

Abbreviations: MD (microfluidic device); MM (maintenance medium); DM (differentiation medium); *PDK4* (pyruvate dehydrogenase kinase 4); *PEPCK* (phosphoenolpyruvate carboxylase); *G6PASE* (glucose-6-phosphatase); *PPARA* (peroxisome proliferator-activated receptor α); *CPT1A* (carnitine palmitoyltransferase 1 α); *ACOX1* (acyl-CoA oxidase 1); *FXR* (farnesoid X receptor); *CYP7A1* (cytochrome P450 enzyme cholesterol 7α-hydroxylase); *PGC-1A* (peroxisome proliferator γ-activated receptor coactivator 1-α).

List of Abbreviations

2D	Two-dimensional cell culture
4-MU	4-methylumbeliferone
5-AZA	5-azacytidine
α-MEM	Minimum essential medium Eagle with alfa modification
ABC	Adenosine triphosphate-binding cassete
ACC	Acetyl-CoA carboxylase
ACOX1	Acyl-CoA oxidase 1
ADME	Absorption, distribution, metabolism and excretion
ADP	Adenosine diphosphate
AFP	α-fetoprotein
Akt	Protein kinase B
ALB	Albumin
AMP	Adenosine monophosphate
ATP	Adenosine triphosphate
BA	Bile acids
BM	Basal medium
bmMSC	Bone marrow mesenchymal stem cells
BMP	Bone morphogenic protein
BSA	Bovine serum albumin
BSEP	Bile salt export pump
cAMP	Cyclic adenosine monophosphate
CAR	Constitutive activated receptor
CD	Cluster of differentiation
cDNA	Complementary deoxyribonucleic acid
ChREBP	Carbohydrate response element binding protein
CoA	Coenzyme A
CPT1	Carnitine palmitoyltransferase 1
CREB	cAMP response element-binding protein
CK	Cytokeratin
CYP450	Cytochrome P450 superfamily
CYP7A	Cytochrome P450 enzyme cholesterol 7α-hydroxylase
CytC	Cytochrome C
DAPI	4',6-diamidino-2-phenylindole
DM	Differentiation medium
DMSO	Dimethyl sulfoxide
ECOD	7-ethoxycoumarin-O-deethylase
EGF	Epidermal growth factor
EROD	7-ethoxyresorufin-O-deethylase
ERR	Estrogen-related receptors

F6P	Fructose-6-phosphate
FA	Fatty acid
FAD	Flavin adenine dinucleotide
$FADH_2$	Flavin adenine dinucleotide (reduced form)
FBS	Fetal bovine serum
FGF	Fibroblast growth factor
Foxa	Forkhead box
FXR	Farnesoid X receptor
G6P	Glucose-6-phosphate
G6Pase	Glucose-6-phosphatase
GATA	GATA binding factor
GCK	Glucokinase
GLUT	Glucose transporter
GSTs	Glutathione transferases
HBSS	Hank's balanced salt solution
HepaRG	Human hepatoma cell line
HepG2	Human hepatoma cell line
HGF	Hepatocyte growth factor
Hhex	Hematopoietically-expressed homeobox protein
HLA-DR	Human leukocyte antigen - antigen D related
HLC	Hepatocyte-like cells
HNF-4α	Hepatocyte nuclear factor 4α
hnMSCs	Human umbilical cord matrix mesenchymal stem cells-derived
hnMSCs-HLCs	Hepatocyte-like cells derived from hnMSCs
IMDM	Iscove's modified Dulbecco's medium
iPSCs	Induced pluripotent stem cells
ITS	Insulin-transferrin-selenium
Klf	Krüppel-like family of transcription factors
LCFA	Long-chain fatty acids
L-PK	Liver pyruvate kinase
MD	Microfluidic device
MM	Maintenance medium
MSCs	Mesenchymal stem cells
NAD^+	Nicotinamide adenine dinucleotide
NADH	Nicotinamide adenine dinucleotide (reduced form)
NADPH	Nicotinamide adenine dinucleotide phosphate (reduced form)
NEAA	Non-essential amino acids
NRF	Nuclear respiratory factor
OATPs	Organic anion-transporting polypeptides
OATs	Organic anion transporters

OCT	Organic cation transporters
Oct	Octamer transcription factor
OSM	Oncostatin M
PAS	Periodic acid Schiff
PBS	Phosphate buffered saline
PDC	Pyruvate dehydrogenase complex
PDK	Pyruvate dehydrogenase kinase
PKA	Protein kinase A
PEPCK	Phosphoenolpyruvate carboxylase
PFA	Paraformaldehyde
PFK-2/FBP-2	6-phosphofructo-2-kinase/fructose-2,6-bisphosphatase
PGC-1α -1β	Peroxisome proliferator γ-activated receptor coactivator 1-α 1-β
PPARα	Peroxisome proliferator-activated receptor α
P/S/A	Penincilin/streptomicin/ amphotericin B
PXR	Pregnane X receptor
qRT-PCR	Quantitative real-time polymerase chain reaction
rpHep/hpHep	Rat primary hepatocytes/human primary hepatocytes
RT	Room temperature
SCD	Stearoyl-CoA desaturases
SEM	Standard error of the mean
SHP	Small heterodimer partner
SLCA2	Solute carrier family 2
SM	Starvation medium
SOX	Sex determining region Y (Sry)-related high mobility group (HMG)-box
SREBP	Sterol regulatory element-binding protein
STM	Septum transversum mesenchyme
SULTs	Sulfotransferases
TAG	Triacylglycerol
TCA	Tricarboxylic acid
UCP	Uncoupling protein
UGTs	Uridine 5’-diphosphate glucuronosyltransferases
VLDL	Very low density lipoproteins

I. Introduction

I. 1. Liver Function and Structure

Liver is an important organ that regulates the metabolism of the whole body and homeostasis. It is located under the lower ribs, in the right-hand side and weights between 1.2 and 1.6 kg [1]. Upon food digestion in the gastrointestinal tract, glucose, amino acids and fatty acids are absorbed into the bloodstream and through the portal vein circulation system, before reaching the liver [2]. The hepatic artery provides nutrients and oxygen while the portal vein carries substances absorbed by the small intestines. Liver functions include the uptake of nutrients and storage of important molecules, such as glycogen and glucose. The liver is also involved in processes of biotransformation and excretion, through bile secretion, granting its protection role against exogenous and potentially toxic substances [3]. It synthesizes urea as a mean of ammonia detoxification [4] and protein synthesis, such as albumin and coagulant proteins.

The human liver is arranged in 4 lobules composed of 60 % of hepatocytes (parenchymal cells), which represent approximately 80 % of the total liver mass [5]. The non-parenchymal cells (40 %) consist of sinusoidal endothelial cells (form the lining of the blood vessels), a population of macrophages termed Kupffer cells, Ito or stellate cells (fat storing cells), biliary epithelial cells and immune cells, such as lymphocytes and leukocytes [6]. The hepatic acinus is the liver structure of 1-2 mm in length [7], defined as the population of hepatocytes supplied by one portal triad, *i.e.*, a microcirculatory functional unit influenced by the flow of blood from the microcirculation (Figure 1) to the central vein [7].

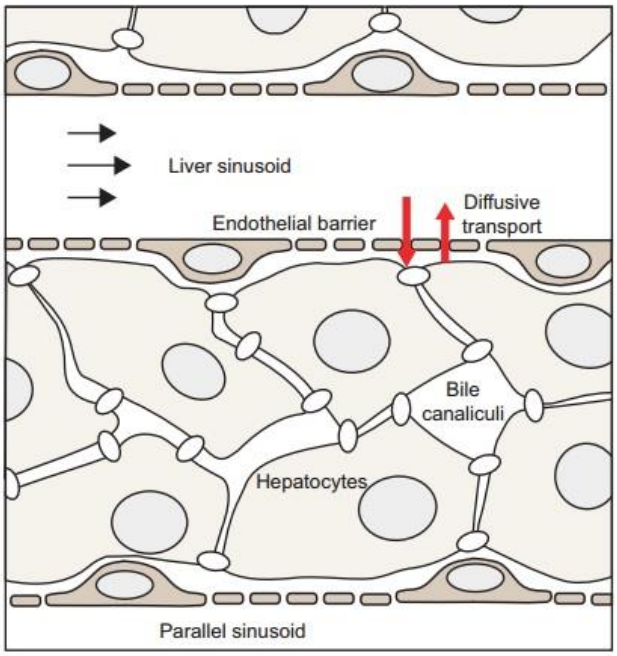

Figure 1 - Cell microenvironment in the liver. Hepatocytes can be in contact with sinusoids, uptaking or secreting substances into the blood, or other hepatocytes through tight junctions, defining bile canaliculi (from Bettinger C, Borenstein JT, Tao SL, 2013) [7].

Hepatocytes are epithelial cells organized into plates that are separated by sinusoids (vascular channels) [5]. Between hepatocytes and endothelial cells is the space of Disse. The blood from the portal vein and hepatic artery mixes together and its subsequent capillaries flows through the space of Disse, where hepatocytes are exposed and are able to extract toxins and nutrients. Ito cells can also be found in the space of Disse. These cells are responsible for the production of collagen. Finally, Kupffer cells are liver macrophages found within the liver sinusoid [5]. These cells can convert heme into bilirubin [8,9].

Mature hepatocytes have a polygonal shape and can be binucleated [10]. They have a polarized organization, forming a cell layer that separates sinusoidal blood from the canalicular bile [11], therefore they contact with two flow systems involving i) uptake, processing and secretion of blood components and ii) synthesis and secretion of bile [12]. Hepatocyte functions such as transformation of carbohydrates; protein, bile salts, phospholipids and cholesterol synthesis; biomolecules storage; modification and excretion of exogenous and endogenous substances make them the most relevant cells for hepatic *in vitro* studies.

I. 1. 1. Biotransformation

In drug development the liver is one of the key organs to be considered since it is highly exposed to xenobiotics due to entrance of compounds directly to portal circulation, contributing to the first pass effect. This effect avoids the systemic exposure to high concentration of xenobiotics, protecting the whole body from potential toxic effects. Most of oral drugs are poorly hydrosoluble to facilitate its absorption. However, in order to be excreted, molecules need to be converted into more hydrophilic species, through a biotransformation process. Thus, hepatocytes present important mechanisms for molecules' biotransformation into metabolites and its elimination. Although more abundant in the liver, biotransformation is a ubiquitously process. It is divided in three different phases. Phase I reactions include oxidation, reduction or hydrolysis resulting in an increase of compound polarity. Most phase I reactions are catalysed by cytochrome P450 (CYP450) enzymes. Phase II reactions allow to conjugate polar compounds to water-soluble groups. These conjugation reactions are mainly performed by uridine 5'-diphosphate-glucuronosyltransferases (UGTs), sulfotransferases (SULTs) and glutathione transferases (GSTs). These derivatives can then be excreted through kidney or bile. Phase III reactions involve active membrane transporters. These transporters can be of two types, namely influx and efflux. Influx transporters are responsible for the uptake of molecules into hepatocytes and are located on sinusoidal/basolateral membrane, comprising OATPs (organic anion-transporting polypeptides particularly important for drug transport), OATs (organic anion transporters) and OCT (organic cation transporters); and efflux transporters relevant for bile secretion, located on canalicular/apical membranes, including members of adenosine triphosphate-binding cassete (ABC), such as multidrug resistance proteins [3]. Liver also regulates glucose homeostasis and there are two important glucose transporters expressed in this organ. GLUT1, in hepatocytes proximal to the hepatic venule, and GLUT2, in hepatocytes' sinusoidal membrane [13]. GLUT1 is expressed in all mammalian cells and is responsible for basal glucose uptake, in the fed state [14].

GLUT2 has a higher K_M and is expressed in hepatocytes, promoting glucose efflux, following gluconeogenesis, in fasted state [13, 14]. Hepatocyte-specific deletion of *GLUT2* blocks glucose uptake but does not affect glucose release in the fed state, suggesting that it can be released through other transporters, such as GLUT1 [2].

Thus, a hepatic *in vitro* model which is competent regarding biotransformation allows to assess therapeutic and toxic profile of a drug candidate.

I. 1. 2. Metabolic Homeostasis

There are several gene pathways regulating the metabolic homeostasis of our body, which are activated or inhibited according to the levels of glucose in the blood that, in a physiologic context, are kept between 4 and 7 mM [15]. Glucose control is crucial since it is the "fuel" for all organs, especially the brain where prolonged hypoglycaemia can cause acute brain damage. On the other hand, hyperglycaemia is a serious consequence of diabetes and the hyperosmolar hyperglycaemic state can be fatal due to electrolyte imbalance and dehydration [15].

Within the human body, glucose concentration is regulated mainly by two pancreatic hormones, insulin and glucagon, with antagonist effects. Insulin is secreted by pancreatic β cells. It is stored in secretory vesicles and is released, according to the intracellular adenosine triphosphate/ adenosine diphosphate (ATP/ADP) ratio that is related to the glucose availability in pancreatic β cells, particularly elevated after feeding. On the other hand, when glucose levels are low, glucagon, which is processed in pancreatic α-cells, and glucocorticoids are released. Glucose is both a substrate and an end product for cells. Therefore, two opposite states need to be considered: high glucose (fed state) and low glucose (fasting or starvation) [15] (Figure 2).

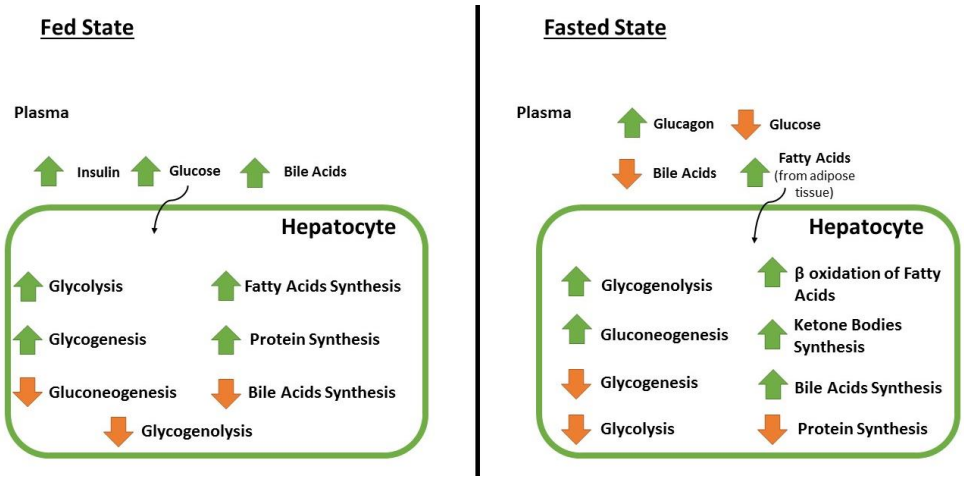

Figure 2 - Overview of the fed/fasted states: the effect in hepatocytes metabolism. The fed state is characterized by insulin release from the pancreatic β cells and glucose uptake. Insulin induces anabolic reactions such as glycogenesis, protein synthesis and fatty acid synthesis. It also induces glycolysis for basal energy expenditures. In the opposite state, the fasted state, glucagon is released by pancreatic α cells and catabolic reactions are induced: glycogenolysis, gluconeogenesis and β oxidation, in order to produce energy. Bile acids are synthesized because a lower amount reaches the liver, through the portal vein, in the fasted state.

In the fed state, nutrients absorbed into the bloodstream (glucose, fatty acids and amino acids) reach the liver through the portal vein. Glucose is converted into pyruvate, through

glycolysis, in the cytoplasm, being oxidized, through the tricarboxylic acid (TCA) cycle and oxidative phosphorylation in the mitochondria, to produce ATP. If energy is not needed, glucose is stored as glycogen or converted into fatty acids and amino acids in the liver. Hepatocytes generate triacylglycerol (TAG) through free fatty acid esterification. TAG is then stored in lipid droplets or secreted as very low density lipoproteins (VLDL), into circulation. Amino acids are used to synthesize proteins, glucose or other biomolecules [2]. These functions are controlled by insulin, which stimulates the uptake of glucose by peripheral tissues, causing a quick removal of glucose from blood. It induces energy storage and anabolic reactions, namely glycogen synthesis (glycogenesis) in liver and muscle, and fatty acid synthesis in liver and adipose tissue, in the fed state [15]. Insulin also stimulates glycolysis and in the liver, insulin blocks glycogenolysis (hydrolization of glycogen to generate glucose) and gluconeogenesis [16].

In the fasted state, fuel substrates are released into the circulation, from the liver, to be metabolized, in peripheral tissues, according to the body's needs. Glucagon release provokes a rise in intracellular cyclic adenosine monophosphate (cAMP), in the liver. Liver provides glucose when nutrients are scarce and the alteration of cAMP levels is the main mechanism by which liver releases glucose in the blood, through the induction of gluconeogenesis and glycogenolysis [17]. β oxidation of fatty acids is unable to produce gluconeogenic substrates. However, it produces ATP, which is necessary for gluconeogenesis. Protein degradation occurs during prolonged starvation, releasing amino acids, which can serve as gluconeogenic substrates [2].

I. 1. 2. 1. Glucose Metabolism - Glycolysis and Gluconeogenesis

Liver selects metabolic fuels (glucose or fatty acids) according to nutrient availability and hormonal signalling.

Glucose enters hepatocytes, via GLUT2 and is phosphorylated by glucokinase (GCK), generating glucose-6-phosphate (G6P). G6P can be used as a precursor for glycogen synthesis, can be metabolized to pyruvate through glycolysis and then enter the TCA cycle to be completely oxidized to generate ATP or it can generate nicotinamide adenine dinucleotide phosphate (NADPH) via the pentose phosphate pathway, required for lipogenesis and biosynthesis of other molecules. In the fasted state, G6P in the endoplasmic reticulum is dephosphorylated by glucose 6-phosphatase (G6Pase), releasing glucose [2].

Glycolysis is mainly controlled by the kinases GCK, 6-phosphofruto-1 kinase (PFK), liver pyruvate kinase (L-PK) and pyruvate dehydrogenase kinases (PDKs) (Figure 3). These enzymes present low levels of activity in the fasted state, increasing in the postprandial state. Insulin and carbohydrates, in the fed state, stimulate the kinase activity of 6-phosphofructo-2-kinase/fructose-2,6-bisphosphatase (PFK-2/FBP-2), inducing the glycolytic pathway [2]. However, insulin suppresses *PDK4*, which is a negative regulator of the mitochondrial pyruvate dehydrogenase complex (PDC), by phosphorylation, thus increasing pyruvate consumption and glycolysis [18]. In fact, fasted PDK4 knockout mice present hypoglycaemia, since PDC activity is increased and pyruvate enters TCA cycle for complete oxidation, thus not being available as a gluconeogenic substrate [19].

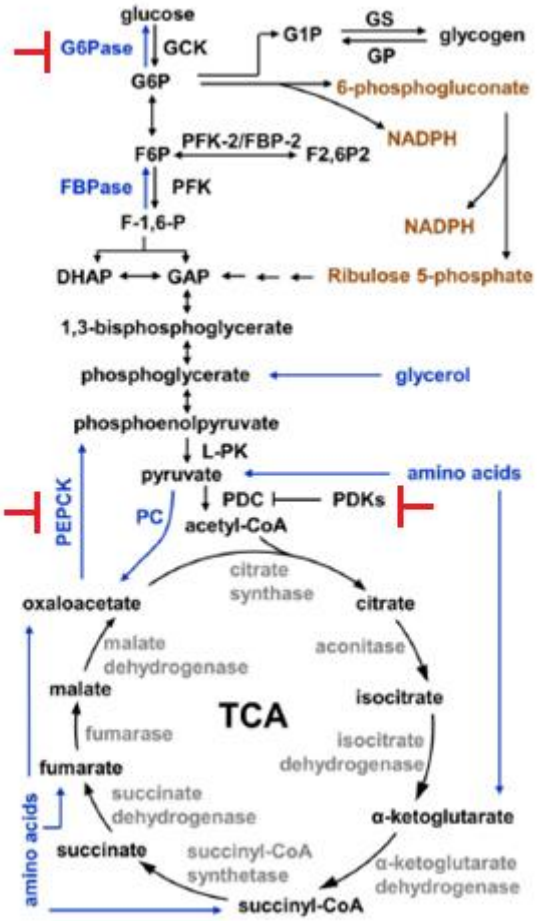

Figure 3 - Glucose Metabolism Pathways. Gluconeogenic pathways are marked in blue, and the pentose phosphate pathway is marked in orange. Insulin inhibits G6Pase, PEPCK and PDKs.
Abbreviations: GCK (glucokinase); G6Pase (glucose-6-phosphatase); G6P (glucose 6-phosphate); G1P (glucose 1-phosphate); GP (glycogen phosphorylase); GS (glycogen synthase); PFK (6- phosphofructo-1 kinase); FBPase (fructose 1,6 bisphosphatase); F-1,6-P (fructose 1,6-biphosphatase); GAP (glyceraldehyde 3-phosphate); DHAP (dihydroxyacetone phosphate); L-PK (liver pyruvate kinase); PC (pyruvate carboxylase); PDC (pyruvate dehydrogenase complex); PDKs (pyruvate dehydrogenase kinases); (adapted from L. Rui 2014) [2].

In short periods of fasting, liver uses glycogenolysis to produce and release glucose. In contrast, during longer periods, after glycogen being depleted, hepatocytes synthesize glucose through gluconeogenesis, using lactate, pyruvate, glycerol and amino acids. Prolonged periods of fasting increase cAMP levels in liver [20]. cAMP response element-binding protein (CREB), a gluconeogenic transcription factor, is activated by protein kinase A (PKA)-mediated phosphorylation, inducing the expression of *G6PASE*, cytoplasmic phosphoenolpyruvate carboxylase (*PEPCK*) and peroxisome proliferator γ-activated receptor coactivator 1-α (*PGC-1A*) [2]. Herein, hepatocytes use other sources for gluconeogenesis, *e.g.* lactate, which can be generated in the liver or delivered from extrahepatic tissues through circulation. Lactate is oxidized to generate pyruvate by lactate dehydrogenase. Afterwards, in the mitochondria, pyruvate is converted to oxaloacetate by pyruvate carboxylase. PEPCK converts cytoplasmic oxaloacetate to phosphoenolpyruvate, which is a key step in gluconeogenesis (Figure 3). Mice

with liver-specific deletion of PEPCK are unable to produce glucose via gluconeogenesis from lactate and amino acids, leading to accumulation of TCA cycle intermediates and hepatic steatosis [21], which demonstrates the role of PEPCK in maintaining equilibrium in fuel substrates. Phosphoenolpyruvate ultimately is converted to fructose-6-phosphate (F6P). F6P generates G6P, which is transported into the endoplasmic reticulum and dephosphorylated by G6Pase to generate glucose (Figure 3). Specific deletion of G6Pase in mice leads to hepatomegaly with glycogen accumulation and steatosis [22], showing the importance of G6Pase in the conversion of glycogen into glucose. PGC-1α was shown to be elevated in the fasted state and in disease models of diabetes and insulin resistance [23], stimulating gluconeogenesis by coactivating hepatocyte nuclear factor 4α (HNF-4α) [20]. This is an interesting fact since it correlates a tissue that is highly enriched in HNF-4α with the primarily place where gluconeogenesis takes place, the liver. Insulin release in response to increasing glucose levels, phosphorylates Akt (or Protein kinase B), stimulates the phosphorylation of PGC-1α and decreases the ability of PGC-1α to activate gluconeogenic genes [24].

I. 1. 2. 2. Fatty Acid Metabolism – Lipogenesis and Fatty Acid Oxidation

In the fed state, when carbohydrates are abundant, glucose is used as the main metabolic fuel whereas the liver uses it to synthesize fatty acids. Carbohydrates provided in meals drive lipogenesis (Figure 4). Pyruvate is the link between glycolysis and lipogenesis, providing a carbon source. Pyruvate can be originated from glucose through glycolysis, converted back to carbohydrates via gluconeogenesis, or to fatty acids through a reaction with acetyl-CoA (lipogenesis). In the mitochondria, pyruvate generates acetyl-coA and oxaloacetate and when these molecules react with each other citrate is formed and is exported to cytoplasm. Citrate is then split into oxaloacetate and acetyl-CoA, being the last carboxylated to form malonyl-CoA. Both malonyl-CoA and NADPH, obtained from the conversion of malate (after reduction of oxaloacetate) into pyruvate by malic enzyme, are precursors of palmitic acid. This is elongated by fatty acyl-CoA elongases, generating long-chain fatty acids (LCFAs – with more than 16-carbon-chain). LCFAs can then produce TAG or unsaturated fatty acids [2].

Fatty acids can also be obtained from the bloodstream, after nutrient absorption or after being released from adipose tissue. Fatty acids are either esterified with glycerol 3-phosphate, generating TAG or, with cholesterol, producing cholesterol esters. These products can be stored in hepatocytes as lipid droplets or released as VLDL into circulation. Fatty acids are also used for phospholipids synthesis that contribute to cell membranes composition [2].

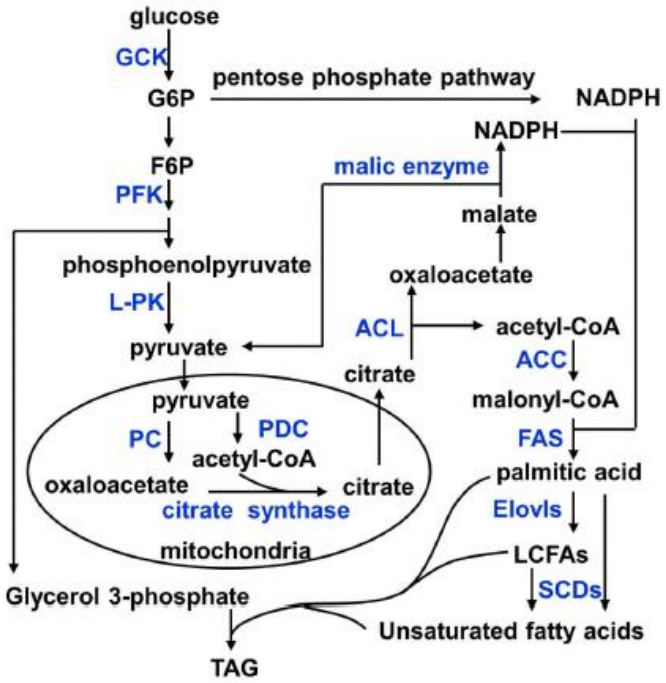

Figure 4 - Lipogenic Pathway. Insulin stimulates the synthesis of TAG and fatty acids.
Abbreviations: GCK (glucokinase); G6P (glucose 6-phosphate); F6P (fructose-6-phosphate); L-PK (liver pyruvate kinase); PC (pyruvate carboxylase); PDC (mitochondrial pyruvate dehydrogenase complex); NADPH (nicotinamide adenine dinucleotide phosphate); ACL (ATP-citrate lyase); ACC (acetyl-CoA carboxylase); FAS (fatty acid synthase); Elovls (fatty acyl-CoA elongases); LCFAs (long-chain fatty acids); SCDs (stearoyl-CoA desaturases); TAG (triacylglycerol); (from L. Rui, 2014) [2].

Transcriptional factors and coregulators of glycolytic and lipogenic genes are important for the control of these pathways. Carbohydrate response element binding protein (ChREBP) stimulates the expression of lipogenic genes (*e.g.* malic enzyme) [25]. An isoform of the sterol regulatory element-binding protein (SREBP) family of transcription factors, SREBP-1c, is responsible for the insulin-dependent increase in gene expression of lipogenic enzymes required for fatty acid and triglyceride synthesis [25].

In the fed state, insulin stimulates i) hepatic lipogenesis, inducing SREBP-1c [26] and ii) glycolysis, thus providing lipogenic precursors. Insulin induces PGC-1α phosphorylation by Akt, impairing the ability of PGC-1α to stimulate β oxidation [24].

On the other hand, β oxidation is induced in the fasted state, which provides energy for hepatocytes and ketone bodies, serving as substrates to be metabolized in peripheral tissues. Glucagon interacts with peroxisome proliferator-activated receptor α (PPARα) [27], the main regulator of β oxidation and promotes it both in mitochondria and peroxisomes (Figure 5). In fact, deletion of PPARα in mice showed a massive lipid accumulation in the liver, hypothermia, hypoglycaemia and elevated plasma levels of free fatty acid [28], impairing fatty acid oxidation. PGC-1α is also a coactivator of PPARα [29]. β oxidation takes place in the mitochondria, thus LCFAs must be translocated from cytoplasm. This transport is mediated by carnitine palmitoyltransferase 1 (CPT1), which is inhibited by malonyl-CoA [2], a rate-limiting step in this pathway.

Nevertheless, PGC-1β is reported to have opposite effects. Some authors state that it is another PPARα coactivator and its liver-specific overexpression increases the expression of β oxidative genes [30] while other authors observed that the expression *PGC-1B* in the liver induces hepatic lipogenesis, increasing TAG synthesis and VLDL secretion [31]. In fact, whole-body ablation of *PGC-1B* in mice resulted in impaired mitochondrial function and hepatic steatosis [32]. Acyl-CoA oxidase (ACOX) is a rate-limiting enzyme of β oxidation in peroxisomes, being targeted by PPARα [33]. ACOX null mice result in hepatic steatosis [34].

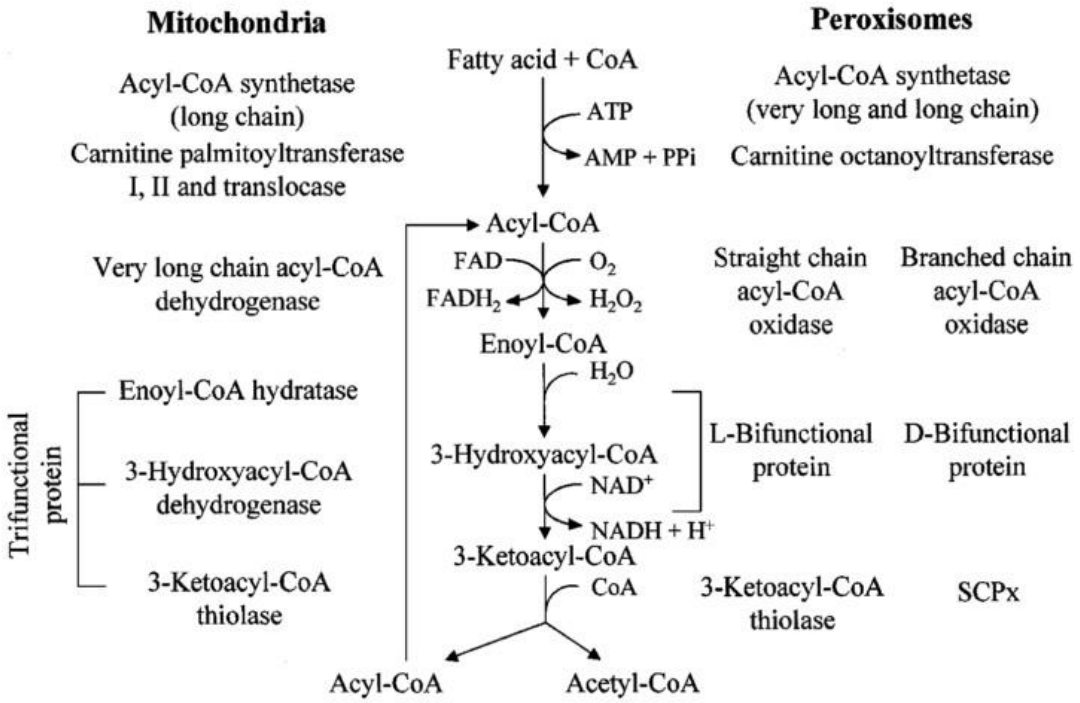

Figure 5 – Mitochondrial and peroxisomal β oxidation pathways. Fatty acid oxidation is induced in the fasted state. The end products are acyl-CoA and acetyl-CoA.
Abbreviations: ATP (adenosine triphosphate); AMP (adenosine monophosphate); PPi (inorganic pyrophosphate); FAD (flavin adenine dinucleotide); $FADH_2$ (FAD reduced form); NAD^+ (nicotinamide adenine dinucleotide; NADH (reduced form of nicotinamide adenine dinucleotide); SCP_X (sterol carrier protein x); (from Reddy et al, 2001) [35].

I. 1. 2. 3. Bile Acid Metabolism

Bile acids regulate cholesterol homeostasis and contribute to the digestion and lipid absorption. Cholesterol is an essential component of membranes and a precursor for steroids and bile acid synthesis whose uptake is performed in the intestine through lipoprotein particles, designated as chylomicrons. Such particles consist of triglycerides, phospholipids, cholesterol and proteins. After the delivery of TAG to peripheral tissues, the cholesterol remnants of chylomicrons reach the liver where they are used for bile acid synthesis or incorporated in VLDL, which are redirected to blood circulation. When cholesterol is in excess, its conversion into bile acids is increased to allow its elimination (in the faeces). An important part of the bile acids pathway is the enterohepatic cycle, which consists on its secretion into the gut, followed by reabsorption in the small intestine and redelivery to the liver, avoiding the loss of these energy-

costly molecules, cholesterol and bile acid derivatives. 90 % of bile acids are reabsorbed in the intestine and return to the liver. Therefore, in the fed state, high amounts of bile acids reach the liver through the portal vein. Upon starvation, there is a decrease in the levels of circulating bile acids [36]. On the other hand, when there is cholesterol demand, *de novo* synthesis occurs in liver and intestine [15].

The synthesis of bile acids consists in a series of enzymatic reactions which take place in the liver and contribute to the conversion of the hydrophobic cholesterol to a more water-soluble molecule. The first and rate-limiting step in the bile synthesis pathway is that catalysed by the cytochrome P450 enzyme cholesterol 7α-hydroxylase (CYP7A) [37]. The size of the bile acid pool is controlled tightly, in a feedback system [37]. Farnesoid X receptor (FXR) senses bile acids and it responds by inhibiting its synthesis [15], since its accumulation beyond a certain level becomes cytotoxic [37]. FXR downregulates a CYP7A isoform, CYP7A1, limiting liver bile acid accumulation [37].

In rat hepatocytes, insulin was shown to negatively regulate FXR gene expression [38]. On CYP7A1, insulin was shown to have a dual effect. Physiological insulin concentrations rapidly induce *CYP7A1* expression while prolonged insulin treatment represses it [39]. However, there is no consensus regarding bile acids regulation by PGC-1α. There are reports that FXR is induced by PGC-1α [40,41] and the latter is elevated in fasting conditions, stimulating gluconeogenesis. Therefore, *CYP7A1* expression is decreased due to inhibition by FXR. On the other hand, some authors claim that PGC-1α interacts with *CYP7A1* promoter [36]. Thus, after prolonged fasting, *CYP7A1* transcription increases and this may help to prepare the gastrointestinal tract for absorption of fats in a future meal [36].

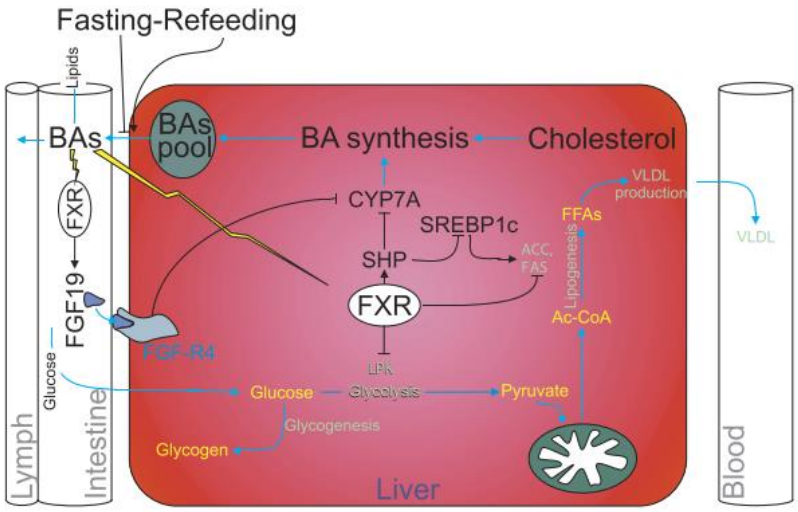

Figure 6 - Roles of FXR and CYP7A1 during fasting and refeeding. In the postprandial state, bile acids are released from gallbladder into the gut to facilitate lipid absorption. Carbohydrates, such as glucose, and bile acids are reabsorbed and reach hepatocytes, through the portal vein. When bile acids enter hepatocytes, FXR is activated to inhibit their synthesis by repressing CYP7A.
Abbreviations: FXR (farnesoid X receptor); BAs (bile acids); SHP (small heterodimer partner); CYP7A (cholesterol 7α-hydroxylase); Ac-CoA (acetyl-CoA); FFAs (free fatty acids);VLDL (very low density proteins); LPK (L-pyruvate kinase); SREBP (sterol regulatory element-binding protein); ACC (acetyl-CoA carboxylase); FAS (fatty acid synthase); FGF (fibroblast growth factor); (from Lefebvre et al, 2009) [42].

I. 2. Metabolic Syndrome

The International Diabetes Federation estimates that a quarter of the adults worldwide suffers from metabolic syndrome. This disease increases the heart attack risk by 2-fold with an associating 3-fold higher mortality. It represents a higher risk of developing cardiovascular diseases and the risk of developing type II diabetes is five times higher in diseased people, compared with healthy people [43].

The metabolic syndrome is a combination of obesity, dyslipidaemia (elevation of triglycerides in plasma), insulin resistance and hypertension, which are interrelated [44]. The main mechanism of its pathophysiology is insulin resistance (metabolic syndrome is also known as insulin resistance syndrome) where liver, skeletal muscle and adipose tissue cells become progressively less sensitive to insulin. Ultimately, glucose absorption no longer occurs [43]. The cause for insulin resistance is an increase in circulating free fatty acids, released from an expanded mass of adipose tissue. These free fatty acids decrease insulin-mediated glucose uptake in muscle tissue, leading to a reduction in insulin sensitivity. Insulin resistance results in hyperinsulinaemia, as a compensation mechanism for the defect in insulin action to maintain a normal level of blood glucose, which is elevated since it is not removed by the cells. The lack of insulin action causes failure to suppress gluconeogenesis in the liver and to mediate glucose uptake in muscle and adipose tissue, causing glucose intolerance. The pancreatic β cells, responsible for the production of insulin, become worn out. Once the pancreas reaches a state where it can no longer produce enough insulin, high glucose levels are observed in the blood (hyperglycaemic) and type II diabetes is diagnosed. In the liver, free fatty acids increase the production of TAG, glucose and secretion of VLDL [43]. Since insulin, under a physiologic state, should stimulate glycogen synthase in the fed state [2], in a pathologic situation, in the liver, glucose conversion to glycogen is reduced and lipid accumulation through TAG is increased. In fact, insulin has an antilipolytic function but when insulin resistance occurs, insulin can no longer act as antilipolytic and there is an increased level of lipolysis of triacylglycerol in the adipose tissue, producing even more fatty acids. This may create further lipolysis due to additional inhibition of the antilipolytic effect of insulin. Therefore, hypertriglyceridemia is an important criterion for the diagnosis of the metabolic syndrome since it reflects insulin resistance. Other characteristic presented in the metabolic syndrome is dyslipidaemia [44], *i.e*., there is an increase in secretion of VLDL into the systemic circulation due to increased free fatty acid flux to the liver. Hypertension is another symptom in people with metabolic syndrome, since insulin is a vasodilator in people with normal weight. It also affects the reabsorption of sodium in the kidneys. When insulin resistance occurs, insulin loses its vasodilatory effects but the effect on renal reabsorption of sodium continues. In addition, the increase of fatty acids in circulation can cause vasoconstriction, all leading to hypertension [44].

Abdominal obesity and increased waist circumference are key causative factors of the metabolic syndrome, according to the International Diabetes Federation [43]. However, there are also people with normal weight who can be metabolically obese, presenting increased amount of visceral adipose tissue. This type of adipose tissue is related with a higher flux rate of fatty acids

to the liver, through the splanchnic circulation, while abdominal fat is related with the release into the systemic circulation of lipolysis products.

I. 3. Stem Cells

Stem cells are an important resource for biomedical applications due to their ability to continuously self-renew in culture (maintaining its undifferentiated state), to differentiate into distinct cell types, and to secrete several molecules such as immunomodulatory factors [45,46]. These cells can be divided into embryonic, fetal, neonatal and adult, according to their origin. Other possible categorization of stem cells is the division through their differentiation potential: totipotent (can give rise to an entire organism), pluripotent (the epiblast which is capable of giving rise to cells from the three germ layers, through gastrulation, such as mesoderm, endoderm and ectoderm), multipotent (which can only differentiate into cells from a particular germ layer) and unipotent cells (which can only differentiate into one cell type). Embryonic stem cells present a pluripotent potential. However, the access to these cells poses ethical, technical and legal concerns. More recently, Yamanaka et al [47] were able to generate induced pluripotent stem cells (iPSCs), with a combination of four transcription factors: Oct3/4, Sox2, Klf4 and c-Myc. iPSCs may be derived from somatic tissues of patients and allows the use of human cells with the same genetic makeup as the patients. However, the reprograming protocols still have very low yields [48]. iPSCs also present safety issues regarding teratoma formation and genetic stability [49].

An alternative source of stem cells is the umbilical cord. This source does not raise such ethical issues, since after birth this tissue was discarded [50]. It contains mesenchymal stem cells, hematopoietic stem cells, which are more primitive than those found in bone marrow or in adipose tissue [51].

I. 4. Mesenchymal Stem Cells (MSCs)

Mesenchymal stem cells (MSCs) are a subset of multipotent stem cells that can be isolated from fetal blood, liver and bone marrow [52], adult bone marrow [53], amniotic fluid and placenta [54], adipose tissue [55], peripheral blood [56], umbilical cord blood [57] and umbilical cord matrix [58, 59].

The International Society for Cellular Therapy defined the following parameters for the characterization of MSCs: plastic-adherence when in culture; expression of CD105, CD73 and CD90 surface markers and lack of the expression of CD45, CD34, CD14 or CD11b, CD79α or CD19 and HLA-DR. Finally, since they are considered to be multipotent, they should be able to differentiate into mesodermal lineages derivatives, such as adipocytes, chondrocytes and osteoblasts [60].

MSCs were firstly harvested from bone marrow (bmMSC) [61] which are the most well studied source of MSCs. However, the harvesting constitutes an invasive procedure with low yields. Neonatal tissues such as placenta and umbilical cord blood or matrix have awakened interest due to its more primitive origin and non-invasive method of harvesting. Neonatal MSCs,

in particular, present less of donor variability compared with other sources of MSCs due to donor age, clinical history or lifestyle. By analysing MSC karyotype during the culture process, it was concluded that MSCs maintained a normal karyotype, as oppose to embryonic stem cell lines, which accumulated mutations [62]. When comparing MSC recovery from umbilical cord blood with umbilical cord matrix, results showed that the latter is a richer source of MSC, the isolation efficiency is higher and the growth kinetics are higher as well, compared with bmMSCs [63].

Furthermore, the presence of early endodermal markers in MSCs derived from the umbilical cord matrix such as GATA-4 and HNF-4α allows to hypothesize that these cells may undergo endoderm-specific differentiation, possibly originating liver cells [62] and not only adipocytes, chondrocytes and osteoblasts. Most importantly, transcription factors important for the liver development (GATA-6, SOX9 and SOX17) and liver progenitor markers (DKK1, DPP4, DSG2, CX43 and K19) were demonstrated to be higher expressed in this type of MSCs compared with other MSC sources [58]. These results provide evidence that human umbilical cord matrix could be a promising MSC source to generate hepatocyte-like cells (HLCs) for *in vitro* applications, such as disease modelling, drug screening, toxicological studies and, ultimately, regenerative medicine applications.

I. 5. Deriving human hepatocyte-like cells (HLCs) from stem cells by mimicking liver embryogenesis

There are several sources of hepatocytes that can be used in *in vitro* models, such as the use of primary hepatocytes (either from human or animal sources), *post-mortem* tissues or immortalized cell lines. The use of primary hepatocytes poses problems due to its availability and, once in culture, there is a decrease in expansion capacity and rapid loss of functionality [6]. On the other hand, *post-mortem* tissues usually only represent the late-stage characteristics of pathology progression. Animal models are also frequently used in studies but they fail to describe efficiently the human body complexity and raise obvious ethical issues. Immortalized cell lines (*e.g.* HepG2) have a great expansion capacity. However, these lines are derived from tumours and may contain genetic and metabolic abnormalities. Thus, they do not represent accurately liver physiology. These drawbacks demonstrate the need for reliable physiological hepatic models for biomedical applications or pharmaceutical industry. Stem cells are a fundamental source for these purposes due to its ability to self-renew and differentiate into mature cells [6].

Hepatocyte differentiation has been described from human bmMSCs [64, 65], MSCs derived from human adipose tissue [66] and MSCs derived from human umbilical cord matrix (hnMSCs) [67]. *In vitro* stem cell differentiation aims at mimicking embryonic organogenesis. Thus, liver development can be divided into four stages: i) endoderm induction; ii) foregut and hepatic competence induction; iii) hepatoblast and liver bud formation and iv) differentiation of hepatoblast into hepatocyte. These steps involve the interaction of multiple signalling pathways and other developing structures of the embryo. The differentiation protocols include mainly the addition of cytokines and growth factors.

During gastrulation, the definitive endoderm emerges as a sheet of cells from the anterior end of the primitive streak. Endoderm forms the primitive gut which is subdivided into foregut, midgut and hindgut [68]. Liver originates from the ventral foregut endoderm [69].

Nodal is an important signalling pathway for the pattern formation and differentiation processes during gastrulation, stimulating the expression of a group of endoderm transcription factors (*e.g.* SOX17 and Foxa1-3), in a concentration-dependent manner where high doses of Nodal induce endoderm [70]. Endoderm starts to acquire the shape of a gut tube epithelium, surrounded by mesoderm. This new structure is further patterned into foregut, midgut and hindgut. Foregut is a precursor of the liver and expresses the transcription factor Hhex [68]. *In vitro*, this phase is mimicked by exposure to fibroblast growth factor (FGF) and epidermal growth factor (EGF), which induce *Hhex* gene expression [71,72]. Regarding Wnt/β-catenin signalling, the correct temporal sequence is essential for liver development. During gastrula, low levels of β-catenin are observed in the anterior endoderm and are important to maintain foregut identity. However, later in development, Wnt and FGF signalling promote hepatic development, having the opposite effect [73]. The developing heart and septum transversum mesenchyme (STM) release FGF and bone morphogenic protein (BMP) respectively, inducing hepatic fate in the ventral foregut endoderm [74,75]. The first sign of the embryonic liver is the hepatic diverticulum. After hepatic fate commitment by FGF and BMP signals, hepatoblasts begin to express liver markers (Hhex, GATA-4 and GATA-6) and there is a transition in the hepatic epithelium from a columnar to a pseudostratified epithelium, promoted by the homeobox gene *Hhex* [76]. The hepatic epithelium is surrounded by a laminin rich basement membrane and endothelial precursors, embedded in the STM. At this point, basal lamina breaks down. Hepatoblasts form the liver bud, invading the STM [68]. Liver bud then becomes the major fetal hematopoietic organ since it is vascularized and colonized by hematopoietic cells, inducing a period of fast tissue growth. Liver genes, such as *HNF-4A*, albumin (*ALB*), cytokeratin19 (*CK-19*) and α-fetoprotein (*AFP*) are expressed shortly after hepatic specification [68]. STM and hepatic mesenchyme promote hepatoblast proliferation and survival through secretion of FGF, BMP, retinoic acid and hepatocyte growth factor (HGF) [71,77–79]. In order to promote *in vitro* hepatoblast formation, HGF combined with insulin-transferrin-selenium (ITS), nicotinamide and dexamethasone are added to cell culture medium since they are liver-specific factors reported to act synergistically [80].

Hepatoblasts are bipotent cells. They can either differentiate into hepatocytes or into biliary epithelial cells. These cells express genes associated with both adult hepatocytes (*HNF-4A*, *ALB*, and cytokeratin-18, *CK-18*) and biliary epithelial cells (*CK-19*). Hepatoblasts in contact with the portal vein increase *CK-19* expression while those which are not in contact with portal veins differentiate into mature hepatocytes [68]. Hematopoietic cells in liver, during mid-gestation produce a cytokine called oncostatin M (OSM), which promotes hepatocyte differentiation. OSM also induces the expression of *G6PASE* and glycogen accumulation [81]. HGF, which originally appeared in serum of partially hepatectomized rats, was shown to stimulate proliferation of adult hepatocytes, being an important factor for liver regeneration [81]. OSM and HGF, along with dexamethasone and Wnt, promote the expression of *ALB* and *HNF-4A* [68]. It was shown that

dexamethasone induces hepatocyte maturation, suppressing growth while HGF and EGF are associated with cells at the intermediate hepatoblast phase. Dexamethasone, in the absence of HGF and EGF, induces exclusively hepatocyte maturation [82].

The use of epigenetic modifiers combined with growth factors has also been attempted in differentiation protocols. Epigenetic modifiers produce changes in genome function without changing the DNA sequence. In the differentiation protocol used in this work two epigenetic modifiers have been used: dimethyl sulfoxide (DMSO) and 5-azacytidine (5-AZA). DMSO [$(CH_3)_2SO$] is an amphipatic molecule with two apolar domains and one polar domain, being soluble in both aqueous and organic media [83]. DMSO was previously shown to induce hepatic differentiation of mesenchymal stem cells and fetal liver stem/progenitor cells [84–86]. The mechanism by which it induces hepatic differentiation is not fully understood but some authors associate it to histone hyperacetylation-inducing effects [87] which facilitates DNA transcription [88]. Chetty et al studied DMSO in order to improve pluripotent stem cell differentiation [89]. It was shown that DMSO, by activating a regulator of the G1 phase of the cell cycle, the retinoblastoma protein, increases the competency of pluripotent stem cells to respond to differentiation signals, across all germ layers [89]. G1 phase has been associated with a differentiated status [90]. 5-AZA is a cytidine analogue which inhibits DNA methylation and has also been reported to induce hepatic differentiation from mesenchymal stem cells [91, 92]. It is a potent inhibitor of DNA-cytosine methyltransferases [93]. The inhibition of DNA methylation increases the expression of genes in a selective environment, which is the combination of small molecules used in the differentiation medium. 5-AZA was the first hypomethylating compound to be approved by the U.S. Food and Drug Administration to treat myelodysplastic syndrome. Cells must be in a proliferative in order to allow this cytidine analogue to be incorporated into the DNA [94].

I. 6. Microfluidic Devices

The use of MSCs-derived HLCs is an important breakthrough for liver studies, since, it does not involve the use of immortalized cell lines or animal models. Thus, it contributes to create models that resemble human biology more closely and that better predict the efficacy and safety of new drugs. Ultimately it contributes for implementing the principle of the 3R's: methods that replace the use of animal models (replacement); methods that minimise the number of animals used in an experiment (reduction); and methods that improve animal welfare (refinement) [95].

Two-dimensional (2D) models were already proven to fail to predict living tissue behaviours because they do not mimic *in vivo* cellular organization, do not involve interaction with other cell types and do not present media flows as what happens *in vivo* [6,96]. Microfluidic devices are now being used for *in vitro* applications due to its low reactant consumption, the possibility of modelling important aspects of microenvironment, such as creating dynamic flows and, according to its design, it can add an extra level of physiologic complexity, *e.g.* by allowing co-culture of different types of cells. These devices are a possibility to overcome the limitations of current methods, introducing the organ-on-a-chip concept. It combines biology and engineering to improve control over experimental conditions thus exploring techniques to control substrate

feature size, shape and topography on the same scale (µm or nm) that cells experience within our body [97]. Microfluidics, due to ability to create flows, can be especially useful when studying pharmacokinetics and pharmacodynamics. Pharmacokinetics (PK) refers to the movement of a drug within the body overtime, involving absorption, distribution, metabolism and excretion (ADME) [98]. A reported physiologically based pharmacokinetic model has separate compartments, representing different organs, connected by blood circulation. This will allow to predict the concentration profile of a drug and its metabolites [99]. Pharmacodynamics (PD) is related to how the body processes the drug [100]. It can predict the pharmacological effect of a drug at the target site [99]. A microfluidic device combining PK and PD was created, by Sung JH et al, representing liver (using HepG2), marrow and tumour [99].

Hepatocytes are mostly considered for *in vitro* drug toxicity testing and disease modelling. Together with the possibility of creating dynamic interactions between compounds and hepatocytes and between hepatocytes and other types of cells, brought by the use of microfluidic devices, the necessary characteristics for a relevant *in vitro* model are created. Microfluidic devices can provide a dynamic medium flow similar to blood circulation. There are reports of a microfluidic design which allows the culture of primary human and rat hepatocytes, mimicking mass transport features of the human liver sinusoid [101]; a microfluidic culture system which can predict hepatic clearance (a relevant pharmacokinetic parameter to be considered in drug discovery) [102]; a microfluidic device which allows to study interactions between hepatocytes receiving or not receiving HGF (important for liver injury studies, immunology and developmental biology) [103]; drug-metabolism studies using a microfluidic hepatic co-culture platform [104]; and modelling of nonalcoholic fatty liver disease in a microfluidic device [105]. Regarding multiple cellular interactions, there are microfluidic devices designed for culturing different cell types, creating the called multi-organ-chip [106]. TissUse is a German company that developed a platform allowing different cell types to be in contact through media flow [107]. Maschmeyer et al [106,108] developed multi-organ-chips that included liver (using HepaRG cell line), intestine, skin and kidney equivalents [106,108], mainly created to assess systemic toxicity of drugs. These devices contain a support with temperature control and micro-pumps, which provides a pulsatile fluid flow. However, these complex features require expertise while working and make them expensive. Nevertheless, the main advantages of using a microfluidic culture system is the possibility of creating medium flow, becoming closer to the *in vivo* conditions, and the bigger control of cell disposition and architecture. Therefore, these culture systems would be an interesting approach to study cell-to-cell interactions that can be regulated by secreting cellular factors or direct contact. Besides, cell–cell interaction within same or different cell types is another essential part of microenvironment making these devices important candidates for studying the metabolic syndrome where the interaction between liver cells, adipocytes and myofibroblasts is essential.

The microfluidic device herein adopted was the Xona Microfluidics Standard Neuron Device, mainly used in neuroscience field, allowing the fluidic isolation of axons and dendrites [109]. Despite not having pumps for a more controlled fluid flow, these devices are rather simple to use and can be adapted to other cell types. Herein, we adapted the HLCs differentiation process and

culturing to this device in order to enable further tests with one of the other cell lines involved in the metabolic syndrome. In fact, in the future, with some modifications, these platforms will possibly allow the culture of different cell types, in the context of the metabolic syndrome.

I. 7. Motivation and Aims

The metabolic syndrome is a combination of risk factors, such as dyslipidaemia, insulin resistance and hypertension, commonly associated with type II diabetes, which increase the probability of having cardiovascular problems [43, 110]. Therefore, the economic burden caused by these health problems needs to be considered specially, because there is a prediction that the incidence of diabetes will double by 2025, along with the cardiovascular-related illness [43]. In 2003, it was estimated that for the 25 European Union countries the total direct health care costs of diabetes in people between 20 and 79 years old represented 7.2 % of the total healthcare expenditures for these countries (64,9 thousand millions international dollars) [43].

Metabolic syndrome's pathophysiology involves the interaction of different organs, namely, liver, adipose tissue and skeletal muscle. The novelty brought by the microfluidic devices is that it allows to study interactions between different cell types with control of fluid flow, similar to the blood [111]. These characteristics allow *in vitro* studies to better mimic what happens *in vivo*. In the context of the metabolic syndrome, the possibility of studying crosstalk between cells is of particular interest, namely crosstalk between hepatocytes and the other two cell types. The increased release of free fatty acids from an expanded mass of adipose tissue induces insulin resistance, causing the glucose homeostasis dysregulation [43]. The lack of insulin sensitivity in the liver fails to suppress gluconeogenesis, increasing glucose production; reduces glycogen synthesis and increases the production of TAG and VLDL secretion [43]. Therefore, to fully understand the mechanisms underlying metabolic syndrome, hepatocytes have a relevant role and studying its behaviour is of utmost importance.

Regarding hepatic *in vitro* studies, the maintenance of primary hepatocytes in culture is difficult due to its phenotypic instability over culture time; whereas the availability of human samples is scarce [6]. To overcome these limitations, cell lines may be an alternative, since they are highly available and present a stable phenotype [6]. However, most hepatocyte cell lines may contain genetic abnormalities are derived from tumours and do not present the same drug-metabolizing characteristics of human hepatocytes [6]. Therefore, there is still the demand for functional hepatocyte sources of human origin. HLCs, derived from stem cells, can be an alternative. hnMSCs represent an ethically acceptable, widely available and safe source, compared to embryonic stem cells [45,46,62]. Furthermore, there are reports showing that MSCs derived from the umbilical cord present early endoderm markers and that they express transcription factors related to liver development and liver progenitor markers [59,63].

Based on such information, the major objective of this thesis was to adapt HLCs derived from hnMSCs to a microfluidic device that would enable the *in vitro* study of the metabolic syndrome. Traditionally, hepatocytes' culture medium has high concentrations of dexamethasone and insulin, which are necessary to induce a more mature phenotype [80]. However, these interfere

with glucose homeostasis [112]. Additionally, the collagen coating used in the differentiation process is of a gel type [86], which may present drawbacks such as the formation of clots of micrometres' order within the channels of the microfluidic device. In this context, we firstly adapted the HLCs to both a new medium with lower concentrations of dexamethasone and insulin and to a new collagen coating.

Secondly, since insulin and glucagon control blood glucose levels and the energy metabolism of hepatocytes, we studied HLCs' response to the stimuli of these two hormones, through gene expression. In addition, HLCs' adaption to fasting was also studied. Lastly, we aimed to maintain HLCs in this microfluidic device up to two weeks to demonstrate whether these could be used in this type of cell culture for further studies regarding the metabolic syndrome.

In sum, the specific questions addressed in this thesis were:

1. Do HLCs in a thin collagen coating and cultured in a medium with lower concentration of insulin and dexamethasone maintain their biotransformation activity, the presence of hepatic markers, glycogen storage, urea and albumin production throughout culture time?
2. Are HLCs able to respond to insulin and glucagon stimuli and fasting, altering their energy metabolism accordingly?
3. Can we maintain HLCs in microfluidic devices over a reasonable culture time, allowing the development of an alternative *in vitro* HLC-based culture model for further mechanistic studies?

II. Materials and Methods

II. 1. Reagents

Cell culture supplements were purchased from Lonza, unless otherwise stated. Trypsin-EDTA, fetal bovine serum (FBS), insulin-transferrin-selenium solution (ITS), non-essential amino acids supplement (NEAA), rat-tail type I collagen and human insulin were purchased from Gibco®/Life Technologies. 7- ethoxyresorufin and 7-ethoxycoumarin were purchase from Alfa Aesar. Hepatocyte growth factor (HGF), fibroblast growth factors (FGF-2 and FGF-4) and oncostatin-M (OSM) were purchased from Peprotech. Finally, Iscove's modified Dulbecco's medium (IMDM), alpha modified Eagle's medium (α-MEM), epidermal growth factor (EGF), dexamethasone, DMSO, nicotinamide, 5-AZA, trypan blue, periodic acid, Schiff's reagent, Mayer's hematoxylin, amylase, Hank's balanced salt solution (HBSS), 4-methylumbelliferone (4-MU), β-glucuronidase/arylsulfatase, resorufin, amphotericin B and glucagon were acquired from Sigma-Aldrich®.

II. 2. Cell Culture

hnMSCs were isolated as described by Miranda et al [45] and Santos et al [46] and expanded as undifferentiated cells in α-MEM supplemented with 10 % of FBS (growing medium). Briefly, cell expansion consisted on passages every 2-3 days, when a 70-80 % confluence was reached. HepG2 cells (purchased from ATCC (HB-8065; American Type Culture Collection (ATCC) were cultured in α-MEM supplemented with 10 % FBS, 1 mM of sodium pyruvate and 1 % NEAA. Cryopreserved human primary hepatocytes (hpHeps; pool of 10 donors) were purchased from Invitrogen™ (Carlsbad, CA, USA; HEP10, A12176), thawed on cryopreserved hepatocyte recovery medium (CHRM; CM7000, Invitrogen™) and manipulated according to manufacturer instructions. Rat primary hepatocytes (rpHeps) were isolated from Wistar rats 3- to 6-month old, weighting 200 to 400 g, obtained from Charles River Laboratories and cultured according to Miranda et al [113]. Prior to each experiment, the animals were kept in a separate cage for at least 24 hours, with *ad libitum* access to food and water. All applicable institutional and governmental regulations concerning the ethical use of animals were followed, according to the European guidelines for the protection of animals used for scientific purposes (European Union Directive 2010/63/EU) and the Portuguese Law nº 113/2013. Cell cultures of hnMSCs, HepG2, hpHeps and freshly isolated rpHeps were maintained at 37 °C in a humidified atmosphere with 5 % CO2 in air. Cell viability was assessed through trypan blue exclusion method.

II. 3. Collagen Coating

Rat-tail collagen and commercial rat-tail collagen were used in this work. The protocol for rat-tail extraction was based on Rajan et al [114]. Briefly, rat-tails were washed twice in 70 % ethanol prior to skin removal using surgical material. Tendon fibres were pulled out, separated from bone and cartilaginous tissue and suspended in PBS. Fibres were then washed three times and

immersed for 1 hour in 70 % EtOH before being transferred into 0.1 % acetic acid and stirred during 48 hours at 4 °C, for fibre acid digestion. The solution was centrifuged at 16000x*g* for 90 minutes at 4ºC. The supernatant was collected, lyophilized and the resultant solid stored at -80° C until further use.

The extracted rat-tail collagen was dissolved in 0.1 % acetic acid to a stock concentration of 1 mg/mL. The stock solution was diluted in PBS to 0.2 mg/mL in a volume that assures total culture surface coverage. After 1-hour incubation at 37 ºC, cell culture surfaces were washed with PBS before inoculation. The differentiation process occurred using this collagen coating until day 17 and onwards for energy metabolism studies in well plates.

Coating with commercial type I collagen was used for the microfluidic device and in parallel for the cover glasses (VWR®) in 24-well plates. Commercial collagen at a stock concentration of 3 mg/mL was diluted in 0.1 % acetic acid to a final concentration of 0.2 mg/mL. This collagen was used from day 17 onwards. Coating was performed with three overnights to guarantee the formation of a collagen film throughout the culture surface. Collagen was allowed to polymerize each overnight. The device and the well plates were washed three times with PBS and before inoculation, the microfluidic device was washed three times with warmed IMDM and was left at the incubator for medium equilibration.

II. 5. Hepatocyte Differentiation Protocol

The differentiation protocol was performed as described in Cipriano et al [86,96]. hnMSCs were seeded at a density of $1.5x10^4$ cells/cm^2 in plates coated with rat-tail collagen, reaching a cell confluency of 90 % within 24 hours after inoculation. A three-step differentiation protocol (Figure 7) was applied using IMDM with 1 % penicillin-streptomycin-amphotericin B (P/S/A) as basal medium (BM). Briefly, the first step consisted in a 48-hour incubation of BM with 2 % FBS, 10 ng/mL of EGF and 4 ng/mL of FGF-2, for endoderm commitment and foregut induction. In the second step, cells were maintained for 10 days in BM supplemented with 10 ng/mL of FGF-4, 4 ng/mL of FGF-2, 20 ng/mL of HGF, 1 % ITS and 0.61 g/L of nicotinamide, to induce hepatoblast and liver bud formation. At day 10 of differentiation (D10), 1 % DMSO was added. In the third step, at D13, BM was supplemented with 8 ng/mL of OSM, 1 µM of dexamethasone, 1 % DMSO and 1 % ITS, defined as differentiation medium (DM). At D17, as a proliferative step, cells were trypsinized, re-inoculated and maintained in this culture medium supplemented with 20 µM of 5-AZA. At D21, cells could be maintained in DM or changed to maintenance medium (MM), which was BM supplemented with 8 ng/mL of OSM, 100 nM of dexamethasone, 1 % DMSO, 1 nM of insulin and 0.2 % bovine serum albumin (BSA). The concentrations of dexamethasone, insulin and BSA used in MM were based on Estal et al [115]. HLCs culture was maintained up to D34.

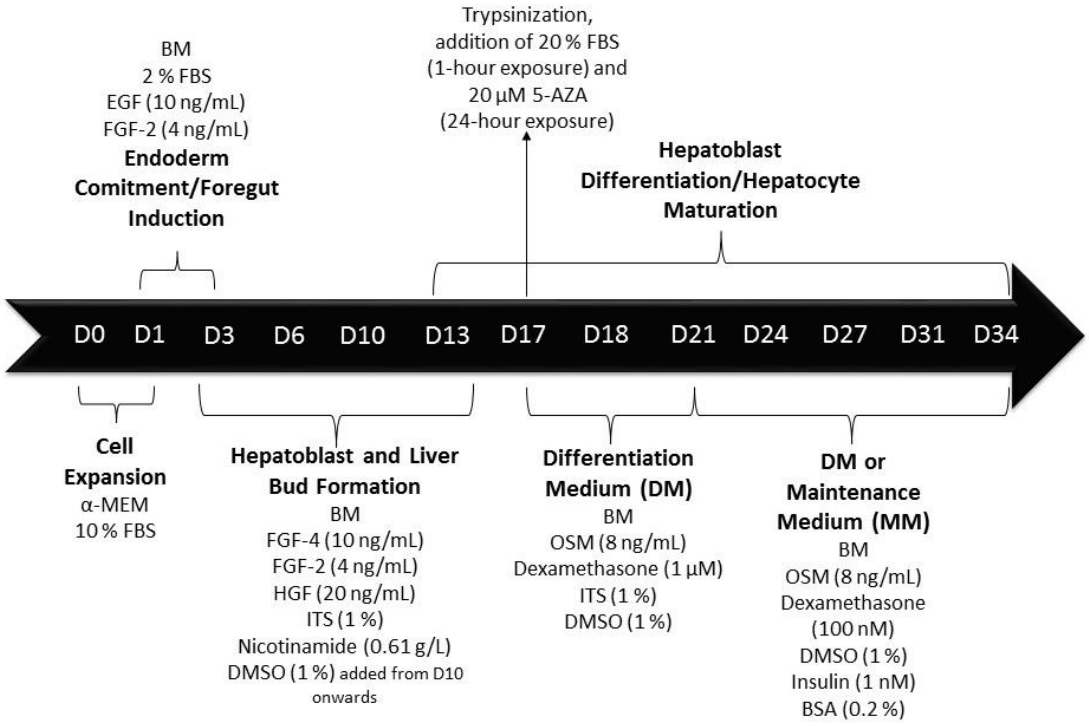

Figure 7 - Hepatocyte Differentiation Protocol. This protocol consisted in three steps: endoderm commitment/foregut induction, hepatoblast and liver bud formation and hepatoblast differentiation/hepatocyte maturation.
Abbreviations: BM (basal medium); FBS (fetal bovine serum); EGF (epidermal growth factor); FGF (fibroblast growth factor); HGF (hepatocyte growth factor); ITS (insulin-transferrin-selenium); DMSO (dimethyl sulfoxide); OSM (oncostatin M); BSA (bovine serum albumin); D0 – D34 (day 0-34 of the differentiation protocol).

II. 6. HLCs Response to Insulin/Glucagon Stimuli

The hormone stimuli assays were performed at D34, as described on Figure 8. Before the insulin stimuli, cells culture medium was changed from MM to starvation medium (SM: DMEM, 1 % P/S, 4 mM of glutamine, 1 % DMSO, 8 ng/mL of OSM and 0.2 % BSA), for an incubation period of 2 hours, to enhance the response to insulin incubation, as described in Correia et al [116].

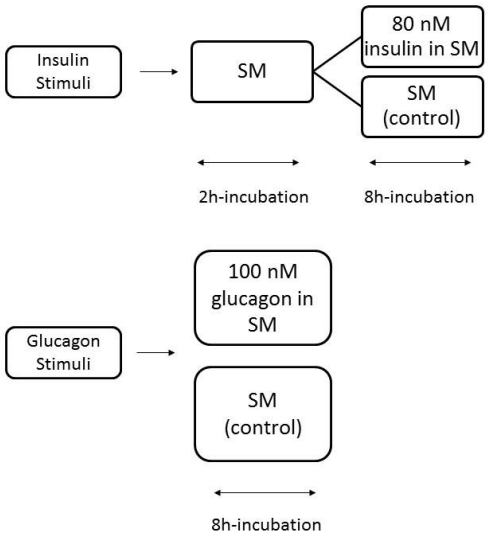

Figure 8 - Insulin and glucagon stimuli protocol. In the insulin stimuli, a 2-hour exposure to SM was performed followed by an 8h-incubation with 80 nM of insulin in SM. Negative control was performed in parallel in which cells were maintained in SM. In the glucagon stimuli, an 8-hour exposure to 100 nM of glucagon in SM was performed. Negative control was performed in parallel in which cells were maintained in SM.
Abbreviations: SM (starvation medium).

II. 7. Microfluidic Device Set-up

II. 7. 1. Set-up

The device herein used was the Xona Microfluidics Standard Neuron Device (SND150) with a 150 µm microgroove barrier. The device is made of polydimethylsiloxane (PDMS) and has four wells and two channels connected by microgrooves, as presented on Figure 9. The wells are 8 mm in diameter. The main channel is 7 mm long. The smaller channels (connecting the wells to the main channel) are 2.07 mm long. All the channels are 100 µm in height and 1.5 mm wide.

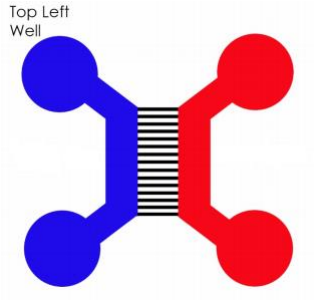

Figure 9 - Microfluidic Device Diagram (from Xona Microfluidics) [109]. This microfluidic device is composed of two channels, allowing the communication between two wells, each. Microgrooves connect the two channels.

The cover glasses (VWR®) used for plasma bonding were firstly submitted to a cleaning procedure consisting on sonication in a water bath for 30 minutes, being rinsed in distilled water, followed by rinsing in 70 % ethanol and three times rinsing in distilled water. As a sterilization procedure, the cover glasses were allowed to dry in a laminar flow hood cabinet, under ultraviolet (UV) light exposure. The next step was to place both the microfluidic device and the cover glass

into a Plasma Cleaner (Harrick Plasma) for plasma bonding procedure, for about 1 minute, at 300 mTorr. The channels were filled with 70 % ethanol until the microfluidic device was used. A cleaned glass slide was placed on top of the chambers to avoid liquid evaporation. The devices were stored at 4 º C, up to 5 months. Before use, the microfluidic channels were washed with water to remove the ethanol.

II. 7. 2. HLCs inoculation

At D17 of differentiation, a suspension containing $7.5x10^4$ cells was centrifuged, at 200x*g* for 5 minutes, and resuspended in 10 µL of DM containing 20 % FBS, in order to inoculate one microfluidic channel. After 1 hour, when most of the cells were adherent, 100 µL of the same DM was added to each one of the four wells to allow further cell adhesion. Up to 1 hour later, 200 µL of DM without FBS containing 20 µM 5-AZA, as a proliferative step, was added to each one of the wells. In parallel, 24-well plates were inoculated at a seeding density of 30 000 cells/cm^2.

II. 8. Quantitative Real-Time Polymerase Chain Reaction (qRT-PCR)

Total RNA was isolated from samples with 0.15-1.0 million of cells using Trizol® (Life Technologies) according to manufacturer instructions and quantified by measuring absorbance at 260 nm using LVis Plate mode (SPECTROstar Omega, BMG Labtech, Ortengerg, Germany). 260/280 nm and 230/280 nm ratios were used as purity measurements for protein and solvent presence, respectively, considering ratios between 1.8-2.2.

cDNA was synthesized from 0.5-1 µg RNA using NZY First-Strand cDNA Synthesis kit (NZYTech) according to the manufacturer instructions. Quantitative real time PCR was performed using PowerUp™ SYBR® Green Master Mix (Life Technologies) which was prepared for a final reaction volume of 15 µL, using 2 µL of template cDNA and 0.333 µM of forward and reverse primers (Table A in chapter VI). Annexes presents the specific primers used in this work. The reaction was performed on 7300 Real-Time PCR System (Applied Biosystems®/ Life Technologies) consisting of a denaturation step at 95 °C for 10 minutes, 40 cycles of denaturation at 95 °C for 15 seconds, annealing at 60 °C for 1 minute and extension at 72 °C for 30 seconds. A dissociation stage was added to determine the melting temperature (Tm) of a single nucleic acid target sequence as a quality and specificity measure. The comparative Ct method ($2^{-\Delta\Delta Ct}$) was used to quantify gene expression, which was normalized to a reference gene (β-actin).

II. 9. Histology

II. 9. 1. Periodic Acid Schiff's (PAS) Staining

Cultured cells were washed with PBS and fixed with 4 % paraformaldehyde (PFA; Sigma-Aldrich®) in PBS at room temperature (RT), for 15 minutes. One sample was incubated with amylase for 15 minutes at 37 ºC allowing to distinguish between positive and unspecific staining since it digests glycogen. Cell surface was oxidized with 1 % Periodic Acid (Sigma-Aldrich®) in water for 10 minutes. A washing step with distilled water for 5 minutes was followed by incubation with Schiff's reagent for 15 minutes. Cells were washed again and counterstained with Mayers'

hematoxylin (Sigma-Aldrich®). The wells were rinsed with distilled water and were observed under light microscope (Olympus CK30 inverted microscope).

II. 9. 2. Immunocytochemistry

For immunocytochemistry staining adherent cells were, firstly, washed with PBS and fixed with 4 % PFA and 4 % sucrose in PBS, at RT, for 15 minutes. The next step was permeabilization with 0.3 % Triton-100 in PBS, for 15 minutes at RT. Afterwards, blocking buffer containing 2.5 % BSA, 2 % FBS in PBS was applied for 30 minutes at RT. Incubation with primary antibody was carried out at 4ºC overnight. The following primary antibodies were used: CK-18 (mouse monoclonal IgG; Santa Cruz Biotechnology®), organic anion-transporting polypeptide-C (OATP-C; mouse monoclonal IgG; Santa Cruz Biotechnology®), multidrug resistance protein-2 (MRP-2; rabbit policlonal IgG; Santa Cruz Biotechnology®), ALB (rabbit polyclonal IgG; Santa Cruz Biotechnology®) and HNF-4α (mouse monoclonal IgG; Perseus Proteomics Inc.). 1h-incubation with secondary antibody was performed at RT. All antibodies were diluted in blocking buffer. The final step was to apply DAPI (Sigma-Aldrich®) and aqua-poly/mount coverslipping medium (Polysciences). The coverslides were observed on an inverted fluorescence microscope (Axiovert 200M, Carl Zeiss) coupled with a monochrome camera (AxioCam MNC, Carl Zeiss). Sample fluorescence was examined in fluorescence at excitation/emission wavelengths of 590/617 nm (goat anti-rabbit Alexa Fluor 594; Life Technologies), 495/519 nm (donkey anti-mouse Alexa Fluor 488; Life Technologies) and 358/461 (DAPI). Images were acquired using AxioVision Rel. 4.7 software.

II. 10. Urea and Albumin Quantification

Urea and albumin were quantified in cell culture supernatants using a colorimetric urea kit (QuantiChrom™ Urea Assay Kit, BioAssay Systems) and ELISA commercial kit (ICL's Human Albumin ELISA kit), respectively. The absorbance was measured at 520 nm for urea and 450 nm for albumin ELISA in a microplate reader (SPECTROStar Omega, BMG Labtech), according to manufacturer instructions. Data is presented as the rate of production: $\mu g/10^6$ cells.h (for urea) and $pg/10^6$ cells.h (for albumin).

II. 11. Biotransformation Activity

Phase I metabolism reactions were assessed by quantification of 7-ethoxyresorufin-O-deethylase (EROD) and 7-ethoxycoumarin-O-deethylase (ECOD) activities. Phase II metabolism reactions were quantified by measuring UGTs activity.

EROD assay allows to assess human CYP1A1 and CYP1A2 [117] activity. The protocol herein used was adapted from Donato et al [118] and consisted in a 90-minutes cell incubation with IMDM containing 8 μM 7-ethoxyresorufin followed by a 2-hour enzymatic digestion with β-glucuronidase/arylsulfatase. The concentration of the product (7-hydroxyresorufin) was measured at an excitation wavelength of 530 nm and an emission of 590 nm.

ECOD activity reflects human CYP2B6, 1A2 and 2E1 activity [117,119]. The protocol consisted on a 90 minutes' cell incubation with 0.8 mM 7-ethoxycoumarin diluted in IMDM. After 2-hour enzymatic digestion with β-glucuronidase/arylsulfatase, liquid-liquid extractions, with chloroform (collecting the organic phase) and a solution of 1.0 M NaCl and 0.1 M NaOH (collecting the aqueous alkaline phase), the concentration of the product (7-hydroxycoumarin) was measured at an excitation wavelength of 340 nm and an emission wavelength of 460 nm.

UGTs activity was determined by cell incubation with 4-methylumbelliferone (4-MU). The substrate was quantified both before and after cell incubation, in order to evaluate the extent of conversion. The protocol was based on Miranda et al. [119]. Briefly, a 1-hour cell incubation with 100 µM 4-MU solution diluted in HBSS was performed. Afterwards, the supernatant was transferred into a 96-well plate and 4 µL of NaOH at 0.1 M was added per well in order to achieve pH = 11. The fluorescence was measured at an excitation wavelength of 340 nm and an emission wavelength of 460 nm.

II. 12. Protein Quantification

Protein concentration was determined by measuring the absorbance at 280 nm, using LVis plate mode (SPECTROstar Omega, BMG Labtech). Total protein was quantified after cell lysis with 0.1 M NaOH solution at 37 °C overnight, stored at -20 ºC for further analysis and used to normalise urea and albumin quantification as well as biotransformation activity.

II. 13. Statistical Analysis

The results are given as the Average ± SEM. Statistical data analysis was performed using PRISM 6.0 (GraphPad Software). The effects on biotransformation activity and the response of HLCs' regarding energy metabolism were evaluated by two-way ANOVA with Tukey's test in order to determine whether the biotransformation activity of each compound was significantly altered by the medium composition over culture time, the effect of medium composition, the effect of fasting and exposure to insulin and glucagon in gene expression and to evaluate differences between groups and controls. $p < 0.05$ was considered statistically significant.

III. Results and Discussion

Metabolic syndrome is a disease commonly associated to type II diabetes and to a higher risk of developing heart problems [43]. It depends on the interaction between different organs such as adipose tissue, skeletal muscle, pancreas and liver. However, further understanding of the role of each organ and the mechanisms leading to this disease is still necessary, namely that of the liver. Human hepatocytes cannot be maintained in culture during a reasonable time in order to allow long-term studies of cellular interaction [6]. Therefore, new hepatocyte models resembling the human physiology are demanded for disease modelling and for the development of new potential therapies. These models seek characteristics closer to the human physiology. Despite immortalized cell lines and animal models being more available those are not the ideal models for these studies. Differentiation protocols of stem cells are being developed and adopted by the scientific community to overcome these drawbacks. Moreover, microfluidic devices can be regarded as an alternative model since these systems allow the study of interactions between different cell types and even the creation of organ-on-a-chip concept [97]. In this study, we attempted to culture HLCs derived from hnMSCs in a microfluidic device (Xona Microfluidics Standard Neuron Device - SND150) and checked their competence for energy metabolism studies.

III. 1. HLCs could be adapted to commercial rat-tail type I collagen coated surfaces

With the ultimate goal of adapting the cells to a microfluidic device, the surface coating was firstly optimized. *In vitro* cultures of epithelial cells, such as hepatocytes, require specialized coating of culture surface with extracellular matrix proteins, namely collagen, contributing to a better attachment and maintenance of differentiated properties [120]. Two types of collagen were used throughout this work: rat-tail type I collagen and commercial type I collagen. Collagen extracted from a rat tail at a laboratory scale does not present the same purity of a commercial collagen submitted to purity controls at an industrial scale. Therefore, the use of commercial collagen as a coating contributes to culture definition and to the development of standard *in vitro* methods. The stock solution of rat-tail collagen and the commercial collagen were diluted in acetic acid. The acid solution allows the fibres to be more flexible [120]. However, at an acidic pH, collagen fibres do not polymerize and this is the reason why acetic acid is used to store collagen, in a liquid form. When pH is raised achieving a value close to the normal physiological level (in our laboratory we used PBS, at pH = 7.45) a thick gel layer is formed [120]. Our group has previously optimized a differentiation protocol for deriving HLCs from hnMSCs and characterized them at morphological, biochemical and biotransformation levels [86,96]. However, the collagen coating used in that protocol was optimized using as coating 0.2 mg/mL of rat-tail collagen diluted in PBS. This coating, although inducing a more polygonal shape in HLCs (data not shown), did not enable a homogeneous cell inoculation in the microfluidic device, since the formed gel clogs the channels. An initial step of coating optimization was performed, using cryopreserved HLCs, to assess which

would be the better commercial collagen concentration. 0.1 mg/mL and 0.2 mg/mL were the concentrations tested, diluted in PBS or 0.1 % acetic acid. HLCs seeded in 0.2 mg /mL of commercial collagen diluted in acetic acid provided better morphology, maintaining its adherence until D34 (data not shown). Therefore, this was the coating used in the microfluidic device and on the maintenance of HLCs'.

III. 2. Different dexamethasone and insulin concentrations do not affect HLCs' biotransformation capacity

Our protocol for deriving and culturing HLCs from hnMSCs [86,96] consists in the use DM (Figure 7) that contains high concentrations of dexamethasone (1 µM) and insulin (1.72 µM). Indeed, as abovementioned, dexamethasone is a glucocorticoid that induces hepatocyte maturation, namely phase I metabolic activity [121]. However, glucocorticoids may cause insulin resistance [112] and, therefore, interfere with cell energy metabolism. Being the liver an organ that controls homeostasis, its cells present functions altered by the surrounding environment. Thus, to further study the responses of HLCs in terms of energy metabolism, there was the need to change the medium formulation to closer physiological concentrations by decreasing dexamethasone and insulin concentrations to 100 nM and 1 nM, respectively, as described by Estal et al in the culture of primary mouse hepatocytes [115]. This medium formulation is referred as MM (Figure 7). Pascussi et al demonstrated that this range of dexamethasone concentrations were able to positively control the activation of two nuclear receptors, pregnane X receptor (PXR) and the constitutive activated receptor (CAR) which in turn activated *CYP3A4* transcription [122] yielding the basal expression of CYP3A4 in the absence of xenobiotic inducers, in both MM and DM.

The influence of the alterations regarding media and collagen coating was evaluated on HLCs' morphology, glycogen storage ability, presence of hepatic markers and biotransformation activity. These assays were performed in HLCs cultured in coated coverslips since HLCs in the MD would also be in contact with a coated glass cover. D27 and D34 were chosen as time points for these evaluations because D27 is considered to be the day at which the differentiation process ends [96] whereas D34, on the other hand, represents maintenance of cells in culture for one week long.

We observed that in both MM and DM conditions HLCs presented binucleated cells and a polygonal shape (Figure 10) throughout time in culture, displayed glycogen storage ability (Figure 11) and the presence of specific hepatic markers such as HNF-4α, ALB, the influx transporter OATP-C, located on the sinusoidal membrane, the efflux transporter MRP-2, located on the canalicular/apical membrane, and CK-18 (Figure 12), at D27 and D34, suggesting the maintenance of hepatic phenotype in culture.

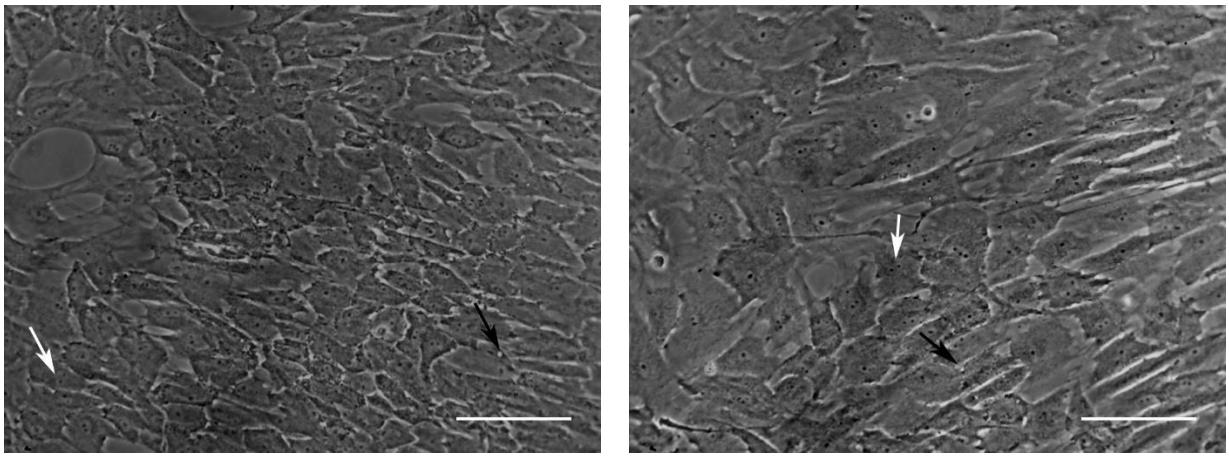

a) b)

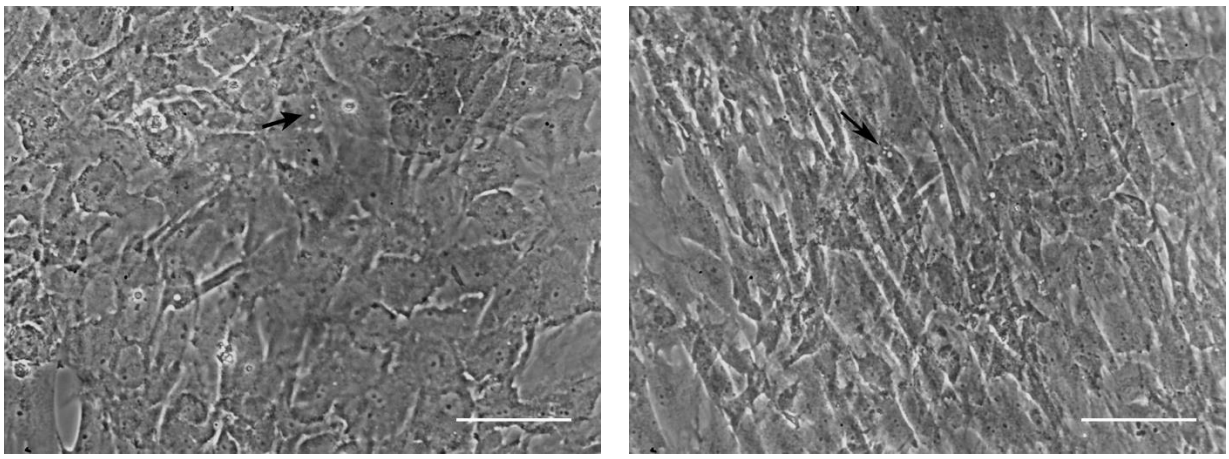

c) d)

Figure 10 - HLCs' morphology in 2D static culture: a) HLCs in MM at D27; **b) HLCs in DM at D27**; **c) HLCs in MM at D34**; **d) HLCs in DM at D34**. White arrows indicate binucleated cell and black arrows indicate lipid droplets. Scale bar = 100 µm.

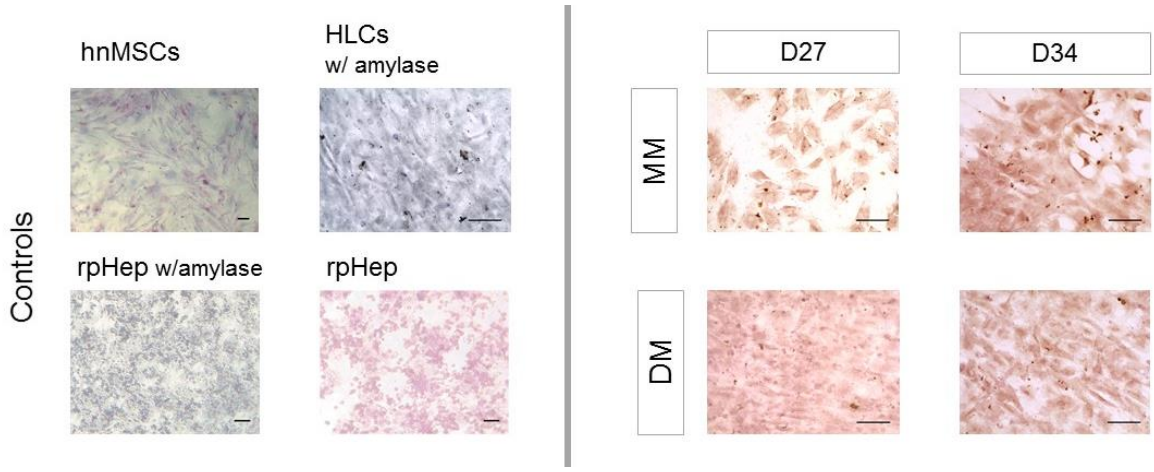

Figure 11 - PAS staining of HLCs at D27 and D34, maintained in MM and DM revealed glycogen storage ability throughout culture time. The controls used were hnMSCs, rpHep and HLCs cultured in DM at D34 incubated with amylase. rpHep was used as a positive control. Scale bar = 100 µm.
Abbreviations: hnMSCs (undifferentiated human neonatal mesenchymal stem cells); rpHep (rat primary hepatocytes); MM (maintenance medium); DM (differentiation medium); D27, D34 (day 27, day 34 of the differentiation protocol)

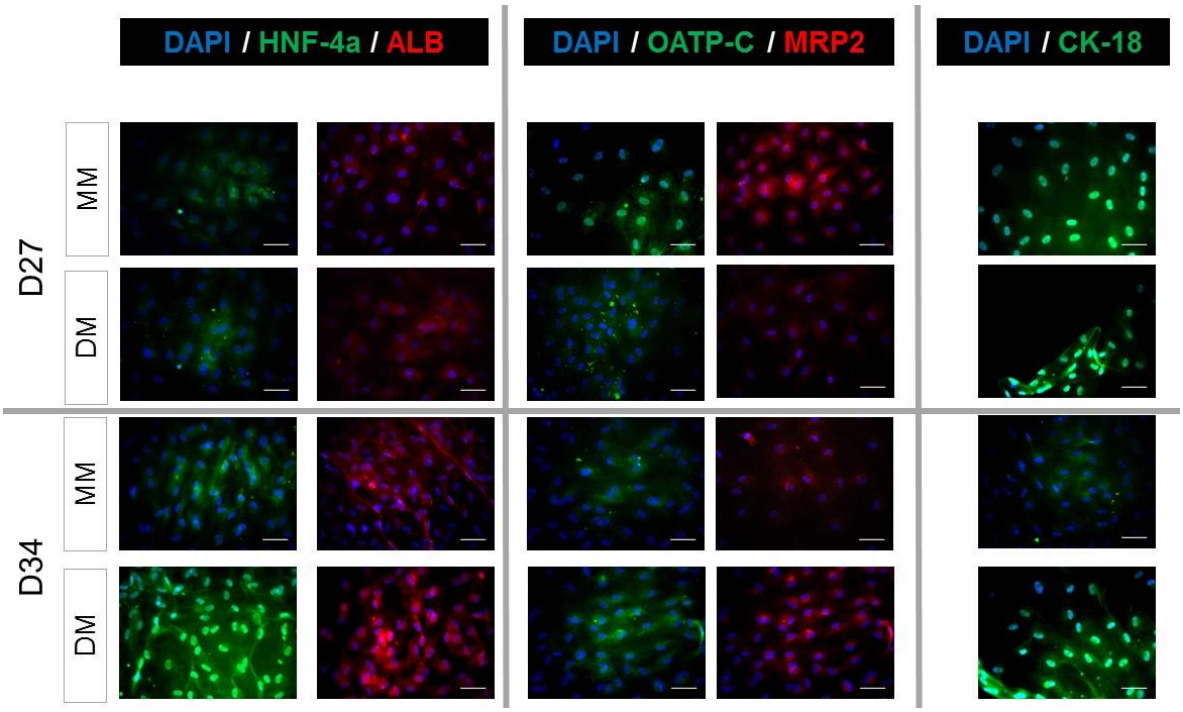

Figure 12 - Immunocytochemical staining revealed the presence of specific hepatic markers in HLCs: HNF-4α, ALB, OATP-C, MRP2 and CK-18 in HLCs maintained in both media, at D27 and D34. Cell nuclei were counterstained with DAPI. Scale bar = 50 µm.
Abbreviations: MM (maintenance medium); DM (differentiation medium); D27, D34 (day 27, day 34 of the differentiation protocol); HNF-4α (hepatocyte nuclear factor-4α); ALB (albumin); OATP-C (organic anion-transporting polypeptide-C); MRP2 (multidrug resistance protein 2); CK-18 (cytokeratin-18).

To assess the effect of the media culture condition on HLCs' biotransformation competence, EROD, ECOD and UGTs activities were also tested. hnMSCs were used as a negative control, in order to verify the maturation process of HLCs, while HepG2, rat primary hepatocytes and human hepatocytes were used as positive controls, since these are the most commonly used cell types for hepatic *in vitro* models.

Extended *in vitro* hepatocyte cultures are hampered by loss of CYP activity. Hence, phase I and II reactions were analysed at D27 and D34 of the differentiation protocol in both MM and DM. EROD activity (Figure 13a), covering CYP1A1/2, showed a slight increase from D27 to D34, in cells maintained in both MM and DM, although not significant ($p > 0.05$). When compared to DM, HLCs in MM presented higher EROD activity in both days (non-significant). Dexamethasone was shown to decrease CYP1A1 activity in adult human hepatocytes [123] being in accordance with our results that demonstrated higher EROD activity in HLCs cultured in lower dexamethasone (MM) than in the DM formulation. In contrast to EROD activity, ECOD assay which covers CYP2B6/1A2/2E1 activities showed a slight decrease in activity from D27 to D34 (non-significant) in both media (Figure 13b). At D27, the activity was similar in HLCs in MM and in DM. At D34, the activity was slightly higher in HLCs maintained in DM, that contains higher concentration of dexamethasone (non-significant). Indeed, dexamethasone is a known inducer of CYP2B6 [124] in human hepatocytes, suggesting that the higher ECOD activity in DM may be related to the presence of a higher concentration of this glucocorticoid.

Phase II enzymes have important roles in the metabolism of xenobiotics [125]. Therefore, their activity was also studied in HLCs exposed to different concentrations of dexamethasone and insulin. Herein, UGTs activity was evaluated since most phase II reactions within the human body are catalysed by these enzymes. Dexamethasone and insulin are known inducers of human UGTs activity [126]. UGTs activity in HLCs showed no significant differences when compared to human hepatocytes ($p > 0.05$) in all tested conditions, being always higher than all other controls (Figure 13c) confirming that HLCs maintained its competence throughout culture time under the different culture media formulations.

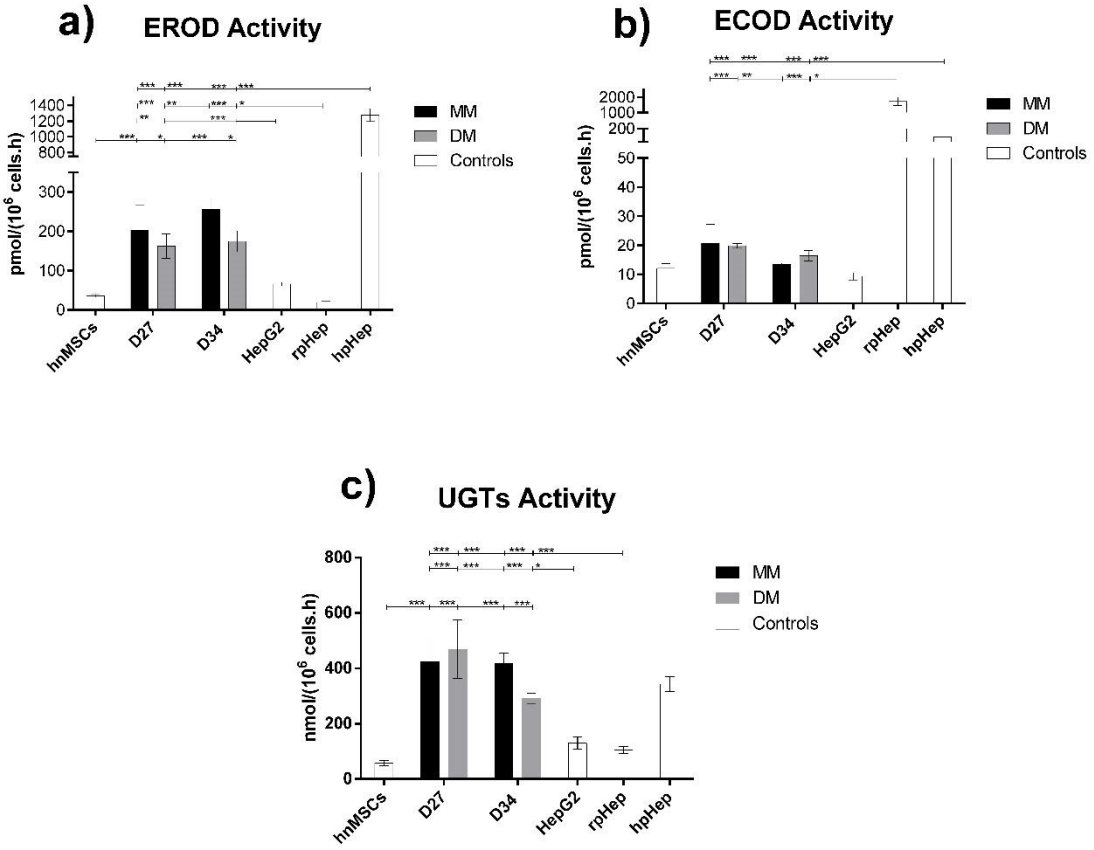

Figure 13 - Effect of culture time and medium composition on Phase I and II activities: a) EROD, b) ECOD and c) UGTs activity. Data is represented as Average ± SEM (n=2-4). Undifferentiated hnMSCs and HepG2 cell line, rpHeps and cryopreserved hpHep are negative and positive controls, respectively (white bars). *, **, *** Significantly differs among the controls with $p < 0.05$, $p < 0.01$ and $p < 0.001$, respectively. Abbreviations: rpHep (rat primary hepatocytes); hpHep (human primary hepatocytes); hnMSC (undifferentiated human neonatal mesenchymal stem cells); MM (maintenance medium); DM (differentiation medium); D27, D34 (day 27, day 34 of the differentiation protocol); EROD (7-ethoxyresorufin-O-deethylase); ECOD (7-ethoxycoumarin-O-deethylase)); UGTs (uridine 5'-diphosphate glucuronosyltransferases).

Overall, HLCs' maintained a hepatic morphology, glycogen storage ability, presence of hepatic markers and biotransformation activities, in DM and MM, not showing significant differences. Based on this data, MM was used for further studies since the concentrations of dexamethasone and insulin are closer to physiological levels and are less probable of interfere with HLCs' energy metabolism. In addition, commercial collagen revealed to be adequate in

maintaining HLCs in culture and it was the coating used for all the studies performed in the microfluidic device.

III. 3. Different dexamethasone and insulin concentrations induce altered gene expression profiles in HLCs

Being the liver an organ that controls homeostasis its cells present functions altered by the surrounding environment. Liver contributes to glucose homeostasis by providing glucose in the fasted state and by storing it as glycogen, in the fed state. When glycogen storages are saturated, the remaining glucose is stored as lipid droplets or secreted as VLDL [2]. As previously observed, HLCs showed formation lipid droplets (Figure 10) and glycogen storage ability (Figure 11). But to understand how HLCs regulate their energy metabolism, we studied the expression of key genes involved in glycolysis and lipogenesis regulation, gluconeogenesis, lipolysis, fatty acids metabolism, bile acids metabolism and mitochondrial function and biogenesis in HLCs cultured in DM and MM, exposed to insulin and glucagon and in SM. The chosen genes are presented in Figure 14.

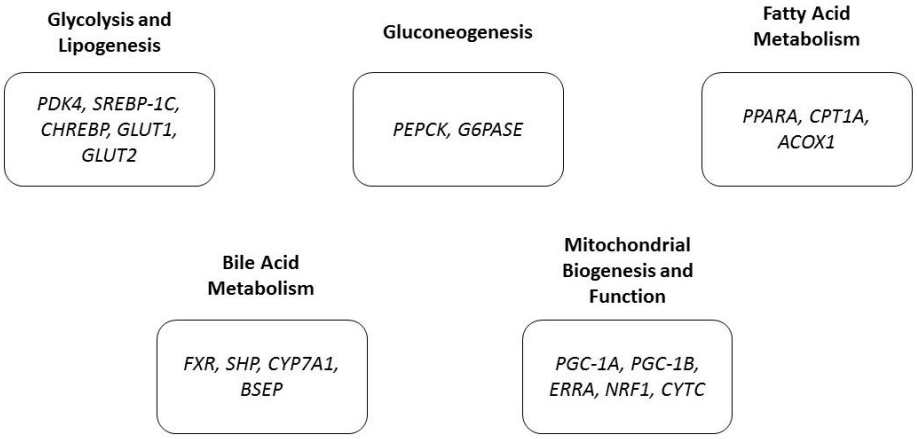

Figure 14 - Genes used for energy metabolism study divided by metabolic pathways: glycolysis and lipogenesis, gluconeogenesis, fatty acid metabolism, bile acid metabolism and mitochondrial biogenesis and function.
Abbreviations: PDK4 (pyruvate dehydrogenase kinase 4); SREBP-1C (Sterol regulatory element-binding protein 1-c); CHREBP (Carbohydrate response element binding protein); GLUT1 (glucose transporter 1); PEPCK (phosphoenolpyruvate carboxylase); G6PASE (glucose-6-phosphatase); PPARA (peroxisome proliferator-activated receptor α); CPT1A (carnitine palmitoyltransferase 1 α); ACOX1 (acyl-CoA oxidase 1); FXR (farnesoid X receptor); CYP7A1 (cytochrome P450 enzyme cholesterol 7α-hydroxylase); PGC-1A (peroxisome proliferator γ-activated receptor coactivator 1-α); PGC-1B (Peroxisome proliferator γ-activated receptor coactivator 1-β); ERRA (Estrogen-related receptor α); NRF1 (nuclear respiratory factor 1); CYTC (cytochrome C).

DM and MM have both equal glucose concentrations (25 mM) but the ratios of insulin to dexamethasone are 1.72 in DM and 0.01 in MM. Therefore, in DM the insulin effect may overlap dexamethasone effect while the opposite happens in MM. Besides, the concentrations of dexamethasone and insulin are also higher in DM. Antagonist effects of dexamethasone and insulin incubation, together with other molecules, with rat hepatocytes in TAG synthesis was

previously reported [127], where the presence of both compounds decreased the activity of an enzyme involved in gluconeogenesis compared with dexamethasone alone.

We studied the gene expression profile of HLCs cultured in MM and DM, in plates, at different culture time points (D27 and D34) using as a reference HLCs subjected to 8h-fasting at D34 since this condition has lower glucose concentration (5 mM) and has no dexamethasone or insulin (Figure 15).

HLCs in DM showed an increased gene expression in all genes tested, except for *GLUT1* and *ERRA* (Figure 15a and e), from D27 to D34, which might be an indicator of HLCs maturation induced by the dexamethasone and insulin concentrations [80] used in the differentiation protocol. Indeed, glucose transporter *GLUT1* expression decreased from D27 to D34 in both MM and DM (only significant in DM). This may be explained due to a transition from a foetal phenotype, which presents higher *GLUT1* expression, to a neonatal phenotype, having little expression in neonatal and adult hepatocytes [128] and HLCs present a similar trend. Regarding, *ERRA*, this gene regulates the transition from glycolysis to fatty acid oxidation [129]. Possibly, the decrease in its expression is related to a continued exposure to high concentrations of insulin, which induces glycolysis and inhibits fatty acid oxidation [2].

In contrast to DM conditions, as expected, when exposed to MM the expression levels of *PEPCK*, *G6PASE*, *ACOX1*, *FXR* and *NRF1* presented the opposite trend being higher at D27 (Figure 15b, c, d and e).

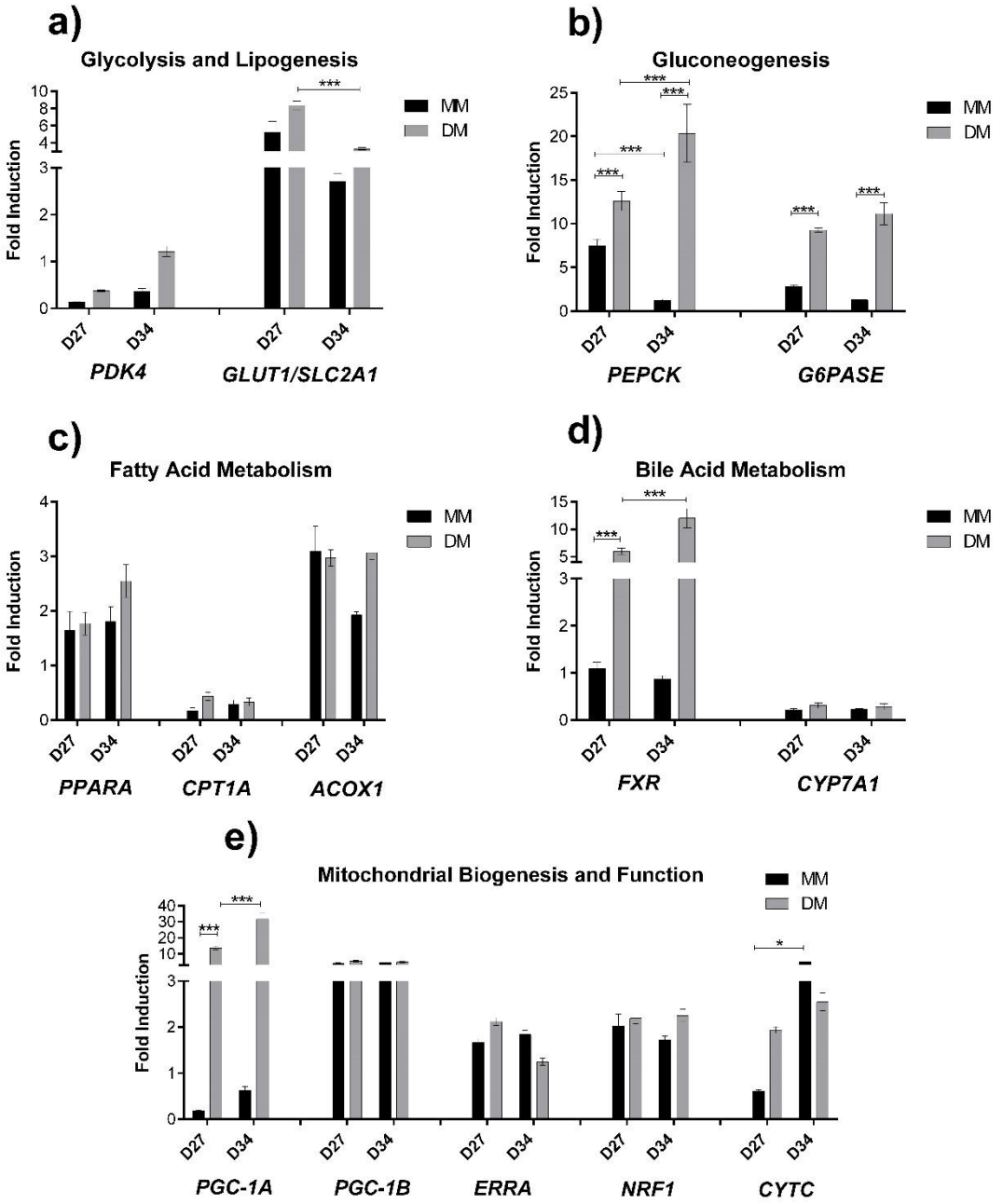

Figure 15 – Gene expression in HLCs throughout culture time in MM and DM regarding a) glycolysis and lipogenesis; b) gluconeogenesis; c) fatty acid metabolism; d) bile acid metabolism and **e) mitochondrial biogenesis and function.** The graphs represent HLCs' evolution in MM and DM relative to 8h-fasting at D34. Data is represented as Average ± SEM (n=2-6). *, **, *** Significantly differs from the different media composition and the days of differentiation with $p < 0.05$, $p < 0.01$ and $p < 0.001$, respectively. Abbreviations: D27 (day 27 of the differentiation protocol); D34 (day 34 of the differentiation protocol), MM (maintenance medium), DM (differentiation medium); *PDK4* (pyruvate dehydrogenase kinase 4); *GLUT1/SLC2A1* (glucose transporter 1/solute carrier family 2 member 1); *PEPCK* (phosphoenolpyruvate carboxylase); *G6PASE* (glucose-6-phosphatase); *PPARA* (peroxisome proliferator-activated receptor α); *CPT1A* (carnitine palmitoyltransferase 1 α); *ACOX1* (acyl-CoA oxidase 1); *FXR* (farnesoid X receptor); *CYP7A1* (cytochrome P450 enzyme cholesterol 7α-hydroxylase); *PGC-1A* (peroxisome proliferator γ-activated receptor coactivator 1-α); *PGC-1B* (peroxisome proliferator γ-activated receptor coactivator 1-β); *ERRA* (estrogen-related receptor α); *NRF1* (nuclear respiratory factor 1); *CYTC* (cytochrome C).

These results suggested that DM was more adequate for enhancing HLCs' metabolic characteristics during culture time, by inducing a continued maturation. However, for the purpose of studying cells adaptation to fasting and/or the response to insulin and glucagon exposure, a

lower gene expression profile, as the one observed in HLCs in MM may allow observing cells adaptation to fasting and/or the response to insulin and glucagon exposure. Therefore, this condition was used in the fasting adaptation (section III. 4) and insulin and glucagon studies (section III. 5).

III. 4. HLCs adapt their response to fasting

Liver needs to adapt its metabolism to face changes in nutrient availability. Particularly, in starvation, liver is able to provide fuel substrates to the rest of the organism. Thus, to possibly establish a relevant hepatic *in vitro* model for energy metabolism studies, HLCs were subjected to fasting.

HLCs at D34 presented metabolic responses more similar to the expected than HLCs in earlier stages of development (data not shown). This observation further suggested that the decrease in gene expression throughout time in HLCs cultured in MM allowed the observation of energy metabolism responses while, in parallel, HLCs display a more mature phenotype. Therefore, energy metabolism studies (response to fasting and to insulin and glucagon stimuli) were performed at D34. Hence, the adaptation of HLCs to fasting [130] was studied by evaluating gene expression of specific genes in HLCs subjected to starvation for a period of 8 and 10 hours relative to HLCs cultured in MM at D34 in order to study the effect of 25 mM of glucose (in MM) and 5 mM of glucose (in SM) on the expression levels of the same genes tested above.

Glucose oxidation through glycolysis is downregulated due to the lack of this substrate during starvation. In our experimental conditions, 8 hours of fasting presented higher expression of *PDK4* than 10 hours of fasting ($p < 0.001$) (Figure 16a), which may be explained by a time course of events leading to glucose homeostasis, in which in a first moment *PDK4* is induced and downregulated afterwards. In fact, in an *in vivo* study by Palou et al, fasting rat revealed a peak in *PDK4* expression at 8 hours of fasting, showing a subsequent decrease [131]. Moreover, *SREBP-1C* and *CHREBP1* induce lipogenesis [2] and upon fasting, it was strongly downregulated (Figure 16a). This is expected since starvation demands the use of fuel substrates and not energy storage. In addition, glucose activates *CHREBP1* transcription [132] and under the condition herein evaluated, this substrate is lacking. *GLUT1* was shown to be upregulated in rat hepatocytes in both fasting and diabetes [133]. However, in HLCs, *GLUT1* was downregulated after 8 hours and maintained its expression, relative to MM, after 10 hours of fasting. Thus, *GLUT1* presented an increase in its expression from 8 to 10 hours of fasting (Figure 16a), suggesting that the expected gene upregulation might be seen if HLCs were submitted to a longer fasting period.

When glycolysis is downregulated, pyruvate can then be directed to gluconeogenesis, due to the need for glucose [2]. Similarly, as expected, *PEPCK* was markedly induced ($p < 0.05$) after 10 hours of fasting, since this condition induces gluconeogenesis [2] in response to the lack of fuel substrates (Figure 16b). *G6PASE* approximately maintained its expression after 10 hours of fasting (Figure 16b). However, after 8 hours of fasting, both *PEPCK* and *G6PASE* showed a slight decrease in expression compared to MM (non-significant). In fact, MM contains dexamethasone and as a glucocorticoid, it induces gluconeogenesis [23]. The effect of the

dexamethasone may overlap the duration of starvation and gluconeogenesis is possibly more induced in MM than after 8 hours of fasting. On the other hand, the effect of 10 hours of fasting caused HLCs to strongly activate gluconeogenesis, suggested by the induced expression of *PEPCK*.

Alternatively to gluconeogenesis, when glycolysis is downregulated due to *PDK4* upregulation [18] a switch from glucose to fatty acids utilization [134] may also occur, inducing *PPARA*. However, in HLCs, *PPARA* and *ACOX1* were not induced upon starvation (Figure 16c), but instead a decrease in its expression from 8 to 10 hours of fasting was observed. *CPT1A*, as a target of *PPARA* [2], was progressively induced with increasing duration of fasting (Figure 16 c). A similar trend was observed in fasting rats where *CPT1A* expression increased from 8 to 24 hours of fasting [131]. In addition, in the same study, *PPARA* expression had a peak after 4 hours, decreasing afterwards while *ACOX1* presented an increasing trend [131]. These observations suggest that, in HLCs, *PPARA* might have been induced some time before 8 hours of fasting and that it caused *CPT1A* upregulation, as a cascade of events downstream. Therefore, it would be interesting to evaluate, in future studies, other time points of fasting in order to observe the evolution of *PPARA*. Regarding *ACOX1*, the trend in rat livers and in HLCs was contrasting, suggesting that in HLCs, *ACOX1* upregulation may have occurred in an anterior time point.

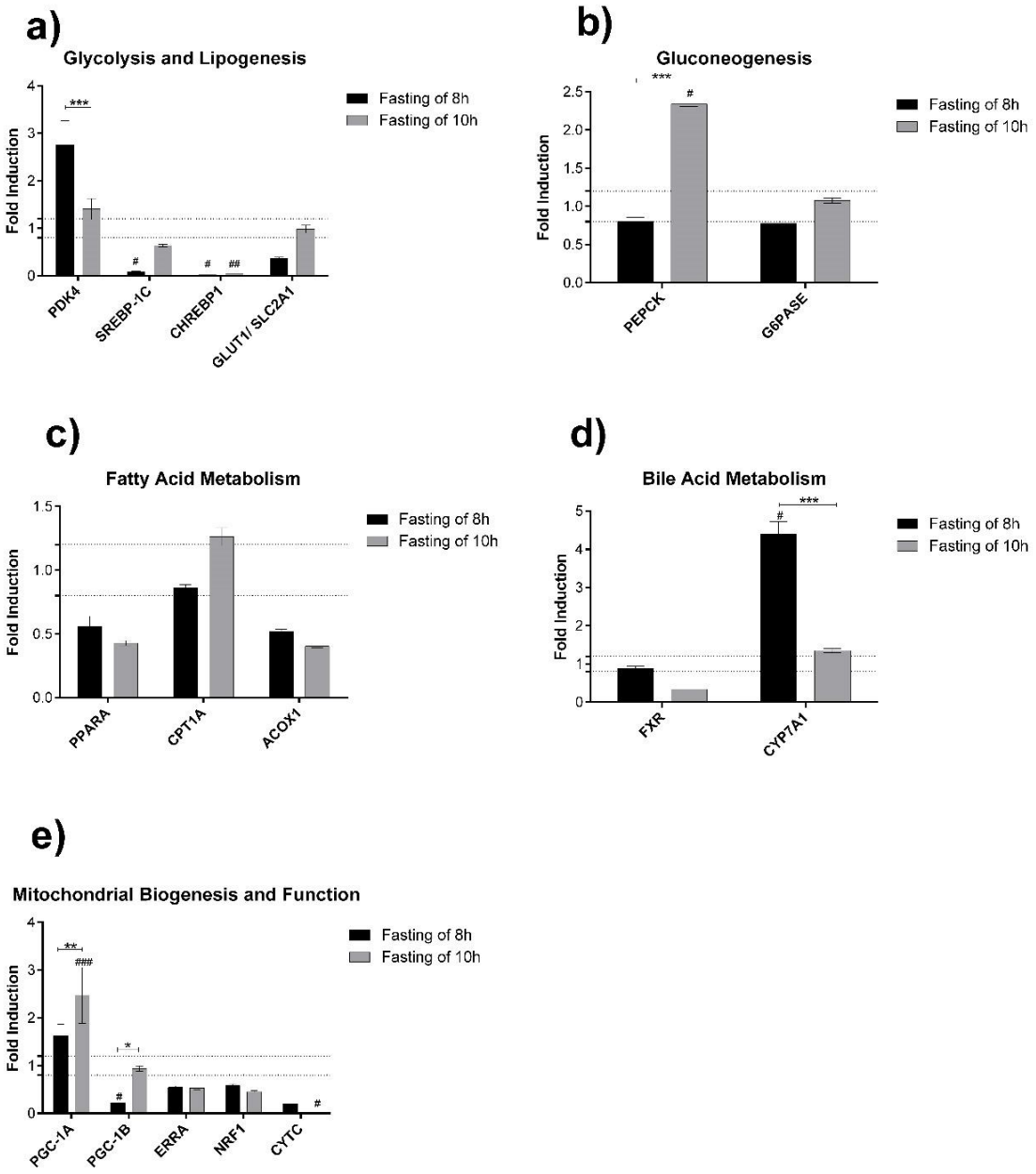

Figure 16 – HLCs' adaptive response to fasting at D34. **Gene expression of specific genes of a) glycolysis and lipogenesis, b) gluconeogenesis, c) fatty acid metabolism, d) bile acid metabolism and e) mitochondrial biogenesis and function.** The graphs represent the fold induction regarding gene expression of HLCs in response to 8h- and 10-fasting relative to MM. Grid lines represent fold induction equal to 0.8 and 1.2. Data is represented as Average ± SEM (n=2-6). *, **, *** Significantly differs from the different media composition and the days of differentiation with $p < 0.05$, $p < 0.01$ and $p < 0.001$, respectively. $^{\#}$, $^{\#\#}$, $^{\#\#\#}$ Significantly induced or repressed expression with $p < 0.05$, $p < 0.01$ and $p < 0.001$, respectively. Abbreviations: *PDK4* (pyruvate dehydrogenase kinase 4); *SREBP-1C* (sterol regulatory element-binding protein 1-c); *CHREBP1* (carbohydrate response element binding protein); *GLUT1/SLC2A1* (glucose transporter 1/solute carrier family 2 member 1); *PEPCK* (phosphoenolpyruvate carboxylase); *G6PASE* (glucose-6-phosphatase); *PPARA* (peroxisome proliferator-activated receptor α); *CPT1A* (carnitine palmitoyltransferase 1 α); *ACOX1* (acyl-CoA oxidase 1); *FXR* (farnesoid X receptor); *CYP7A1* (cytochrome P450 enzyme cholesterol 7α-hydroxylase); *PGC-1A* (peroxisome proliferator γ-activated receptor coactivator 1-α); PGC-1B (Peroxisome proliferator γ-activated receptor coactivator 1-β); *ERRA* (estrogen-related receptor α); *NRF1* (nuclear respiratory factor 1); *CYTC* (cytochrome C).

Mitochondrial biogenesis was also evaluated in fasting conditions. *PGC-1A* was upregulated upon starvation, having its expression higher after 10 hours of starvation compared

to 8 hours of starvation ($p < 0.01$) (Figure 16e). This upregulation was in line with previously reported in mice [23]. PGC-1α induces gluconeogenesis and β oxidation. Upon starvation, HLCs showed an activation of both pathways, more relevant in gluconeogenesis, through upregulation of *PEPCK*, suggesting that the regulation by PGC-1α also occurs in these cells. *CYP7A1* (bile acid metabolism) was upregulated in fasting ($p < 0.05$) (Figure 16d), which may be related to *PGC-1A* activation [135]. Our results are in accordance with the reported *CYP7A1* activation in livers of fasted mice [135], augmenting the synthesis of bile acids. *PGC-1A* upregulation upon fasting allows to infer that it may influence *CYP7A1* expression. The decrease of *CYP7A1* expression with time suggests that this gene follows the same trend of *PDK4* and *CPT1A*. A sequence of events downstream takes place and the expression is progressively decreased. On the other hand, contrary to reported [40,41], *FXR* (bile acid metabolism) was not induced by PGC-1α in HLCs (Figure 16e), upon fasting. FXR senses bile acids and between 8 and 10 hours of fasting, bile acid synthesis was induced through CYP7A1 activation. Nevertheless, beyond a certain pool size of bile acids, their synthesis is inhibited due to cytotoxic effects [37]. Thus, a longer fasting time would possibly result in *FXR* upregulation. PGC-1β is related to mitochondrial biogenesis and function [136]. Opposing to *PGC-1A*, *PGC-1B* in fasted rats and mice showed no alteration in its expression when compared to the fed state [136]. Our results for HLCs showed a downregulation of this gene after 8 hours of fasting ($p < 0.05$), followed by an increase in expression ($p < 0.05$), maintaining it approximately equal to the one presented in MM after 10 hours of fasting (Figure 16e). PGC-1β is related to lipogenesis [31] and upon fasting, there is a lack of substrates to be used in this pathway, thus explaining the observed downregulation. Due to its widespread tissue distribution, PGC-1β may fulfil other functions necessary for the basal cell energy requirements and these results may not be fully explained just by the response to fasting [136]. Estrogen-related receptor α (ERRα) is a nuclear receptor and its functions are related with mitochondrial function. ERRα null mice showed decreased expression of genes coding for fatty acid oxidation enzymes and oxidative phosphorylation components [137]. A study in mice by Herzog et al revealed that ERRα interacts with *PEPCK* promoter, thus inhibiting gluconeogenesis [137]. Our results showed that *ERRA* was downregulated (non-significant), presenting approximately the same level of expression, after 8 and 10 hours of fasting (Figure 16e). This downregulation accompanied by an induction of gluconeogenesis in HLCs, possibly suggests that ERRα was not activated in order to gluconeogenesis occur as a source of energy. In addition, ERRα is reported to induce expression of genes related to mitochondrial biogenesis, such as nuclear respiratory factor 1 (*NRF1*), and respiratory chain cytochrome C (*CYTC*) [137]. However, not much is known about the metabolic regulation of these two genes. Nevertheless, *NRF1* and *CYTC* were downregulated upon fasting in HLCs (non-significant) (Figure 16e), possibly due to the lack of induction of ERRα.

Based on these results, we observed that all the genes tested regarding glycolysis, gluconeogenesis, bile acid metabolism and mitochondrial function respond as expected, except for *G6PASE*, although showing the expected increasing trend. We could conclude that the pathway that better responded to starvation in HLCs is gluconeogenesis (namely *PEPCK* and *PGC-1A* which is also involved), which is actually the first pathway to respond in this condition [14].

In addition, the differentiation protocol is characterized by high concentrations of glucose in the medium. The marked responses in genes regarding gluconeogenesis in HLCs correlates with what happens during the gestation period of several animals, including humans. The mother, in a well fed state, provides glucose and the foetus does not have the need of producing it. However, fasting mothers can induce premature foetal gluconeogenesis [138]. Genes related to fatty acid metabolism may not present the expected physiological responses, because we only considered 8 and 10 hours of fasting. As suggested by genes expression throughout time, we may be missing upregulations. Metabolic pathways are regulated by a cascade of events occurring in different time points. For genes involved in gluconeogenesis regulation, this window of time is adequate whereas fatty acid metabolism and bile acid metabolism may demand earlier and later time points, respectively.

III. 5. HLCs respond to insulin and glucagon exposure

In addition to adapt their functions to starvation, hepatocytes are expected to stimulate or inhibit genes controlling glucose metabolism when exposed to insulin or glucagon. In order to further validate HLCs' regarding energy metabolism competence, cell response to an insulin or glucagon stimuli was evaluated. Herein, the effect of insulin and glucagon was evaluated under SM (5 mM glucose) in cells that were maintained in MM. Human primary hepatocytes maintained in the same culture conditions were used as controls. Table 1 presents the expected responses of each of the genes and the response of HLCs and primary human hepatocytes.

		HLCs		**Primary Hepatocytes**		**Expected Response**	
		Insulin	Glucagon	Insulin	Glucagon	Insulin	Glucagon
Glycolysis	***PDK4***	Down	Up	No change	No change	Down	Up
	SREBP-1C	No change	Up	Down	No change	Up	Down
	CHREBP1	Down	No change	Up	No change	Up	Down
Gluconeogenesis	***PEPCK***	Down	Up	No change	No change	Down	Up
	G6PASE	Down	Up	No change	No change	Down	Up
Fatty acid metabolism	***PPARA***	Down	No change	No change	No change	Down	Up
	CPT1A	No change	No change	No change	No change	Down	Up
	ACOX1	No change	No change	No change	No change	Down	Up
Bile acid metabolism	***FXR***	Down	No change	No change	No change	Down	Up
	CYP7A1	Down	No change	Down	No change	Down	Up
	SHP	No change	No change	Down	No change	Down	Up
	BSEP	Down	Up	No change	No change	Down	Up
Mitochondrial function and biogenesis	***PGC-1A***	Down	No change	No change	Up	Down	Up
	PGC-1B	Up	No change	Up	No change	Unknown	Unknown
	ERRA	No change	No change	Down	No change	Unknown	Unknown
	NRF1	Down	Up	No change	No change	Unknown	Unknown
	CYTC	Down	No change	No change	Up	Unknown	Unknown

Table 1 - Response to insulin and glucagon: overview of HLCs and primary hepatocytes significant response compared to the expected response in literature. "Up" indicates upregulation and "Down" indicates downregulation. Green is associated with responses similar to that of primary hepatocytes or to the expected, yellow is associated to genes that presented responses similar to that of primary hepatocytes but was not the expected response and red is associated to the genes that did not respond to the expected in both HLCs and primary hepatocytes.

Physiologically, under high glucose concentrations, insulin is released, while glucagon is released in low glucose concentrations. As mentioned earlier, insulin stimulates glycolysis and lipogenesis [2]. In this work, both HLCs and human hepatocytes when incubated with insulin, inhibited *PDK4* (glycolysis) expression (Figure 17a), indicating increased pyruvate consumption and glycolysis [2], although only significant in HLCs ($p < 0.001$). The opposite response was observed when cells were exposed to glucagon where pyruvate is used to produce energy through catabolic reactions [134] (Figure 17a). On the other hand, *CHREBP1* (lipogenesis pathway) was downregulated in response to insulin ($p < 0.05$) while *GLUT1* (glycolysis pathway) maintained its expression in HLCs (Figure 17a). Moreover, *SREBP-1C* (lipogenesis pathway) was downregulated ($p < 0.05$) in the positive control, *i.e.*, human hepatocytes. In fact, SREBP-1c belongs to a family of transcription factors involved in fatty acid synthesis that are positively controlled by insulin [139]. This gene is activated when senses elevated cholesterol concentration [140]. However, in our experimental conditions, the medium did not contain cholesterol, which can explain why the expression of *SREBP-1C* was inhibited. In addition, 8 hours of insulin exposure may not be adequate to observe the expected upregulation, as mentioned above. Indeed, insulin stimulation in rat hepatocytes with a duration of 6 hours increased *SREBP-1C* expression [139], suggesting that a shorter period of insulin incubation with HLCs would be interesting to study. ChREBP1, on the other hand, is directly activated by glucose [2], and indirectly by insulin since insulin induces lipogenesis. *CHREBP1* was upregulated in primary hepatocytes ($p < 0.05$) and downregulated in HLCs ($p < 0.05$) (Figure 17a) but other mechanisms may induce synergistically the expression of *CHREBP1* towards lipogenesis. Finally, glucose transporter *GLUT2* was only detected in primary hepatocytes, maintaining its expression when exposed to insulin and glucagon (Figure 17a). Rat hepatocytes demonstrated a transient inhibitory insulin effect on GLUT2 [141] and its expression was decreased after a 24-hour incubation. GLUT2 has a high K_M for glucose (15-20 mM) [14]. Therefore, after meals, *GLUT2* is upregulated for the uptake of glucose and storage [14]. Insulin is suggested to act synergistically with glucose abundance in an early period upregulating it and afterwards, by an unknown mechanism of autoregulation, *GLUT2* expression is decreased to basal levels [141]. We can infer that glucagon, acting in a fasted state by promoting glucose, has a similar effect. Firstly, it upregulates *GLUT2* in order to remove glucose, produced through gluconeogenesis, from hepatocytes and its expression is then decreased to basal levels. However, the expected responses of this glucose transporter may not have been observed due to low glucose concentration in the media. In HLCs, the upregulation of gluconeogenic genes in response to glucagon (Figure 17b) and the inexistent expression of *GLUT2* could possibly explain the upregulation of *GLUT1* ($p < 0.001$), suggesting that the latter is used for glucose output, in accordance with previous observations [2].

Gluconeogenesis is upregulated by glucagon in order to produce glucose for extrahepatic tissues, after glycogen depletioned [2]. Therefore, as expected, *PEPCK* and *G6PASE* were upregulated when medium contained glucagon and downregulated in response to insulin, in both HLCs and primary hepatocytes (Figure 17b). Moreover, HLCs presented more marked changes in gluconeogenic genes than human hepatocytes, being more downregulated ($p < 0.05$ for

PEPCK and p < 0.001 for *G6PASE*) or upregulated (p < 0.001 for both genes) when incubated with insulin and glucagon, respectively. This may be due to high glucose concentration of the medium of the differentiation protocol. On the other hand, hepatocytes have other energy substrates since they present more lipid droplets than HLCs and its constituents can be directed to β oxidation [142]. Furthermore, β oxidation is mainly developed after birth in response to a change from a high-carbohydrate and low-fat diet to a high-fat and low-carbohydrate diet [138]. Thus, glucose may constitute a stimulus to the development of HLCs' pathways related to glucose homeostasis, in particular, gluconeogenesis. Regarding starvation, *PEPCK* had an increased upregulation with the course of time and *G6PASE* had an increased expression when compared to MM, although the latter was not upregulated (Figure 16b). This result suggests that glucagon is an important regulator of the *G6PASE* expression, which is not only induced by fasting.

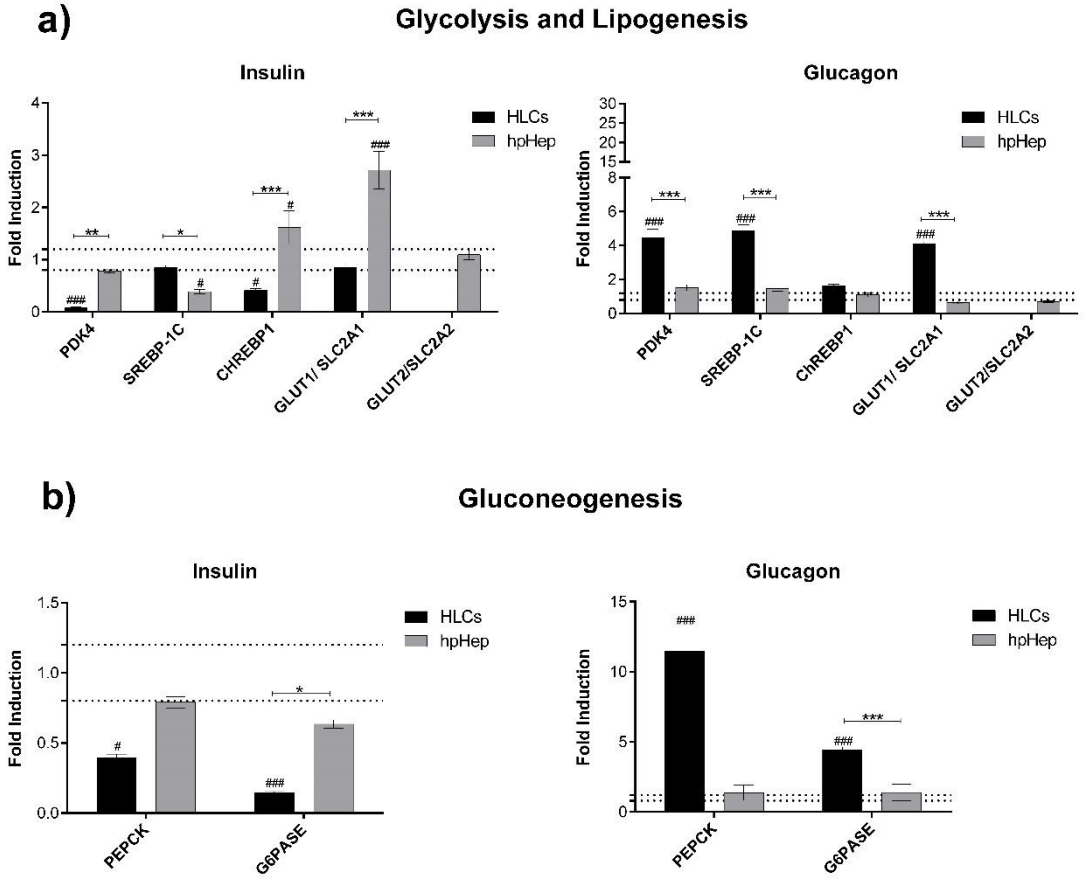

Figure 17 – Gene expression in HLCs in response to insulin and glucagon regarding a) glycolysis and lipogenesis and b) gluconeogenesis. Grid lines represent fold induction equal to 0.8 and 1.2. Data is represented as Average ± SEM (n=2-6). *, **, *** Significantly differs from the different media composition and the days of differentiation with p < 0.05, p < 0.01 and p < 0.001, respectively. #, ##, ### Significantly induced or repressed expression with p < 0.05, p < 0.01 and p < 0.001, respectively.
Abbreviations: HLCs (hepatocyte-like cells); hpHep (human cryopreserved hepatocytes); *PDK4* (pyruvate dehydrogenase kinase 4); *SREBP-1C* (sterol regulatory element-binding protein 1-c); *CHREBP1* (carbohydrate response element binding protein); *GLUT1/SLC2A1* (glucose transporter 1/solute carrier family 2 member 1); *GLUT2/SLC2A2* (glucose transporter 2/solute carrier family 2 member 2); *PEPCK* (phosphoenolpyruvate carboxylase); *G6PASE* (glucose-6-phosphatase).

The oxidation of fatty acids is downregulated by insulin and stimulated by glucagon [27] to obtain energy and PPARα promotes β oxidation [2]. Longuet et al reported that glucagon signalling activates a PPARα-dependent cascade of events, enhancing fatty acid oxidation in mice [130]. This

nuclear receptor targets *ACOX1*, the rate-limiting enzyme of the partial oxidation of LCFAs in peroxisomes and *CPT1A* [33]. *PPARA* was downregulated, in HLCs, in response to insulin ($p < 0.05$) and upregulated upon glucagon treatment in HLCs and human hepatocytes (non-significant) (Figure 18a). However, in HLCs just *PPARA* was responsive while target genes of PPARα did not show different responses to insulin or glucagon (Figure 18a). This may indicate that this pathway is not fully developed in HLCs. In fact, hepatocytes isolated from guinea pig were able to oxidize fatty acids only 12 hours after birth [143]. The lack of fatty acids in the medium could also be the reason why the genes related to fatty acids metabolism do not present the excepted expression. Interestingly, *PPARA* expression of HLCs that were subjected to starvation was downregulated (Figure 16d), suggesting that glucagon regulates its expression.

Regarding bile acids metabolism, insulin downregulated *FXR* in both HLCs ($p < 0.05$) and human hepatocytes (non-significant) while glucagon resulted in its upregulation (non-significant) (Figure 18b). The downregulation of *FXR* induced by insulin is in line with previously reported in rat hepatocytes cultured in low glucose concentrations (5 mM) [38]. Small heterodimer partner (SHP) is a target of FXR [38] (Figure 6), being involved in the inhibition of cholesterol conversion to bile acids. Since *FXR* was downregulated by insulin, we may infer that *SHP* expression will not be induced, as observed (Figure 18b). *CYP7A1* was also downregulated in HLCs ($p < 0.01$) and primary hepatocytes ($p < 0.05$) during prolonged exposure to insulin (Figure 18b), which is in accordance with previous observations [39]. However, *SHP* and *CYP7A1* expression had no differences when cells were incubated with glucagon. FXR positively regulates bile salt export pump (BSEP), excreting bile acids from the hepatocytes into bile canaliculus [15]. *BSEP* was downregulated when human hepatocytes were exposed to insulin and glucagon (Figure 18b). However, in HLCs, *BSEP* was upregulated in response to glucagon, possibly due to induction by FXR. We may infer that the expected responses were not observed may be due to the lack of cholesterol and bile acids in the medium [144]. CYP7A1 synthesizes bile acids from cholesterol and since this substrate was not available in culture, this enzyme may not be expressed because it is not necessary. Glucagon induced different responses in *FXR* and *CYP7A1*, when compared to fasting. Several papers suggest that FXR upregulation occurs through the action of PGC-1α upon fasting [40,41]. However, in HLCs, *FXR* was upregulated by glucagon but it was downregulated when HLCs were in fasting conditions (Figure 16d). Based on this observation, glucagon may have additional mechanisms for the regulation of FXR.

PGC-1α is a regulator of mitochondrial biogenesis [145]. In both HLCs and hepatocytes, glucagon treatment caused *PGC-1A* upregulation ($p < 0.05$ for hepatocytes) whereas insulin repressed it ($p < 0.05$ for HLCs) (Figure 18c) as expected [17]. PGC-1α is also a transcription factor relevant for the regulation of liver metabolism in several ways [2] co-activating genes regarding gluconeogenesis (*PEPCK* and *G6PASE*) [15]. Therefore, by downregulating *PGC-1A*, insulin inhibits gluconeogenesis, which is not needed since this hormone is released in well fed situations. *PGC-1A* was upregulated in fasting conditions, as well (Figure 16e). PGC-1β is related to lipogenesis, among other mitochondrial functions [31]. In response to insulin, both HLCs ($p < 0.01$) and hepatocytes ($p < 0.001$) presented *PGC-1B* upregulation (Figure 18c). The

physiological response of PGC-1β to hormonal signalling has not yet been clarified. However, since insulin also induces lipogenesis, this may be a possible response. On the other hand, glucagon caused a decrease in the upregulation of *PGC-1B* (Figure 18c), allowing to infer that a longer incubation with this hormone would induce a downregulation, which would be expected since lipogenesis is repressed by glucagon [130]. Upon fasting, this gene was downregulated, although with an increasing trend (Figure 16e). Due to the involvement in several mitochondrial functions and wide tissue distribution, it is difficult to explain what should be its role in metabolism homeostasis [136]. Regarding the remaining genes related to mitochondrial function, *ERRA*, *NRF1* and *CYTC* were mostly downregulated by insulin (Figure 18c). ERRα was shown to repress gluconeogenesis [146], which might explain the strong repression shown by human hepatocytes. In HLCs, *ERRA* essentially presented the same level of expression in response to glucagon and insulin (Figure 18c). Glucagon mostly induced an increase in expression of these genes when compared to insulin (Figure 18c). PGC-1α was reported to have stimulatory effects in ERRα, Nrf1 and CytC [147]. Therefore, the trend presented in gene expression may reveal a possible upregulation if the incubation time with glucagon would be longer. The response of this set of genes to glucagon contrasts with their response to fasting (Figure 16e), in which they were mainly inhibited. Thus, it is difficult to conclude what would occur in a physiological context, which is a combination of the two studied conditions: decrease of the levels of glucose (fasting condition) and release of glucagon (glucagon response).

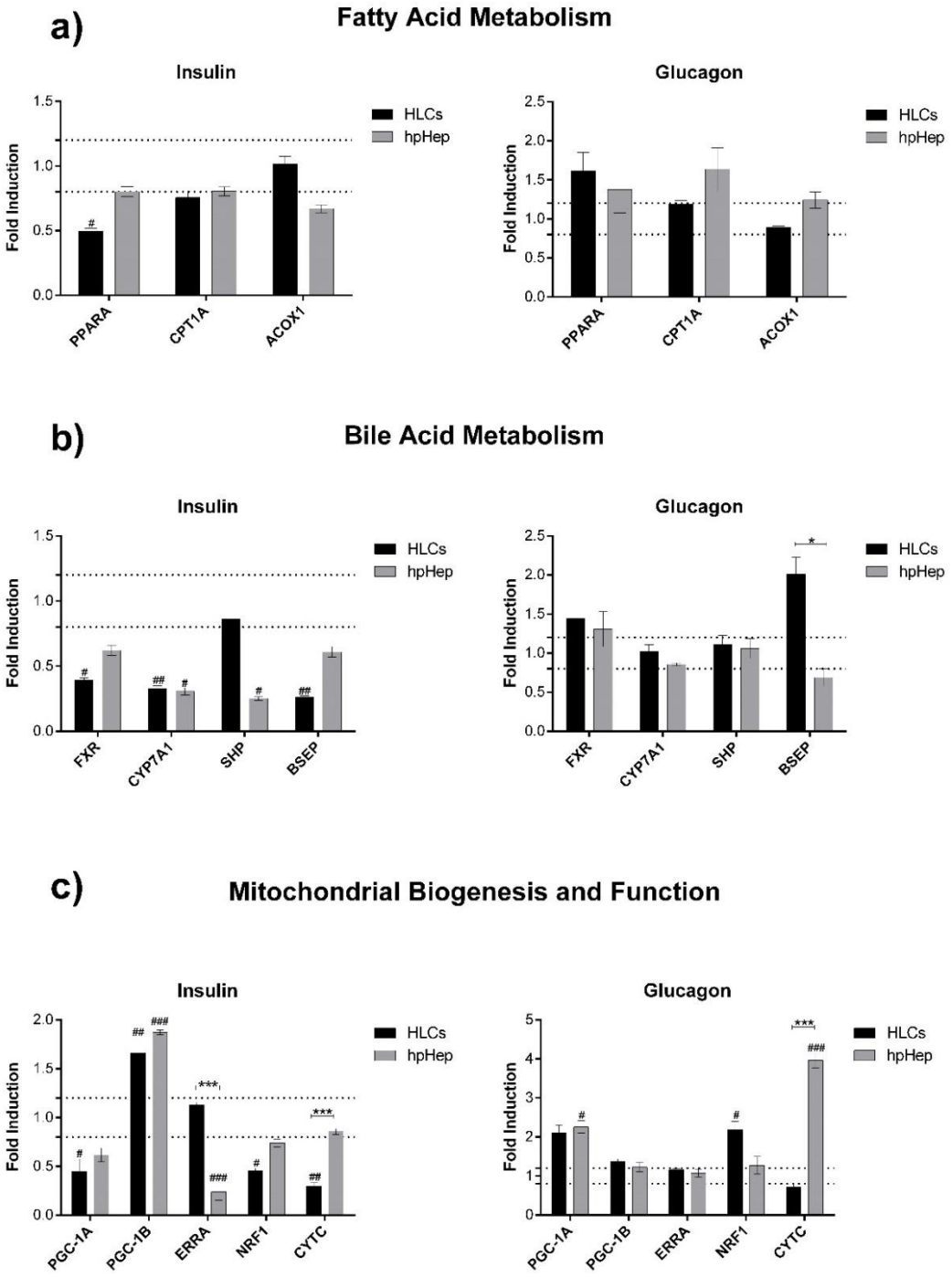

Figure 18 – Gene expression in HLCs in response to insulin and glucagon regarding a) fatty acid metabolism, b) bile acid metabolism and c) mitochondrial biogenesis and function. Grid lines represent fold induction equal to 0.8 and 1.2. *, **, *** Significantly differs from the different media composition and the days of differentiation with $p < 0.05$, $p < 0.01$ and $p < 0.001$, respectively. #, ##, ### Significantly induced or repressed expression with $p < 0.05$, $p < 0.01$ and $p < 0.001$, respectively.
Abbreviations: HLCs (hepatocyte-like cells); hHep (human cryopreserved hepatocytes), *PPARA* (peroxisome proliferator-activated receptor α); *CPT1A* (carnitine palmitoyltransferase 1 α); *ACOX1* (acyl-CoA oxidase 1); *FXR* (farnesoid X receptor); *CYP7A1* (cytochrome P450 enzyme cholesterol 7α-hydroxylase); *PGC-1A* (peroxisome proliferator γ-activated receptor coactivator 1-α); *PGC-1B* (peroxisome proliferator γ-activated receptor coactivator 1-β); *ERRA* (estrogen-related receptor α); *NRF1* (nuclear respiratory factor 1); *CYTC* (cytochrome C).

In sum, gluconeogenesis is the pathway where HLCs presented more accentuated and expected responses, compared with human hepatocytes. Glucose is a medium component present in high concentrations during all the differentiation process. Therefore, this biomolecule possibly stimulates pathways that regulate its use. In addition, genes upregulating gluconeogenesis are functional in foetuses if the mother is submitted to fasting [138], suggesting the early development of this pathway. *PDK4*, which is related to glycolysis, also showed significant downregulation and upregulation when HLCs were exposed to insulin and glucagon, respectively. Considering fatty acid oxidation, in HLCs just *PPARA* was responsive, being downregulated when exposed to insulin. Genes downstream may show a downregulating trend if the exposure to insulin was prolonged. Genes regarding bile acid metabolism responded to insulin stimuli but did not show significant responses to glucagon, except for *BSEP*, suggesting the need for optimization of hormone concentration or time incubation. PGC-1α induces gluconeogenesis gene expression and interacts with PPARα, activating fatty acid oxidation [148] and is a co-activator of FXR, inhibiting bile acid synthesis. Our results showed that when *PGC-1A* was upregulated, these genes were also. Godoy et al demonstrated that including bile salts in hepatocytes culture increased expression of mature liver function genes (*e. g. BSEP*) [144].

Thus, it would be interesting to use a medium containing biomolecules frequently in contact with hepatocytes such as fatty acids, cholesterol and bile acids and adapt their concentration to the one found in fasted and fed states. Incubation with these compounds might produce different responses, possibly bringing this model closer to an *in vivo* situation.

III. 6. HLCs can be maintained up to two weeks in the microfluidic device

The results obtained above suggest a dual effect of MM and DM in HLCs' culture. MM enables the observation of responses related to energy metabolism homeostasis, by lowering gene expression, while DM induces a more mature phenotype in HLCs. In addition, it was noticed that HLCs were responsive to insulin and glucagon and adapted their metabolism to fasting, demonstrating their competence for energy metabolism studies. Moreover, HLCs cultured in coverslips coated with commercial type I collagen maintained their phenotype, biotransformation activity, glycogen storage ability and presence of hepatic markers throughout time in culture. Therefore, we proceeded to adapt HLCs to the microfluidic device (MD).

HLCs were inoculated at D17. After 20 minutes, they started to adhere to the microfluidic channel and, after 1 hour, they acquired a polygonal shape (Figure 19).

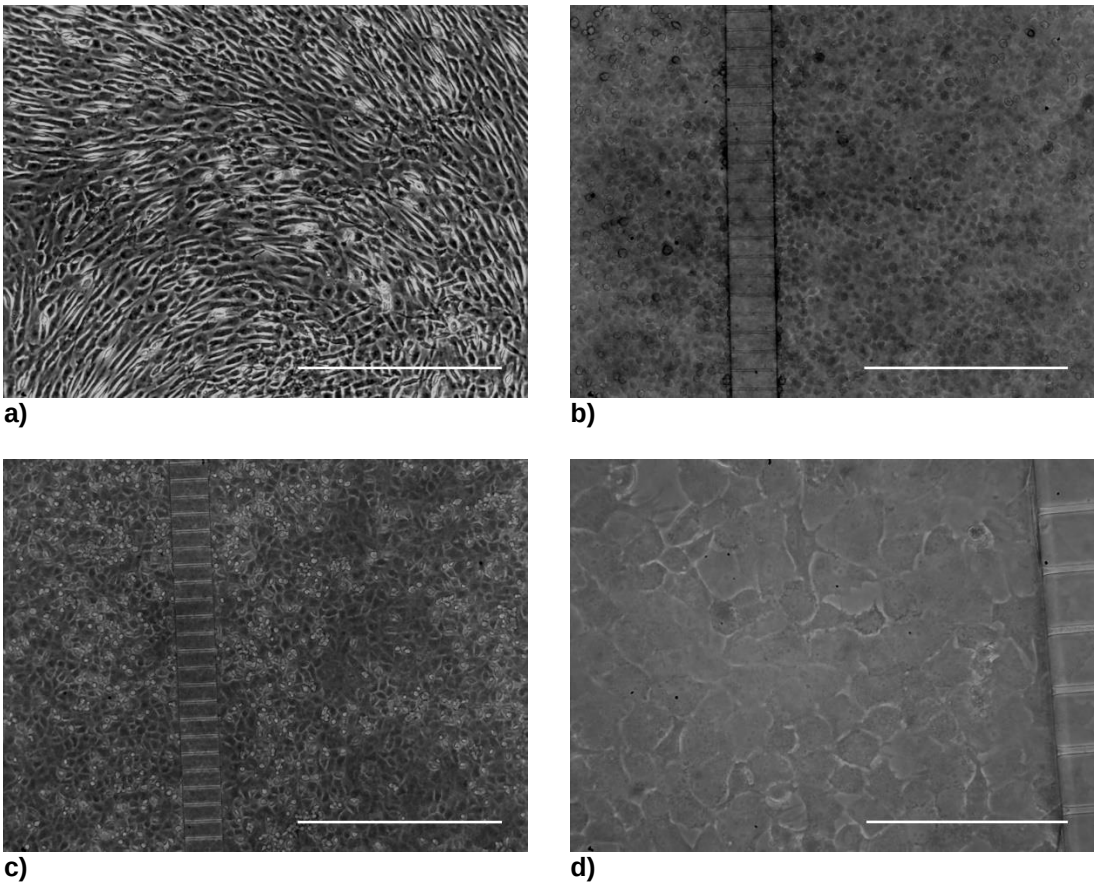

Figure 19 – HLCs morphology at D17 and the change from a fibroblast-like shape to a polygonal shape throughout the day of inoculation, in the microfluidic device: a) HLCs before trypsinization (scale bar = 500 µm); **b) HLCs 20 minutes after device inoculation** (scale bar = 500 µm); **c) HLCs 1 hour after device inoculation** (scale bar = 500 µm); **d) HLCs 2 hours after device inoculation** (scale bar = 100 µm).

Cell loading at high pressures leads to cell damage and death while low pressures cause low cell-cell contact, an important feature to be considered [7], especially in hepatocytes. To avoid such effect, most of the works in this field use a pressure pump that allows a controlled cell loading (always at the same speed and pressure) and a controlled medium flow. However, this was not possible in this particular MD. Cells were loaded manually, which may not result in equal pressure

and velocity of loading among all the inoculations. However, no cell damage was observed when inoculating the cells in our MD and therefore further adopted. The density of cell suspension is also a parameter to be considered when using MDs since high densities lead to channel blocking due to clumping while low densities may cause low cell-cell contact [7]. Moreover, since cell-cell interactions are particularly important in maintaining a functional hepatocyte culture [149], an inoculum that enabled channel confluency and cell adherence throughout time in culture was adopted, *i.e.*, 75 000 cells in 10 µL of medium. These features present the complexity of inoculating MDs highlighting the need for controlling these parameters when working at microscales.

The main goals were to inoculate and verify if HLCs could be maintained in this device until D34 (in MM and DM) in order to develop a model for energy metabolism studies, in the context of the metabolic syndrome. HLCs' morphology at D27 and D34 in the MD is shown in Figure 20.

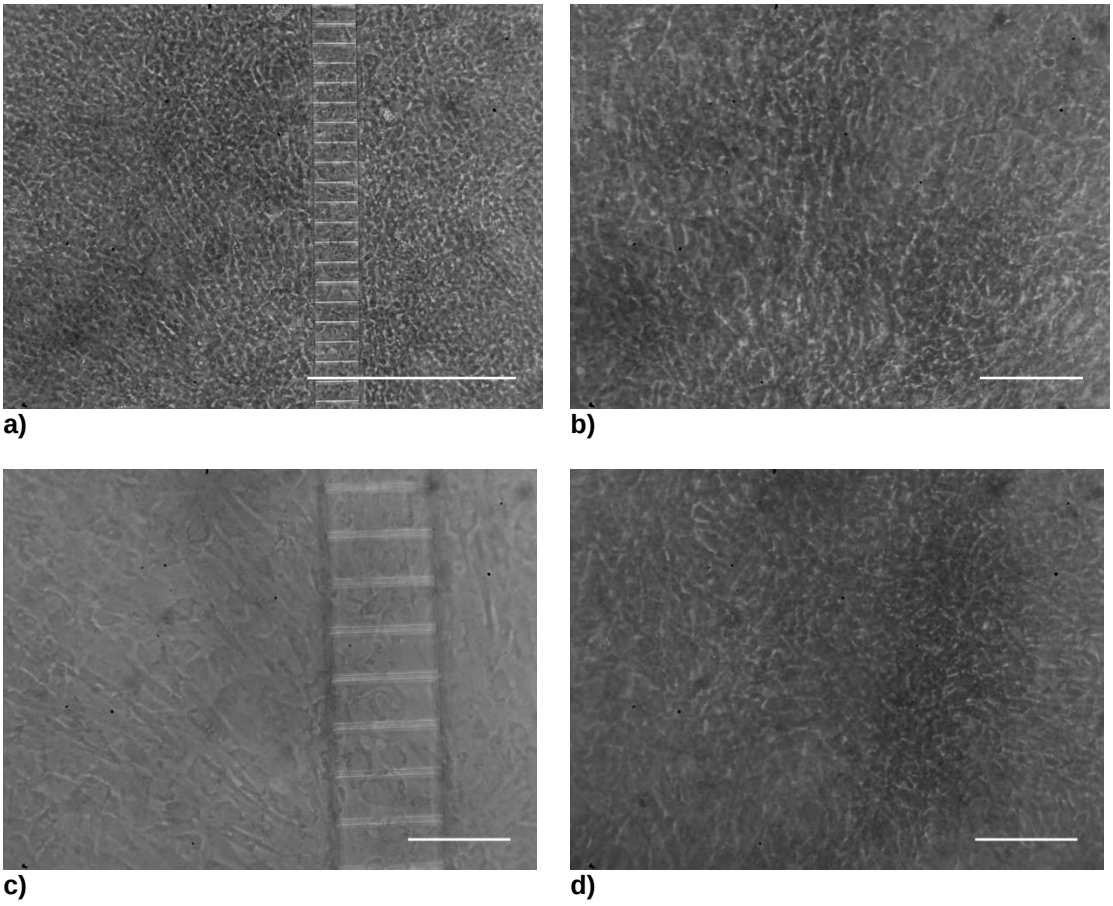

Figure 20 - HLCs' morphology throughout culture time in the MD: **a) HLCs at D27 in MM** (scale bar = 500 µm); **b) HLCs at D27 in DM** (scale bar = 100 µm); **c) HLCs at D34 in MM** (scale bar = 100 µm); **d) HLCs at D34 in DM** (scale bar = 100 µm).

To assess if HLCs in the microfluidic device maintained their phenotype throughout culture time, urea and albumin production were quantified, at D27 and D34, in MM and DM. HLCs cultured in MM showed an increase from D27 to D34 in urea production, while HLCs cultured in DM showed the opposite trend, although non-significant in both media compositions (Figure 21a). There are reports that insulin stimulates albumin production in rat liver cells [150] and our results (Figure 21b) showed that albumin production was higher in DM than in MM, in both days (non-significant). These data suggests the maintenance of a hepatic phenotype in the MD.

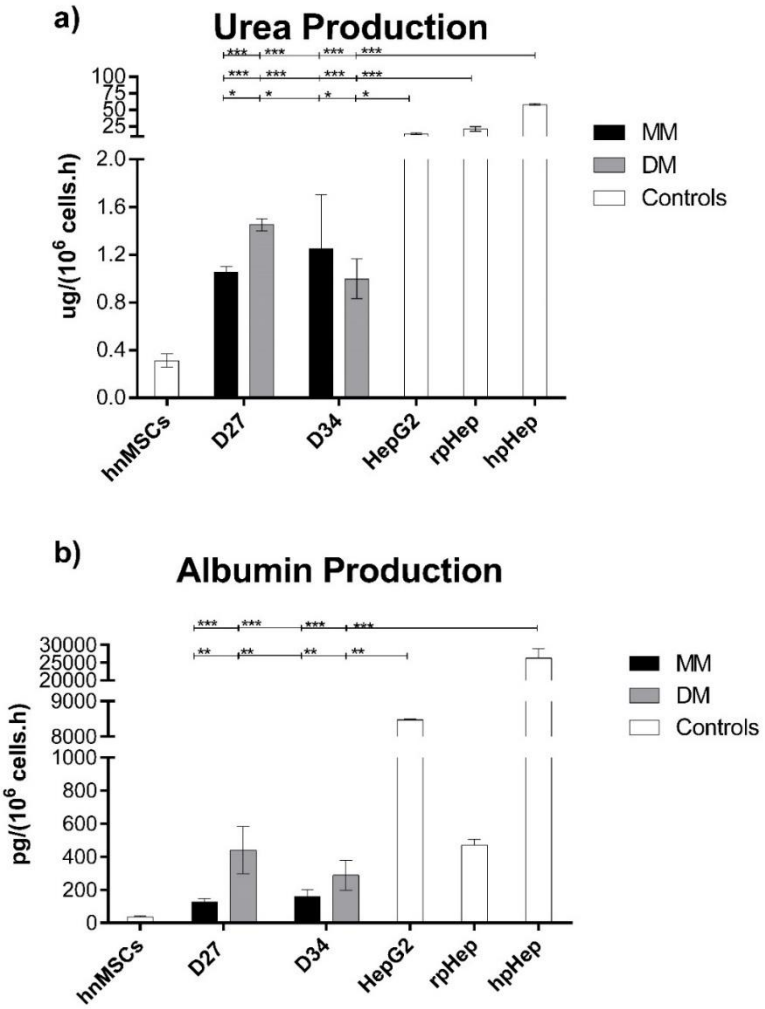

Figure 21 - Effect of culture time on a) urea and **b) albumin production in HLCs cultured in the microfluidic device, in MM and DM at D27 and D34, in the microfluidic device.** Data is represented as Average ± SEM (n=4-5). Undifferentiated hnMSCs and HepG2 cell line, rpHep and hpHep are negative and positive controls, respectively (white bars). *, **, *** Significantly differs among the controls with $p < 0.05$, $p < 0.01$ and $p < 0.001$, respectively.
Abbreviations: rpHep (rat primary hepatocytes), hpHep (human primary hepatocytes) and hnMSC (undifferentiated human neonatal mesenchymal stem cells), MM (maintenance medium), DM (differentiation medium); D27 (day 27 of the differentiation protocol); D34 (day 34 of the differentiation protocol).

Additionally, in order to further understand the evolution of HLCs' characteristics throughout the culture time in the MD, we compared the level of gene expression of D34 relative to D27 (Figure 22), in MM and DM. The influence of MM and DM in gene expression profile of

HLCs cultured in plates was discussed in section III. 3. Thus, the traditional 2D static system was used as a control in this analysis, allowing to compare gene expression in a novel culture system (MD) to a culture system extensively used and optimized (considering HLCs' biotransformation activity and biochemical characteristics) in this laboratory. However, gene expression analysis of HLCs cultured in the MD considered a smaller group of genes, namely *PDK4*, *G6PASE*, *PEPCK*, *PPARA*, *CPT1A*, *ACOX1*, *FXR*, *CYP7A1* and *PGC-1A*, due to lower sample quantity, since each microfluidic device has approximately 150 000 cells. Nevertheless, this subset of genes still includes glycolysis/lipogenesis, gluconeogenesis, fatty acid metabolism, bile acid metabolism and mitochondrial function and biogenesis.

Regarding MM, we observed a decrease in the level of expression from D27 to D34 in all the genes tested, in the MD (Figure 22a). Therefore, the MD did not improve maturation when compared to plates.

In the MD, *PEPCK*, *G6PASE* and *PGC-1A* showed increased expression at D34 compared to D27, when HLCs were maintained in DM (Figure 22b). In particular, *G6PASE* and *PGC-1A* had greater differences ($p < 0.001$) between the two days when compared to plates.

CYP7A1 expression was not detected in HLCs in the device, at D27.

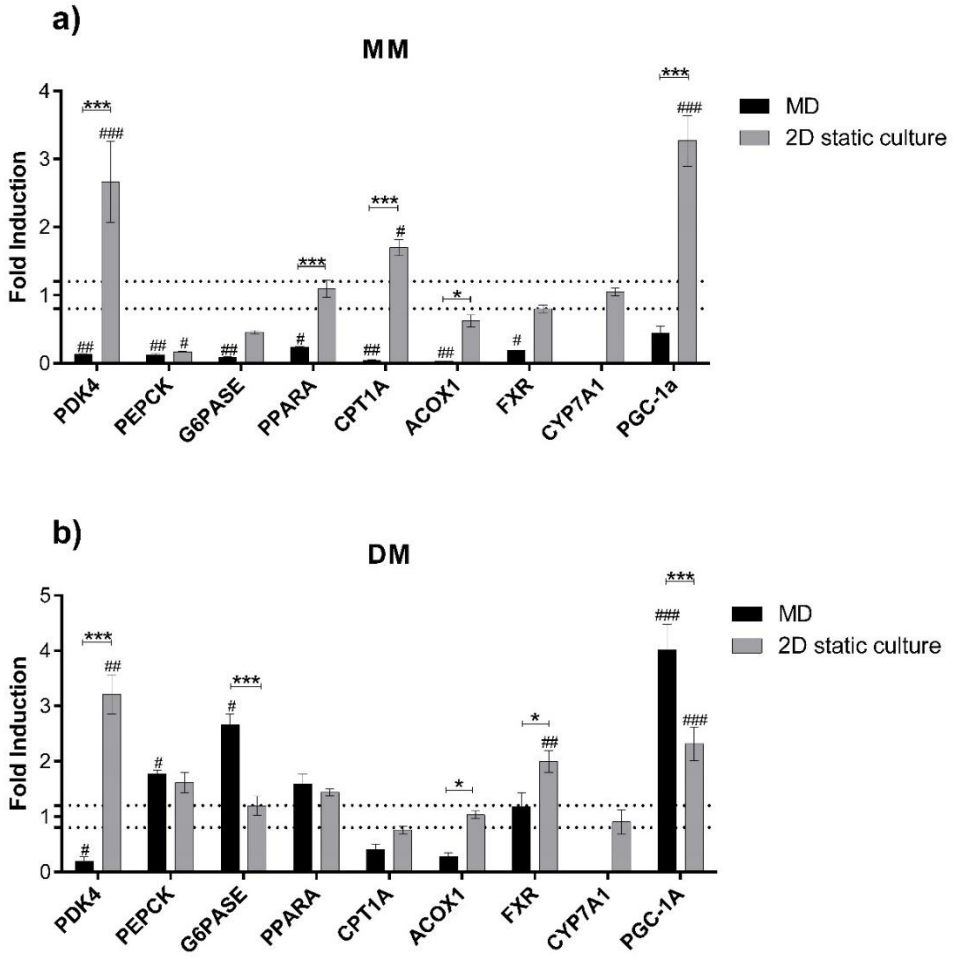

Figure 22 - Gene expression levels in HLCs in the microfluidic device and in plates throughout culture time, in a) MM and **b) DM.** The graphs represent the fold induction regarding gene expression of HLCs in MM and DM at D34 relative to D27. Grid lines represent fold induction equal to 0.8 and 1.2. Data is represented as Average ± SEM (n=2-4). *, **, *** Significantly differs from the different media composition and the days of differentiation with $p < 0.05$, $p < 0.01$ and $p < 0.001$, respectively. $^{\#}$, $^{\#\#}$, $^{\#\#\#}$ Significantly induced or repressed expression with $p < 0.05$, $p < 0.01$ and $p < 0.001$, respectively.
Abbreviations: MD (microfluidic device); MM (maintenance medium); DM (differentiation medium); *PDK4* (pyruvate dehydrogenase kinase 4); *PEPCK* (phosphoenolpyruvate carboxylase); *G6PASE* (glucose-6-phosphatase); *PPARA* (peroxisome proliferator-activated receptor α); *CPT1A* (carnitine palmitoyltransferase 1 α); *ACOX1* (acyl-CoA oxidase 1); *FXR* (farnesoid X receptor); *CYP7A1* (cytochrome P450 enzyme cholesterol 7α-hydroxylase); *PGC-1A* (peroxisome proliferator γ-activated receptor coactivator 1-α).

These data suggest that HLCs present different characteristics when cultured in MD or in standard static 2D cultures. Indeed, in the MD, medium flow is promoted, creating conditions more similar to what happens *in vivo*. Moreover, HLCs were seeded in the MD at a much higher inoculum (450 000 cells/cm^2 in the MD and 30 000 cells/cm^2 in plates). These observations, further highlight the differences between the two culture systems.

As a mean to analyse the differences between these two culture systems, we further compared expression levels of the genes studied above of HLCs cultured in the MD relative to the gene expression of HLCs cultured in plates in MM or in DM (Figure 23), in both days.

HLCs in MM presented higher expression of all the genes, in the MD than in plates, at D27 (Figure 23a). However, at D34, *PGC-1A* continued to show significantly higher expression in the MD ($p < 0.001$) (Figure 23a). *PDK4*, *PEPCK, G6PASE* were also higher expressed at D34 in

the MD than in plates, although not significant. As observed above, *CYP7A1* was not detected at D27 in MM, in MD.

On the other hand, *PDK4* and *CPT1*A had higher expression in MD than in plates, in both days, when in DM (Figure 23b), although only significant for *PDK4* at D27 ($p < 0.01$). However, at D34, the difference in expression between MD and plates decreased. The remaining genes had similar expression in both days, in plates and in MD. *CYP7A1* at D27 was not detected in MD but it was detected in plates, suggesting a possible need for longer adaption of HLCs to the MD.

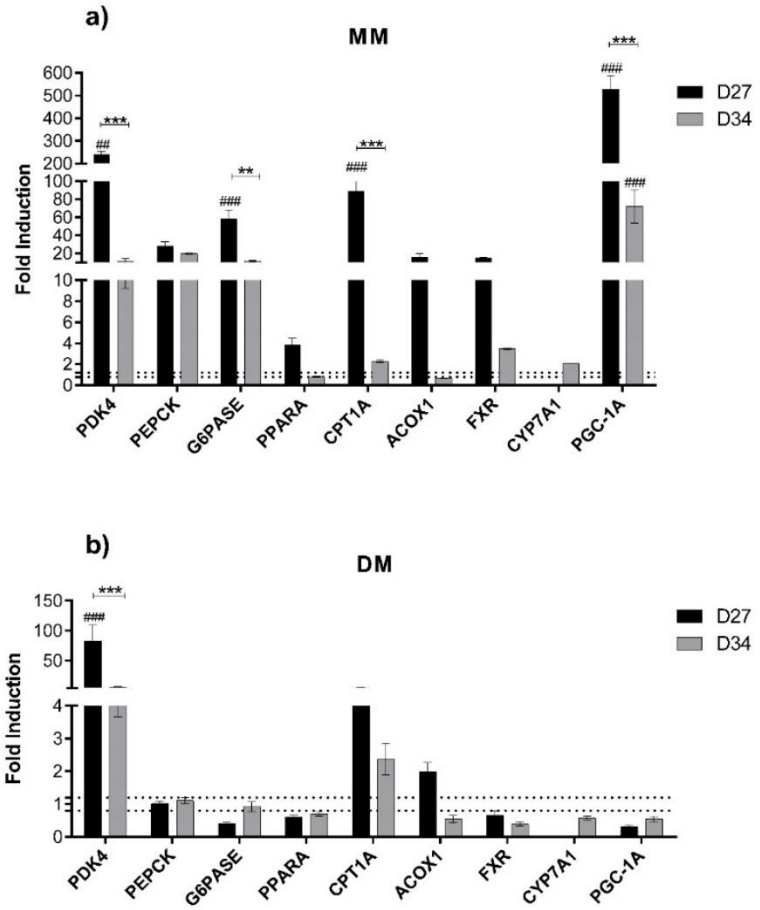

Figure 23 - Gene expression levels in HLCs (D27 and D34) in the microfluidic device relative to plates in a) MM and **b) DM, in both days.** The graphs represent the fold induction regarding gene expression of HLCs cultured in MD relative to plates. Grid lines represent fold induction equal to 0.8 and 1.2. Data is represented as Average ± SEM (n=2-4). *, **, *** Significantly differs from the different media composition and the days of differentiation with $p < 0.05$, $p < 0.01$ and $p < 0.001$, respectively. #, ##, ### Significantly induced or repressed expression with $p < 0.05$, $p < 0.01$ and $p < 0.001$, respectively.
Abbreviations: MD (microfluidic device); MM (maintenance medium); DM (differentiation medium); *PDK4* (pyruvate dehydrogenase kinase 4); *PEPCK* (phosphoenolpyruvate carboxylase); *G6PASE* (glucose-6-phosphatase); *PPARA* (peroxisome proliferator-activated receptor α); *CPT1A* (carnitine palmitoyltransferase 1 α); *ACOX1* (acyl-CoA oxidase 1); *FXR* (farnesoid X receptor); *CYP7A1* (cytochrome P450 enzyme cholesterol 7α-hydroxylase); *PGC-1A* (peroxisome proliferator γ-activated receptor coactivator 1-α).

Finally, to compare the effect between the medium used to maintain HLCs for energy metabolism studies with the medium used in the differentiation protocol, gene expression of HLCs cultured in MM relative to gene expression of HLCs in DM was evaluated in the MD and plates, in both days (Figure 24).

At D27, we observed that all the considered genes presented higher expression in MM compared to DM in the MD, namely *PEPCK* ($p < 0.001$), *G6PASE* ($p < 0.001$), *CPT1A* ($p < 0.01$), *ACOX1* ($p < 0.01$), *PGC-1A* ($p < 0.001$) (Figure 24a). Moreover, these genes and *PPARA* significantly differ in its expression in the MD when compared to plates. At D34, genes related to gluconeogenesis, *G6PASE*, *PEPCK* and *PGC-1A*, continued to be significantly more expressed in the MD ($p < 0.001$) while this set of genes was strongly repressed in plates ($p < 0.01$) (Figure 24b). This observation was possibly due to higher influence of dexamethasone relative to insulin in MM, inducing gluconeogenesis [23], since the ratio of insulin to dexamethasone is 0.01 in this medium condition.

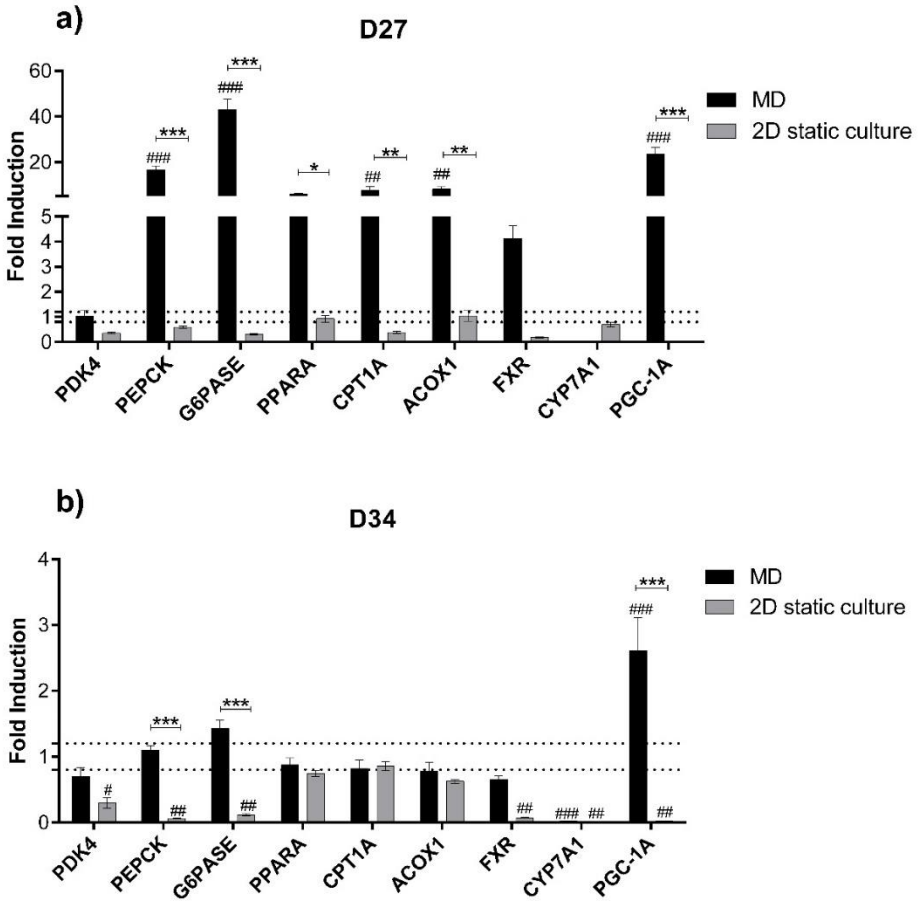

Figure 24 - Gene expression levels in HLCs cultured in the microfluidic device or in 2D static cultures in a) D27 and b) D34. Fold induction of gene expression in HLCs cultured in MM relative to HLCs cultured in DM. Grid lines represent fold induction equal to 0.8 and 1.2. Data is represented as Average ± SEM (n=2-4). *, **, *** Significantly differs from the different media composition and the days of differentiation with $p < 0.05$, $p < 0.01$ and $p < 0.001$, respectively. #, ##, ### Significantly induced or repressed expression with $p < 0.05$, $p < 0.01$ and $p < 0.001$, respectively.
Abbreviations: MD (microfluidic device); MM (maintenance medium); DM (differentiation medium); *PDK4* (pyruvate dehydrogenase kinase 4); *PEPCK* (phosphoenolpyruvate carboxylase); *G6PASE* (glucose-6-phosphatase); *PPARA* (peroxisome proliferator-activated receptor α); *CPT1A* (carnitine palmitoyltransferase 1 α); *ACOX1* (acyl-CoA oxidase 1); *FXR* (farnesoid X receptor); *CYP7A1* (cytochrome P450 enzyme cholesterol 7α-hydroxylase); *PGC-1A* (peroxisome proliferator γ-activated receptor coactivator 1-α).

In summary, some important conclusions can be taken regarding cell culture in this MD:

1. Cell characteristics throughout time in the MD - MM induced higher gene expression at D27, in all genes tested while in plates *PDK4, PPARA*, *CPT1A* and *PGC1-A* were higher expressed at D34. On the other hand, HLCs in DM maintained or enhanced expression of all genes at D34, except for *PDK4*, *CPT1A* and *ACOX1*, while in plates, all genes were higher expressed at D34;
2. MD *vs* static 2D cultures – regarding MM, gene expression in MD at D27 was greater in all genes tested than in plates and at D34, *PDK4*, *PEPCK*, G*6PASE* and *PGC-1A* ($p < 0.001$) continued to have greater expression in the MD. On the other hand, at D27, DM induced greater expression in *PDK4* ($p < 0.001$), *CPT1A* (non-significant) and *ACOX1* (non-significant) in the MD while at D34, just *PDK4* and *CPT1A* continued to have higher expression in the MD;
3. MM *vs* DM in the MD – at D34, *PEPCK*, *G6PASE* and *PGC-1A* ($p < 0.001$) continued to have greater expression in HLCs cultured in MM than in HLCs cultured in DM.

Overall, MM enhanced gene expression in the MD by comparison to 2D static cultures. Although a decrease in expression from D27 to D34 was observed, it was not significant. On the other hand, DM induced higher gene expression in plates from D27 to D34, as seen in chapter III. 2. for most of the genes tested. Therefore, DM, being used for HLCs maturation, is not suitable within the MD.

Concluding, there are differences regarding MD and static 2D culture systems. MM induced higher gene expression in the MD than in plates, at D27. At D34, this trend was not maintained except for genes that regulate gluconeogenesis such as *PEPCK*, *G6PASE* and *PGC-1A*. In fact, higher concentrations of dexamethasone (instead of insulin) in MM induces gluconeogenesis [23]. Thus, opposite trends when comparing HLCs cultured (in the MD and plates) in MM or DM were observed. The differences between these two systems are based on the inoculum and the possibility of creating a flow, by a daily addition of 30 µL of medium from the bottom wells to the upper wells. HLCs in the MD were cultured at a higher inoculum than in plates. In fact, high density cultures (>200 000 cells/cm^2) enhance cell function. In a study performed by Zhang et al, HepG2 seeded at high densities in a microfluidic device presented greater albumin production than 2D static cultures [151]. We can infer that the decrease in concentrations of insulin and dexamethasone (in MM), which are important in the differentiation protocol, may be supplanted by increased cell-to-cell contact in the MD. The enhancement of tight junctions mimics the *in vivo* liver configuration where high density of hepatocytes is in close contact [151]. However, this trend is maintained up to D34 just for a set of genes regulating gluconeogenesis. In addition, fluid friction and shear stress are parameters that further approximate this culture system to liver microenvironment, since *in vivo* liver regeneration is related to portal pressure [152]. Furthermore, cells cultured in MD were maintained in small medium volumes, where diffusion of growth factors and secreted biomolecules is limited because surface-to-volume ratio is very high and molecular diffusion resembles what occurs physiologically [153].

IV. Conclusions and Future Perspectives

To understand the pathophysiological development of the metabolic syndrome, the regulation of energy metabolism in hepatocytes needs to be studied.

The work presented in this thesis showed that if hnMSCs-derived HLCs were changed from a medium already proved to induce a more mature phenotype [86] to a medium with less dexamethasone and insulin (MM), biotransformation activity, glycogen storage, presence of hepatic markers and urea and albumin production could be maintained throughout culture time. However, HLCs cultured in MM could not maintain a stable gene expression, decreasing throughout culture time, from D27 to D34. Indeed, DM induced an increase in gene expression until D34, in plates, leading to a more mature phenotype. Nevertheless, MM allowed testing HLCs response to insulin and glucagon stimuli and their adaptation to fasting. Gluconeogenesis was the pathway that showed more similar responses to the physiological state, being significantly repressed when incubated with insulin and significantly activated in response to glucagon. Some of the genes related to fatty acid oxidation and bile acid metabolism did not respond entirely as expected, although displaying a possible trend of regulation, possibly due to the lack of fatty acids, cholesterol and bile acids in the culture media [144]. In the future, we would like to add these molecules to the medium. Other interesting parameter to be studied would be gene expression in other time points, allowing to further understanding trends of response. In addition, all organs in the human body are in interaction with each other and liver, in particular, is responsible for regulating homeostasis. Therefore, it needs to receive signals from other sources to regulate its metabolism accordingly. Thus, crosstalk between different types of cells is important to observe changes in energy metabolism. Perhaps, this is the reason for most of the studies in the field of metabolism being made in animal models.

Following the energy metabolism studies, HLCs were successfully inoculated into a MD, maintaining functionality during culture time. Thus, a future step of this work would be the study of HLCs response to insulin, glucagon and fasting in the MD. Nevertheless, differences between 2D static culture and MD culture were noticed, namely that most of the genes of HLCs in MM presented higher gene expression in the MD than in plates, in both days. In addition, genes related to gluconeogenesis were higher expressed in HLCs cultured in MM than in HLCs in DM, possibly because MM presents lower insulin effect than DM. However, further information regarding MD culture will be gathered once the response to fasting and to hormone signalling is evaluated in the MD culture.

The differentiation process of hnMSCs into HLCs takes approximately one month. For future studies of cellular interaction, it would also be more convenient to have HLCs ready to be inoculated. Therefore, we tried to inoculate cryopreserved HLCs [154] into MDs. However, we could not reproduce the process (data not shown). The process of thawing of HLCs and posterior inoculation of the MD still needs to be optimized since these cells did not present the same characteristics as freshly differentiated HLCs. In fact, cryopreserved hepatocytes do not have the same functional levels and do not demonstrate the same morphology as freshly isolated ones [155].

Cryopreserved cells are more sensitive and need more time to adhere, being not yet compatible with the timing of the MD operation, at the day of inoculation. In the future, we intend to optimize the inoculation of cryopreserved HLCs into MDs and also adapt these cells to study metabolic responses.

In conclusion, this work demonstrates that HLCs obtained by a specific differentiation protocol are capable of responding to insulin and to glucagon and to adapt their metabolism to fasting. Although the medium composition should be optimized in order to better mimic the composition of blood in the human body, containing additional biomolecules [144], we could successfully inoculate these cells into a MD and maintain them for up to two weeks. We hope that future studies in the context of metabolic syndrome using HLCs and other relevant cell types, such as adipocytes and myofibroblasts, in similar MDs, will be useful to create a better understanding of this pathology and thus designing therapeutic strategies.

V. References

1. Normal Liver Physiology. http://biomed.brown.edu/Courses/BI108/BI108_2002_Groups/liver/webpage/NormalLiver.htm. Accessed February 17, 2016.
2. Rui L. Energy Metabolism in the Liver. *NIH Public Access*. 2014;72(2):181-204. doi:10.1038/nature13314.A.
3. Mazzoleni G, Steimberg N. New Models for the In Vitro Study of Liver Toxicity : 3D Culture Systems and the Role of Bioreactors. *Intechopen*. 2009.
4. Chemistry for Biologists: Excretion and the liver. http://www.rsc.org/Education/Teachers/Resources/cfb/excretion.htm.
5. Physiology and Pathophysiology of liver inflammation, damage and repair. http://www.jpp.krakow.pl/journal/archive/08_08_s1/pdf/107_08_08_s1_article.pdf. Accessed February 17, 2016.
6. Godoy P, Hewitt NJ, Albrecht U, et al. Recent advances in 2D and 3D in vitro systems using primary hepatocytes, alternative hepatocyte sources and non-parenchymal liver cells and their use in investigating mechanisms of hepatotoxicity, cell signaling and ADME. *Arch Toxicol*. 2013;87(8):1315-1530. doi:10.1007/s00204-013-1078-5.
7. Bettinger C, Borenstein JT, Tao SL. *Microfluidic Cell Culture Systems*. Elsevier, William Andrew; 2013.
8. Bilirubin. http://chemistry.elmhurst.edu/vchembook/634bilirubin.html.
9. Naito M, Hasegawa G, Ebe Y, Yamamoto T. Differentiation and function of Kupffer cells. *Med Electron Microsc*. 2004;37(1):16-28. doi:10.1007/s00795-003-0228-x.
10. Hepatic Histology: Hepatocytes. http://www.vivo.colostate.edu/hbooks/pathphys/digestion/liver/histo_hcytes.html. Accessed April 4, 2016.
11. Gissen P, Arias IM. Structural and functional hepatocyte polarity and liver disease. *J Hepatol*. 2015;63(4):1023-1037. doi:10.1016/j.jhep.2015.06.015.
12. Treyer A, Müsch A. Hepatocyte polarity. *Compr Physiol*. 2013;3(1):243-287. doi:10.1002/cphy.c120009.
13. Karim S, Adams DH, Lalor PF. Hepatic expression and cellular distribution of the glucose transporter family. *World J Gastroenterol*. 2012;18(46):6771-6781. doi:10.3748/wjg.v18.i46.6771.
14. Berg J, Tymoczko J, Stryer L. Biochemistry. *Biochemistry*. 2002. http://www.ncbi.nlm.nih.gov/books/NBK21154/.
15. Desvergne B, Michalik L, Wahli W. Transcriptional regulation of metabolism. *Physiol Rev*. 2006;86(2):465-514. doi:10.1152/physrev.00025.2005.
16. Saltiel AR, Kahn CR. Insulin signalling and the regulation of glucose and lipid metabolism. *Nature*. 2001;414(6865):799-806. doi:10.1038/414799a.
17. Jiang G, Zhang BB. Glucagon and regulation of glucose metabolism. *AmJPhysiol EndocrinolMetab*. 2003;284(4):E671-E678. http://www.ncbi.nlm.nih.gov/pubmed/12626323.
18. Jeong JY, Jeoung NH, Park K-G, Lee I-K. Transcriptional regulation of pyruvate dehydrogenase kinase. *Diabetes Metab J*. 2012;36(5):328-335. doi:10.4093/dmj.2012.36.5.328.
19. Jeoung NH, Wu P, Joshi MA, et al. Role of pyruvate dehydrogenase kinase isoenzyme 4 (PDHK4) in glucose homoeostasis during starvation. *Biochem J*. 2006;397(3):417-425. doi:10.1042/BJ20060125.
20. Yoon JC, Puigserver P, Chen G, et al. Control of hepatic gluconeogenesis through the transcriptional coactivator PGC-1. *Nature*. 2001;413(6852):131-138. doi:10.1038/35093050.
21. Burgess SC, Hausler N, Merritt M, et al. Impaired Tricarboxylic Acid Cycle Activity in Mouse Livers Lacking Cytosolic Phosphoenolpyruvate Carboxykinase. *J Biol Chem*. 2004;279(47):48941-48949. doi:10.1074/jbc.M407120200.
22. Mutel E, Abdul-Wahed A, Ramamonjisoa N, et al. Targeted deletion of liver glucose-6 phosphatase mimics glycogen storage disease type 1a including development of multiple adenomas. *J Hepatol*. 2011;54(3):529-537. doi:10.1016/j.jhep.2010.08.014.
23. Herzig S, Long F, Jhala US, et al. CREB regulates hepatic gluconeogenesis through the coactivator PGC-1. *Nature*. 2001;413(6852):179-183. doi:10.1038/35093131.

24. Li X, Monks B, Ge Q, Birnbaum MJ. Akt/PKB regulates hepatic metabolism by directly inhibiting PGC-1alpha transcription coactivator. *Nature*. 2007;447(7147):1012-1016. doi:10.1038/nature05861.
25. Iizuka K, Bruick RK, Liang G, Horton JD, Uyeda K. Deficiency of carbohydrate response element-binding protein (ChREBP) reduces lipogenesis as well as glycolysis. *Proc Natl Acad Sci U S A*. 2004;101(19):7281-7286. doi:10.1073/pnas.0401516101.
26. Wan M, Leavens KF, Saleh D, et al. Postprandial hepatic lipid metabolism requires signaling through Akt2 independent of the transcription factors FoxA2, FoxO1, and SREBP1c. *Cell Metab*. 2011;14(4):516-527. doi:10.1016/j.cmet.2011.09.001.
27. Longuet C, Sinclair EM, Maida A, et al. The glucagon receptor is required for the adaptive metabolic response to fasting. *Cell Metab*. 2008;8(5):359-371. doi:10.1016/j.cmet.2008.09.008.
28. Kersten S, Seydoux J, Peters JM, Gonzalez FJ, Desvergne B, Wahli W. Peroxisome proliferator-activated receptor alpha mediates the adaptive response to fasting. *J Clin Invest*. 1999;103(11):1489-1498. doi:10.1172/JCI6223.
29. Vega RB, Huss JM, Kelly DP. The coactivator PGC-1 cooperates with peroxisome proliferator-activated receptor alpha in transcriptional control of nuclear genes encoding mitochondrial fatty acid oxidation enzymes. *Mol Cell Biol*. 2000;20(5):1868-1876. http://www.ncbi.nlm.nih.gov/pubmed/10669761. Accessed August 29, 2016.
30. Bellafante E, Murzilli S, Salvatore L, Latorre D, Villani G, Moschetta A. Hepatic-specific activation of peroxisome proliferator-activated receptor γ coactivator-1β protects against steatohepatitis. *Hepatology*. 2013;57(4):1343-1356. doi:10.1002/hep.26222.
31. Hernandez C, Lin JD, Finck BN, et al. A sweet path to insulin resistance through PGC-1beta. *Cell Metab*. 2009;9(3):215-216. doi:10.1016/j.cmet.2009.02.001.
32. Lelliott CJ, Medina-Gomez G, Petrovic N, et al. Ablation of PGC-1beta results in defective mitochondrial activity, thermogenesis, hepatic function, and cardiac performance. *PLoS Biol*. 2006;4(11):e369. doi:10.1371/journal.pbio.0040369.
33. Burri L, Thoresen GH, Berge RK, Burri L, Thoresen GH, Berge RK. The Role of PPARα Activation in Liver and Muscle. *PPAR Res*. 2010;2010. doi:10.1155/2010/542359.
34. Fan C-Y, Pan J, Chu R, et al. Hepatocellular and Hepatic Peroxisomal Alterations in Mice with a Disrupted Peroxisomal Fatty Acyl-coenzyme A Oxidase Gene. *J Biol Chem*. 1996;271(40):24698-24710. doi:10.1074/jbc.271.40.24698.
35. Reddy JK, Hashimoto T. Peroxisomal beta-oxidation and peroxisome proliferator-activated receptor alpha: an adaptive metabolic system. *Annu Rev Nutr*. 2001;21:193-230. doi:10.1146/annurev.nutr.21.1.193.
36. De Fabiani E, Mitro N, Gilardi F, Galmozzi A, Caruso D, Crestani M. When Food Meets Man: the Contribution of Epigenetics to Health. *Nutrients*. 2010;2(5):551-571. doi:10.3390/nu2050551.
37. Staels B, Fonseca VA. Bile acids and metabolic regulation: mechanisms and clinical responses to bile acid sequestration. *Diabetes Care*. 2009;32 Suppl 2(Suppl 2):S237-45. doi:10.2337/dc09-S355.
38. Duran-Sandoval D, Mautino G, Martin G, et al. Glucose regulates the expression of the farnesoid X receptor in liver. *Diabetes*. 2004;53(4):890-898. doi:10.2337/diabetes.53.4.890.
39. Park W-H, Pak YK. Insulin-dependent suppression of cholesterol 7α-hydroxlase is a possible link between glucose and cholesterol metabolisms. *Exp Mol Med*. 2011;43(10):571-579. doi:10.3858/emm.2011.43.10.064.
40. Zhang Y, Castellani LW, Sinal CJ, Gonzalez FJ, Edwards PA. Peroxisome proliferator-activated receptor-gamma coactivator 1alpha (PGC-1alpha) regulates triglyceride metabolism by activation of the nuclear receptor FXR. *Genes Dev*. 2004;18(2):157-169. doi:10.1101/gad.1138104.
41. Kanaya E, Shiraki T, Jingami H. The nuclear bile acid receptor FXR is activated by PGC-1alpha in a ligand-dependent manner. *Biochem J*. 2004;382(Pt 3):913-921. doi:10.1042/BJ20040432.
42. Lefebvre P, Cariou B, Lien F, Kuipers F, Staels B. Role of bile acids and bile acid receptors in metabolic regulation. *Physiol Rev*. 2009;89(1):147-191. doi:10.1152/physrev.00010.2008.
43. Alberti SG, Zimmet P, Shaw J, Grundy SM. The IDF Consensus Worldwide Definition of the Metabolic Syndrom. 2006:24. https://www.idf.org/webdata/docs/IDF_Meta_def_final.pdf.
44. Shimano H. Pathophysiology of metabolic syndrome. *Nippon rinsho Japanese J Clin Med*. 2004;62(6):1029-1035. doi:10.1097/MAJ.0b013e31823ea214.

45. Miranda JP, Filipe E, Fernandes AS, et al. The human umbilical cord tissue-derived MSC population UCX® promotes early motogenic effects on keratinocytes and fibroblasts and G-CSF-mediatedmobilization of BM-MSCS when transplanted in vivo. *Cell Transplant*. 2015;24(5):865-877. doi:10.3727/096368913X676231.
46. Santos JM, Camões SP, Filipe E, et al. 3D spheroid cell culture of umbilical cord tissue-derived MSCs (UCX®) leads to enhanced paracrine induction of wound healing. *Stem Cell Res Ther*. 2015;6(1):90. doi:10.1186/s13287-015-0082-5.
47. Takahashi K, Tanabe K, Ohnuki M, et al. Induction of Pluripotent Stem Cells from Adult Human Fibroblasts by Defined Factors. *Cell*. 2007;131(5):861-872. doi:10.1016/j.cell.2007.11.019.
48. Medvedev SP, Shevchenko AI, Zakian SM. Induced Pluripotent Stem Cells: Problems and Advantages when Applying them in Regenerative Medicine. *Acta Naturae*. 2010;2(2):18-28. http://www.ncbi.nlm.nih.gov/pubmed/22649638. Accessed September 10, 2016.
49. Vojnits K, Bremer S. Challenges of using pluripotent stem cells for safety assessments of substances. *Toxicology*. 2010;270(1):10-17. doi:10.1016/j.tox.2009.12.003.
50. Moise KJ. Umbilical Cord Stem Cells. *Obstet Gynecol*. 2005;106(6):1393-1407. doi:10.1097/01.AOG.0000188388.84901.e4.
51. Hordyjewska A, Popiołek Ł, Horecka A. Characteristics of hematopoietic stem cells of umbilical cord blood. *Cytotechnology*. 2015;67(3):387-396. doi:10.1007/s10616-014-9796-y.
52. Campagnoli C, Roberts IAG, Kumar S, Bennett PR, Bellantuono I, Fisk NM. Identification of mesenchymal stem / progenitor cells in human first-trimester fetal blood , liver , and bone marrow. 2015;98(8):2396-2403.
53. Jiang Y, Jahagirdar BN, Reinhardt RL, et al. Pluripotency of mesenchymal stem cells derived from adult marrow. *Nature*. 2002;418(6893):41-49. doi:10.1038/nature05812.
54. In 't Anker PS, Scherjon SA, Kleijburg-van der Keur C, et al. Isolation of mesenchymal stem cells of fetal or maternal origin from human placenta. *Stem Cells*. 2004;22(7):1338-1345. doi:10.1634/stemcells.2004-0058.
55. Zuk, PA E Al. Multilineage cells from human adipose tissue: implications for cell-based therapies. *Tissue Eng*. 2001;7(2):211-228. doi:10.1089/107632701300062859.
56. Zvaifler NJ, Marinova-Mutafchieva L, Adams G, et al. Mesenchymal precursor cells in the blood of normal individuals. *Arthritis Res*. 2000;2(6):477-488. doi:10.1186/ar130.
57. Erices a, Conget P, Minguell JJ. Mesenchymal progenitor cells in human umbilical cord blood. *Br J Haematol*. 2000;109(1):235-242. doi:10.1046/j.1365-2141.2000.01986.x.
58. Buyl K, De Kock J, Najar M, et al. Characterization of hepatic markers in human Wharton's Jelly-derived mesenchymal stem cells. *Toxicol In Vitro*. 2014;28(1):113-119. doi:10.1016/j.tiv.2013.06.014.
59. Secco M, Zucconi E, Vieira NM, et al. Multipotent Stem Cells from Umbilical Cord: Cord Is Richer than Blood! *Stem Cells*. 2008;26(1):146-150. doi:10.1634/stemcells.2007-0381.
60. Dominici M, Le Blanc K, Mueller I, et al. Minimal criteria for defining multipotent mesenchymal stromal cells. The International Society for Cellular Therapy position statement. *Cytotherapy*. 2006;8(4):315-317. doi:10.1080/14653240600855905.
61. Friedenstein a J, Piatetzky-Shapiro II, Petrakova K V. Osteogenesis in transplants of bone marrow cells. *J Embryol Exp Morphol*. 1966;16(3):381-390.
62. La Rocca G, Anzalone R, Corrao S, et al. Isolation and characterization of Oct-4+/HLA-G+ mesenchymal stem cells from human umbilical cord matrix: Differentiation potential and detection of new markers. *Histochem Cell Biol*. 2009;131(2):267-282. doi:10.1007/s00418-008-0519-3.
63. Zeddou M, Briquet A, Relic B, et al. The umbilical cord matrix is a better source of mesenchymal stem cells (MSC) than the umbilical cord blood. *Cell Biol Int*. 2010;34(7):693-701. doi:10.1042/CBI20090414.
64. Snykers S, Vanhaecke T, De Becker A, et al. Chromatin remodeling agent trichostatin A: a key-factor in the hepatic differentiation of human mesenchymal stem cells derived of adult bone marrow. *BMC Dev Biol*. 2007;7:24. doi:10.1186/1471-213X-7-24.
65. Dong X, Pan R, Zhang H, Yang C, Shao J, Xiang L. Modification of histone acetylation facilitates hepatic differentiation of human bone marrow mesenchymal stem cells. *PLoS One*. 2013;8(5):e63405. doi:10.1371/journal.pone.0063405.
66. Li X, Yuan J, Li W, et al. Direct Differentiation of Homogeneous Human Adipose Stem Cells Into Functional Hepatocytes by Mimicking Liver Embryogenesis. *J Cell Physiol*. 2014;229(6):801-812. doi:10.1002/jcp.24501.

67. Campard D, Lysy PA, Najimi M, Sokal EM. Native Umbilical Cord Matrix Stem Cells Express Hepatic Markers and Differentiate Into Hepatocyte-like Cells. *Gastroenterology*. 2008;134(3):833-848. doi:10.1053/j.gastro.2007.12.024.
68. Zorn AM. Liver Development. *StemBook*. October 2008. doi:10.3824/stembook.1.25.1.
69. Tremblay KD, Zaret KS. Distinct populations of endoderm cells converge to generate the embryonic liver bud and ventral foregut tissues. *Dev Biol*. 2005;280(1):87-99. doi:10.1016/j.ydbio.2005.01.003.
70. Shen MM. Nodal signaling: developmental roles and regulation. *Development*. 2007;134(6):1023-1034. doi:10.1242/dev.000166.
71. Calmont A, Wandzioch E, Tremblay KD, et al. An FGF response pathway that mediates hepatic gene induction in embryonic endoderm cells. *Dev Cell*. 2006;11(3):339-348. doi:10.1016/j.devcel.2006.06.015.
72. Shen MM. Nodal signaling: developmental roles and regulation. *Development*. 2007;134(6):1023-1034. doi:10.1242/dev.000166.
73. McLin V a, Rankin S a, Zorn AM. Repression of Wnt/beta-catenin signaling in the anterior endoderm is essential for liver and pancreas development. *Development*. 2007;134(12):2207-2217. doi:10.1242/dev.001230.
74. Rossi JM, Dunn NR, Hogan BL, Zaret KS. Distinct mesodermal signals, including BMPs from the septum transversum mesenchyme, are required in combination for hepatogenesis from the endoderm. *Genes Dev*. 2001;15(15):1998-2009. doi:10.1101/gad.904601.
75. Ameri J, Ståhlberg A, Pedersen J, et al. FGF2 Specifies hESC-Derived Definitive Endoderm into Foregut/Midgut Cell Lineages in a Concentration-Dependent Manner. *Stem Cells*. 2009;28(1):N/A-N/A. doi:10.1002/stem.249.
76. Bort R, Signore M, Tremblay K, Martinez Barbera JP, Zaret KS. Hex homeobox gene controls the transition of the endoderm to a pseudostratified, cell emergent epithelium for liver bud development. *Dev Biol*. 2006;290(1):44-56. doi:10.1016/j.ydbio.2005.11.006.
77. Rossi JM, Dunn NR, Hogan BL, Zaret KS. Distinct mesodermal signals, including BMPs from the septum transversum mesenchyme, are required in combination for hepatogenesis from the endoderm. *Genes Dev*. 2001;15(15):1998-2009. doi:10.1101/gad.904601.
78. Wang Z, Dollé P, Cardoso W V., Niederreither K. Retinoic acid regulates morphogenesis and patterning of posterior foregut derivatives. *Dev Biol*. 2006;297(2):433-445. doi:10.1016/j.ydbio.2006.05.019.
79. Liver development | StemBook. http://www.stembook.org/node/512.html. Accessed March 20, 2016.
80. Chivu M, Dima SO, Stancu CI, et al. In vitro hepatic differentiation of human bone marrow mesenchymal stem cells under differential exposure to liver-specific factors. *Transl Res*. 2009;154(3):122-132. doi:10.1016/j.trsl.2009.05.007.
81. Kamiya A, Kinoshita T, Miyajima A. Oncostatin M and hepatocyte growth factor induce hepatic maturation via distinct signaling pathways. *FEBS Lett*. 2001;492(1-2):90-94. doi:10.1016/S0014-5793(01)02140-8.
82. Michalopoulos GK, Bowen WC, Mulè K, Luo J. HGF-, EGF-, and dexamethasone-induced gene expression patterns during formation of tissue in hepatic organoid cultures. *Gene Expr*. 2003;11(2):55-75. http://www.ncbi.nlm.nih.gov/pubmed/12837037. Accessed August 7, 2016.
83. Santos NC, Figueira-Coelho J, Martins-Silva J, Saldanha C. Multidisciplinary utilization of dimethyl sulfoxide: Pharmacological, cellular, and molecular aspects. *Biochem Pharmacol*. 2003;65(7):1035-1041. doi:10.1016/S0006-2952(03)00002-9.
84. Alizadeh E, Zarghami N, Eslaminejad MB, Akbarzadeh A, Barzegar A, Mohammadi SA. The effect of dimethyl sulfoxide on hepatic differentiation of mesenchymal stem cells. *Artif cells, nanomedicine, Biotechnol*. 2014;(May):1-8. doi:10.3109/21691401.2014.928778.
85. Liu W, Liu Z, You N, et al. Several Important In Vitro Improvements in the Amplification, Differentiation and Tracing of Fetal Liver Stem/Progenitor Cells. Kerkis I, ed. *PLoS One*. 2012;7(10):e47346. doi:10.1371/journal.pone.0047346.
86. Cipriano M, Correia J, Castro M, Santos JM, Miranda JP. The Role of Epigenetic Modifiers on Extended Cultures of Functional Hepatocyte-Like Cells Derived From hnMSCs. *Arch Toxicol*. 2016. Epub ahead of prin
87. Snykers S, Vanhaecke T, De Becker A, et al. Chromatin remodeling agent trichostatin A: a key-factor in the hepatic differentiation of human mesenchymal stem cells derived of adult bone marrow. *BMC Dev Biol*.

2007;7(August):24. doi:10.1186/1471-213X-7-24.
88. Eberharter A, Becker PB. Histone acetylation: a switch between repressive and permissive chromatin. Second in review series on chromatin dynamics. *EMBO Rep*. 2002;3(3):224-229. doi:10.1093/embo-reports/kvf053.
89. Chetty S, Pagliuca FW, Honore C, Kweudjeu A, Rezania A, Melton DA. A simple tool to improve pluripotent stem cell differentiation. *Nat Methods*. 2013;10(6):553-556. doi:10.1038/nmeth.2442.
90. Calder A, Roth-Albin I, Bhatia S, et al. Lengthened G1 Phase Indicates Differentiation Status in Human Embryonic Stem Cells. *Stem Cells Dev*. 2012;22(2):120829080827006. doi:10.1089/scd.2012.0168.
91. Seeliger C, Culmes M, Schyschka L, et al. Decrease of global methylation improves significantly hepatic differentiation of Ad-MSCs: Possible future application for urea detoxification. *Cell Transplant*. 2013;22(1):119-131. doi:10.3727/096368912X638946.
92. Yoshida Y, Shimomura T, Sakabe T, et al. A role of Wnt/beta-catenin signals in hepatic fate specification of human umbilical cord blood-derived mesenchymal stem cells. *Am J Physiol Gastrointest Liver Physiol*. 2007;293(5):G1089-98. doi:10.1152/ajpgi.00187.2007.
93. Santi D V, Norment A, Garrett CE. Covalent bond formation between a DNA-cytosine methyltransferase and DNA containing 5-azacytosine. *Proc Natl Acad Sci U S A*. 1984;81(22):6993-6997. http://www.ncbi.nlm.nih.gov/pubmed/6209710. Accessed August 21, 2016.
94. Komashko VM, Farnham PJ. 5-Azacytidine Treatment Reorganizes Genomic Histone Modification Patterns. *Epigenetics*. 2010;5(3):229-240. doi:10.4161/epi.5.3.11409.
95. The 3Rs. https://www.nc3rs.org.uk/the-3rs.
96. Miranda J, Cipriano M, Castro M. Self-Assembled 3D Spheroids and Hollow-fibre Bioreactors improve MSC-Derived Hepatocyte-Like Cell Maturation In Vitro. *Arch Toxicol*. 2016.
97. Beebe DJ, Ingber Cde DE, Den Toonder J. Organs on Chips. *Lab Chip*. 2013;13. doi:10.1039/c3lc90080k.
98. Overview of Pharmacokinetics - Clinical Pharmacology - Merck Manuals Professional Edition. http://www.merckmanuals.com/professional/clinical-pharmacology/pharmacokinetics/overview-of-pharmacokinetics.
99. Sung JH, Kam C, Shuler ML. A microfluidic device for a pharmacokinetic–pharmacodynamic (PK–PD) model on a chip. *Lab Chip*. 2010;10(4):446. doi:10.1039/b917763a.
100. Overview of Pharmacodynamics - Clinical Pharmacology - Merck Manuals Professional Edition. http://www.merckmanuals.com/professional/clinical-pharmacology/pharmacodynamics/overview-of-pharmacodynamics.
101. Lee PJ, Hung PJ, Lee LP. An artificial liver sinusoid with a microfluidic endothelial-like barrier for primary hepatocyte culture. *Biotechnol Bioeng*. 2007;97(5):1340-1346. doi:10.1002/bit.21360.
102. Chao P, Maguire T, Novik E, Cheng K-C, Yarmush ML. Evaluation of a microfluidic based cell culture platform with primary human hepatocytes for the prediction of hepatic clearance in human. *Biochem Pharmacol*. 2009;78(6):625-632. doi:10.1016/j.bcp.2009.05.013.
103. Patel D, Haque A, Gao Y, Revzin A. Using reconfigurable microfluidics to study the role of HGF in autocrine and paracrine signaling of hepatocytes. *Integr Biol (Camb)*. 2015;7(7):815-824. doi:10.1039/c5ib00105f.
104. Novik E, Maguire TJ, Chao P, Cheng KC, Yarmush ML. A microfluidic hepatic coculture platform for cell-based drug metabolism studies. *Biochem Pharmacol*. 2010;79(7):1036-1044. doi:10.1016/j.bcp.2009.11.010.
105. Gori M, Simonelli MC, Giannitelli SM, Businaro L, Trombetta M, Rainer A. Investigating Nonalcoholic Fatty Liver Disease in a Liver-on-a-Chip Microfluidic Device. *PLoS One*. 2016;11(7):e0159729. doi:10.1371/journal.pone.0159729.
106. Maschmeyer I, Lorenz AK, Schimek K, et al. From chip-in-a-lab to lab-on-a-chip: towards a single handheld electronic system for multiple application-specific lab-on-a-chip (ASLOC). 2014. doi:10.1039/c5lc00392j.
107. TissUse • Emulating Human Biology. http://www.tissuse.com/index.html.
108. Maschmeyer I, Hasenberg T, Jaenicke A, et al. Chip-based human liver–intestine and liver–skin co-cultures – A first step toward systemic repeated dose substance testing in vitro. *Eur J Pharm Biopharm*. 2015;95:77-87. doi:10.1016/j.ejpb.2015.03.002.
109. Technology & Science - Xona Microfluidics. http://xonamicrofluidics.com/about/technology-science/.
110. NHLBI N. What Is Metabolic Syndrome? http://www.nhlbi.nih.gov/health/health-topics/topics/ms.
111. Bhatia SN, Ingber DE. Microfluidic organs-on-chips. *Nat Biotechnol*. 2014;32(8):760-772.

doi:10.1038/nbt.2989.

112. Ferris HA, Kahn CR, Barnes P, et al. New mechanisms of glucocorticoid-induced insulin resistance: make no bones about it. *J Clin Invest*. 2012;122(11):3854-3857. doi:10.1172/JCI66180.
113. Miranda JP, Leite SB, Teixeira AP, et al. Merging bioreactor technology with 3D hepatocyte-fibroblast culturing approaches: Improved in vitro models for toxicological applications. *Toxicol Vitr*. 2009;25(4):825-832. doi:10.1016/j.tiv.2011.02.002.
114. Rajan N, Habermehl J, Coté M-F, Doillon CJ, Mantovani D. Preparation of ready-to-use, storable and reconstituted type I collagen from rat tail tendon for tissue engineering applications. *Nat Protoc*. 2006;1(6):2753-2758. doi:10.1038/nprot.2006.430.
115. Estall JL, Ruas JL, Choi CS, et al. PGC-1alpha negatively regulates hepatic FGF21 expression by modulating the heme/Rev-Erb(alpha) axis. *Proc Natl Acad Sci U S A*. 2009;106(52):22510-22515. doi:10.1073/pnas.0912533106.
116. Martínez-redondo V, Agudelo LZ, Sinha I, Zierath JR, Groen AK, Ruas JL. Correia et al, 2015. 2015.
117. Wilkening S, Stahl F, Bader A. Comparison of primary human hepatocytes and hepatoma cell line HepG2 with regard to their biotransformation properties. *Drug Metab Dispos*. 2003;31(8):1035-1042. doi:10.1124/dmd.31.8.1035.
118. Donato MT, Gomez-Lechon MJ, Castell J V. A microassay for measuring cytochrome P450IA1 and P450IIB1 activities in intact human and rat hepatocytes cultured on 96-well plates. 1993.
119. Miranda JP, Rodrigues A, Tostões RM, et al. Extending Hepatocyte Functionality for Drug-Testing Applications Using High-Viscosity Alginate–Encapsulated Three-Dimensional Cultures in Bioreactors. *Tissue Eng Part C Methods*. 2010;16(6):1223-1232. doi:10.1089/ten.tec.2009.0784.
120. Strom SC, Michalopoulos G. Collagen as a substrate for cell growth and differentiation. In: ; 1982:544-555. doi:10.1016/0076-6879(82)82086-7.
121. Pascussi JM, Gerbal-Chaloin S, Drocourt L, Maurel P, Vilarem MJ. The expression of CYP2B6, CYP2C9 and CYP3A4 genes: A tangle of networks of nuclear and steroid receptors. *Biochim Biophys Acta - Gen Subj*. 2003;1619(3):243-253. doi:10.1016/S0304-4165(02)00483-X.
122. Pascussi JM, Drocourt L, Gerbal-Chaloin S, Fabre JM, Maurel P, Vilarem MJ. Dual effect of dexamethasone on CYP3A4 gene expression in human hepatocytes. Sequential role of glucocorticoid receptor and pregnane X receptor. *Eur J Biochem*. 2001;268:6346-6358.
123. Monostory K, Kőhalmy K, Prough RA, Kóbori L, Vereczkey L. The effect of synthetic glucocorticoid, dexamethasone on CYP1A1 inducibility in adult rat and human hepatocytes. *FEBS Lett*. 2005;579(1):229-235. doi:10.1016/j.febslet.2004.11.080.
124. Stephen C. Strom, Ljubomir A. Pisarov, Kenneth Dorko, Melissa T. Thompson, John D. Schuetz and EGS. Use of Human Hepatocytes to Study P450 Gene Induction. 1996;272(1992):388-401.
125. Gomez-Lechon MJ, Tolosa L, Conde I, Donato MT. Competency of different cell models to predict human hepatotoxic drugs. *Expert Opin Drug Metab Toxicol*. 2014;10(11):1553-1568. doi:10.1517/17425255.2014.967680 [doi].
126. Sutherland L, Ebner T, Burchell B. The expression of UDP-glucuronosyltransferases of the UGT1 family in human liver and kidney and in response to drugs. *Biochem Pharmacol*. 1993;45(2):295-301. doi:10.1016/0006-2952(93)90064-4.
127. Pittner RA, Fears R, Brindley DN. Effects of cyclic AMP, glucocorticoids and insulin on the activities of phosphatidate phosphohydrolase, tyrosine aminotransferase and glycerol kinase in isolated rat hepatocytes in relation to the control of triacylglycerol synthesis and gluconeogenesis. *Biochem J*. 1985;225(2):455-462. http://www.pubmedcentral.nih.gov/articlerender.fcgi?artid=1144611&tool=pmcentrez&rendertype=abstract.
128. Polin R, Fox WW, Abman SH. *Fetal and Neonatal Physiology: Expert Consult - Online and Print - Richard Alan Polin, William W. Fox, Steven H. Abman - Google Livros*. Elsevier; 2011.
129. Audet-Walsh É, Giguère V. The multiple universes of estrogen-related receptor α and γ in metabolic control and related diseases. *Acta Pharmacol Sin*. 2015;36121(10):51-61. doi:10.1038/aps.2014.121.
130. Longuet C, Sinclair EM, Maida A, Baggio LL, Charron MJ, Drucker DJ. The glucagon receptor is required for the adaptive metabolic response to fasting. *Cell*. 2009;8(5):359-371. doi:10.1016/j.cmet.2008.09.008.The.
131. Palou M, Priego T, Sánchez J, et al. Sequential changes in the expression of genes involved in lipid

metabolism in adipose tissue and liver in response to fasting. *Pflugers Arch Eur J Physiol*. 2008;456(5):825-836. doi:10.1007/s00424-008-0461-1.

132. Iizuka K, Horikawa Y. ChREBP: A Glucose-activated Transcription Factor Involved in the Development of Metabolic Syndrome. *Endocr J*. 2008;55(4):617-624.
133. TAL M, KAHN BB, LODISH HF. Expression of the Low Km GLUT-1 Glucose Transporter Is Turned on in Perivenous Hepatocytes of Insulin- Deficient Diabetic Rats*. *Endocrinology*. 1991;129(4):1933-1941. doi:10.1210/endo-129-4-1933.
134. Connaughton S, Chowdhury F, Attia RR, et al. Regulation of pyruvate dehydrogenase kinase isoform 4 (PDK4) gene expression by glucocorticoids and insulin. *Mol Cell Endocrinol*. 2010;315(1-2):159-167. doi:10.1016/j.mce.2009.08.011.
135. Shin D-J, Campos JA, Gil G, Osborne TF. PGC-1alpha activates CYP7A1 and bile acid biosynthesis. *J Biol Chem*. 2003;278(50):50047-50052. doi:10.1074/jbc.M309736200.
136. Meirhaeghe A, Crowley V, Lenaghan C, et al. Characterization of the human, mouse and rat PGC1β (peroxisome- proliferator-activated receptor-γ co-activator 1β) gene in vitro and in vivo. *Biochem J*. 2003;373:155-165.
137. Herzog B, Cardenas J, Hall RK, et al. Estrogen-related receptor alpha is a repressor of phosphoenolpyruvate carboxykinase gene transcription. *J Biol Chem*. 2006;281(1):99-106. doi:10.1074/jbc.M509276200.
138. Girard J. Gluconeogenesis in Late Fetal and Early Neonatal Life. *Neonatology*. 1986;50(5):237-258. doi:10.1159/000242605.
139. Azzout-Marniche D, Bécard D, Guichard C, Foretz M, Ferré P, Foufelle F. Insulin effects on sterol regulatory-element-binding protein-1c (SREBP-1c) transcriptional activity in rat hepatocytes. *Biochem J*. 2000;350 Pt 2(Pt 2):389-393. http://www.ncbi.nlm.nih.gov/pubmed/10947952. Accessed September 16, 2016.
140. Foretz M, Pacot C, Dugail I, et al. ADD1/SREBP-1c is required in the activation of hepatic lipogenic gene expression by glucose. *Mol Cell Biol*. 1999;19(5):3760-3768. http://www.ncbi.nlm.nih.gov/pubmed/10207099. Accessed September 16, 2016.
141. Postic C, Burcelin R, Rencurel F, et al. Evidence for a transient inhibitory effect of insulin on GLUT2 expression in the liver: studies in vivo and in vitro. *Biochem J*. 1993;293:119-124.
142. Mashek DG, Khan SA, Sathyanarayan A, Ploeger JM, Franklin MP. Hepatic lipid droplet biology: Getting to the root of fatty liver. *Hepatology*. 2015;62(3):964-967. doi:10.1002/hep.27839.
143. Shipp DA, Parameswaran M, Arinze IJ. Development of fatty acid oxidation in neonatal guinea-pig liver. *Biochem J*. 1982;208:723-730.
144. Godoy P, Widera A, Schmidt-Heck W, et al. Gene network activity in cultivated primary hepatocytes is highly similar to diseased mammalian liver tissue. *Arch Toxicol*. 2016;90(10):2513-2529. doi:10.1007/s00204-016-1761-4.
145. Austin S, St-Pierre J. PGC1a and mitochondrial metabolism – emerging concepts and relevance in ageing and neurodegenerative disorders. *J Cell Sci*. 125:4963-4971. doi:10.1242/jcs.113662.
146. Giguère V. Transcriptional Control of Energy Homeostasis by the Estrogen-Related Receptors. *Endocr Rev*. 2008;29(6):677-696. doi:10.1210/er.2008-0017.
147. Liu C, Lin JD. PGC-1 coactivators in the control of energy metabolism Structure and function of PGC-1. *Acta Biochim Biophys Sin*. 2011;43(4):248-257. doi:10.1093/abbs/gmr007.Advance.
148. Liang H, Ward WF. PGC-1a: a key regulator of energy metabolism.
149. Ben-Ze'ev A, Robinson GS, Bucher NL, Farmer SR. Cell-cell and cell-matrix interactions differentially regulate the expression of hepatic and cytoskeletal genes in primary cultures of rat hepatocytes. *Proc Natl Acad Sci U S A*. 1988;85(7):2161-2165. http://www.pubmedcentral.nih.gov/articlerender.fcgi?artid=279949&tool=pmcentrez&rendertype=abstract. Accessed May 28, 2016.
150. Dich J, Gluud CN, Gluud CN. Effect of Insulin on Albumin Production and Incorporation of 14C-leucine into Proteins in Isolated Parenchymal Liver Cells from Normal Rats BY. 1975:236-243.
151. Zhang MY, Lee PJ, Hung PJ, Johnson T, Lee LP, Mofrad MRK. Microfluidic environment for high density hepatocyte culture. *Biomed Microdevices*. 2008;10(1):117-121. doi:10.1007/s10544-007-9116-9.
152. Niiya T, Murakami M, Aoki T, Murai N, Shimizu Y, Kusano M. Immediate increase of portal pressure, reflecting

sinusoidal shear stress, induced liver regeneration after partial hepatectomy. *J Hepatobiliary Pancreat Surg*. 1999;6(3):275-280. doi:10.1007/s005340050118.

153. Zhang C, Noort D van. Cells in Microfluidics. *TripleC*. 2011;11(1):13-35. doi:10.1007/128.

154. Cipriano M, Belém B, Rodrigues JS, et al. *Of-the-Shelf Hepatocyte-like Cells (HLCs): Characterization of Cryopreserved Human Mesenchymal Stem Cells Derived-HLCs*.; 2016. https://docs.google.com/document/d/17uU5wYDVWIHxnIDLOpb41ar7X1H5X5RV91sgMIvYKVk/edit.

155. Stéphenne X, Najimi M, Sokal EM. Hepatocyte cryopreservation: is it time to change the strategy? *World J Gastroenterol*. 2010;16(1):1-14. doi:10.3748/wjg.v16.i1.1.

VI. Annexes

VI. 1. Primers List

Name	Sequence	Melting Temperature (Tm ºC)
B-actin_F	CATGTACGTTGCTATCCAGGC	87.80
B-actin_R	CTCCTTAATGTCACGCACGAT	87.80
PDK4_F	TCTGAGGCTGATGACTGGTG	80.60
PDK4_R	GGAGGAAACAAGGGTTCACA	80.60
SREBP-1c_F	TGTTTGTTAGTGGGAGGAGTG	86.20
SREBP-1c_R	GAGGTGAGAAGGGACAACTGA	86.20
ChREBP1_F	GTTCCCTCTCTCTGCTCCTTC	86.80
ChREBP1_R	CCACACACACACATCCACAC	86.80
PEPCK_F	GCTTTTCAGCATCTCCAAGGA	80.30
PEPCK_R	GCTTCAAGGCAAGGATCTCTC	80.30
G6PASE_F	CAGAGCAATCACCACCAAGC	80.30
G6PASE_R	ACATTCATTCCTTCCTCCATCC	80.30
PPARA_F	CTGTCATTCAAGCCCATCTTC	81.60
PPARA_R	TTATTTGCCACAACCCTTCC	81.60
FXR_F	AGAACCTGGAAGTGGAACC	81.60
FXR_R	CTCTGCTACCTCAGTTTCTCC	81.60
CYP7A1_R	CCAGAAGCAATGAAAGCAGC	79.30
CYP7A1_F	GGATGTTGAGGGAGGGACT	79.30
PGC-1A_F	GCTGAAGAGGCAAGAGACAGA	80.40
PGC-1A_R	AAGCACACACACCACACACA	80.40
PGC-1B_F	GATGCCAGCGACTTTGACTC	85.90
PGC-1B_R	ACCCACGTCATCTTCAGGGA	85.90
GLUT1_SLC2A1_F	TCTGGCATCAACGCTGTCTTC	83.00
GLUT1_SLC2A1_R	CGATACCGGAGCCAATGGT	83.00
GLUT2_SLC2A2_F	GCTGCTCAACTAATCACCATGC	80.90
GLUT2_SLC2A2_R	TGGTCCCAATTTTGAAAACCCC	80.90
CPT1a_F	TCCAGTTGGCTTATCGTGGTG	80.90
CPT1a_R	TCCAGAGTCCGATTGATTTTTGC	80.90
ACOX1_F	ACTCGCAGCCAGCGTTATG	81.60
ACOX1_R	AGGGTCAGCGATGCCAAAC	81.60
NRF_F	AGGAACACGGAGTGACCCAA	83.00
NRF_R	TATGCTCGGTGTAAGTAGCCA	83.00
ERRA_F	AGGGTTCCTCGGAGACAGAG	71.60
ERRA_R	TCACAGGATGCCACACCATAG	71.60
CYTC_F	CTGATCTGCGGCTACAATTCTG	83.40
CYTC_R	CCCGGAAGAGGACTTGCTT	83.40

Table A - Primers used for RT-qPCR.